Title
Urologic applications of in vivo nuclear magnetic resonance spectroscopy

Author
Vigneron, Daniel B.

Publication Date
1990

Peer reviewed|Thesis/dissertation

UROLOGIC APPLICATIONS OF *IN VIVO* NUCLEAR MAGNETIC RESONANCE SPECTROSCOPY

by

DANIEL B. VIGNERON

DISSERTATION

Submitted in partial satisfaction of the requirements for the degree of

DOCTOR OF PHILOSOPHY

in

PHARMACEUTICAL CHEMISTRY

in the

GRADUATE DIVISION

of the

UNIVERSITY OF CALIFORNIA

San Francisco

UROLOGIC APPLICATIONS OF *IN VIVO* NUCLEAR MAGNETIC RESONANCE SPECTROSCOPY

by
DANIEL B. VIGNERON

ABSTRACT

Nuclear magnetic resonance (NMR) spectroscopy offers the unique opportunity to monitor noninvasively the concentrations of small molecules throughout a living body. This dissertation contains studies assessing the applicability of in vivo NMR spectroscopy for medical investigations in uro-genital organ systems. Section I contains renal studies of NMR spectroscopy. This technique was used to assess renal viability in cold-stored kidneys prior to transplantation. This was accomplished by noninvasive monitoring of phosphomonoester (PME)/inorganic phosphate (Pi) ratios in order to quantitate the severity of cellular ischemic damage in ex vivo rat, dog and human kidneys. These ratios correlated well with electron microscopic evaluation of biopsy specimens and with post-transplantation renal function. This technique was also shown to be capable of determining viable from nonviable kidneys after transplantation, but was unable to differentiate between acute rejection and vascular compromise as causes of the nonviability. Studies of kidneys with obstructed ureters showed that changes in phosphorus metabolite ratios were not very sensitive to deterioration in renal function. At present, the usefulness of ^{31}P NMR in assessing the viability of these kidneys remains unclear.

Section II contains NMR studies of testicular ischemia, the status of spermatogenesis and fertility. The ^{31}P NMR-derived PME/Pi ratios were found to indicate the degree of ischemic cellular injury and, therefore may be clinically useful to detect testicular torsion noninvasively and to predict recoverability. Statistically significant changes in phosphorus metabolite ratios were also observed after hormonal suppression of spermatogenesis in canine and primate testicles. Thus, this technique may have value for medical investigations of infertility.

Section III consists of NMR studies of the prostate and rat prostatic cancer. ^{31}P NMR was shown to be useful in detecting the bioenergetic differences between hormone-sensitive and hormone-resistant cancers, and between treated and untreated hormone-sensitive cancers. The ability to further these studies in canines and humans was attained by the development of a transrectal MR probe capable of providing high resolution MR images and localized ^{31}P NMR spectra of the prostate in situ.

ACKNOWLEDGEMENTS

Most of the work presented in this dissertation is the result of collaborations with radiologists and urologists. I received assistance from a large number of people in both these departments as well in pharmaceutical chemistry. I am very grateful for all of their assistance and regret that I cannot individually mention every person who contributed in some way to my work.

I am deeply appreciative of the support and guidance of my advisor, Tom James, who strived mightily and successfully to keep me and my projects on an even keel through real and imaginary crises. His patience was remarkable and extremely helpful, both directly and as an example. For the every day scientific assistance of Mike Moseley and Mike Wendland, I am especially thankful. The quality of this work would have been much lower without both of their assistance. Mike Wendland's biochemical approaches to *in vivo* spectroscopy were very beneficial to me in planning and rationalizing my studies. Hedi Hricak served as the principal investigator for most of the projects presented herein, and I am very appreciative of her energy, support and goal oriented approach which served to accelerate greatly the progress of these studies. To my friend and energetic co-worker Aria Tzika, words can never adequately express my gratitude and the joy I got out of our work together. Perinchery Narayan directed superbly the prostate studies. I am very appreciative of his focus and the long hours he and Dr. Jajodia put in on these projects. Peter Bretan also put in a

great deal of work on these projects and taught me valuable lessons about drive and dedication which will benefit me in the rest of my career. I would also like to thank every member (during my stint here) of the NMR lab, both *in vivo* and high-res. I learned a great deal from a wide variety of people and am appreciative of all.

I also benefitted from a great deal of personal and professional support (both moral and immoral), from the above and especially from my friends John Thomason, George Seibel, Don Kneller, Gamin Marugg, Jenna Hayward, Mary Meredith, Janice Varr, Lori Barak, Alex and Evan, John Shonle, John Altman, Rey Koslowski, Rene DesJarlais, my incomparable bro's (Dave and Tom), and all the rest. Lastly, I would like to express my deepest appreciation for the great support and fine examples my parents, Betty and Morgan, have offered me since my first scream. I aspire to emulate my mother's enthusiasm and excitement (for science and in general) and my father's thoughtful, caring approach to medicine and science.

I fervently hope I will continue to be so lucky in having opportunities to work and play with the likes of the people mentioned in this section. Many thanks.

TABLE OF CONTENTS

CHAPTER 1.

INTRODUCTION

Since living tissues are transparent to radiofrequency (rf) pulses, nuclear magnetic resonance (NMR) spectroscopy has the potential to obtain signals from nuclei of interest throughout the body. Recent advances in a wide variety of technologies, including large superconducting magnets, electronics, coil design, NMR pulse sequences and signal processing, have made *in vivo* NMR a viable technology with ever increasing clinical and investigative uses. Using linear magnetic field gradients and proper pulse sequences the spatial distribution of protons (primarily in water and fat) can be determined and displayed as a two- or three-dimensional image. This technique, magnetic resonance imaging (MRI), has, in the past few years, become widely used in diagnostic radiology providing, in many instances, images superior in detail and scope to those offered by any other modality (1-4).

The clinical impact of MRI has been especially great in the fields of neuroradiology and musculoskeletal radiology, but its superior soft-tissue resolution has also made it attractive for uro-radiology. MRI has now become an essential urologic imaging technique by providing unique and extremely informative images of pelvic organs and abnormalities (2, 5, 6). MR images offer not only exceptional anatomic detail of urogenital systems but also certain pathologies can be detected by using specific pulse sequences which highlight the changes in proton T1 (spin-lattice) and T2 (spin-spin) relaxation times and/or proton motion indicative of the specific disease or

abnormality. For example, uro-genital cancers are often of higher signal intensity than normal tissues on T2-weighted images, although many exceptions exist (5, 6). Even in those cases where cancer detection is poor, MRI can often be the most accurate method for tumor staging (5-8). MRI has also proven its usefulness for evaluating acute post-transplant renal failure (9, 10). In the normal kidney, cortico-medullary contrast (CMC) exists in T1-weighted images due to the much longer water proton T1's in the medulla. With acute rejection, the CMC is decreased or totally absent and the kidney is swollen. No CMC is observable with chronic rejection. Cyclosporin nephrotoxicity can often be differentiated from acute rejection, since the CMC is, in most cases, retained in the former and is greatly decreased in the latter.

Despite the successes in the use of clinical MRI, there remain many pathologies in which detection, prognosis, determination of optimal therapy and/or therapeutic monitoring are still difficult to achieve using present radiologic modalities. Since NMR spectroscopy has the unique ability to measure noninvasively the concentration of small molecules inside a living body, there has been, in recent years, great interest in developing this technique to provide biochemical information useful to the clinician and the medical scientist. The widespread availability of MR clinical imagers with sufficient field strength and spectroscopy packages (hardware and software) has generated many *in vivo* NMR studies focussing on clinical utility.

The initial research, however, has shown that finding and developing clinical applicability for NMR spectroscopy is far from trivial work. Despite its potential, *in vivo* NMR spectroscopy has

suffered from many short-comings and technical obstacles, making this technique complicated and limited in its present applicability. The reasons given for the slow development of clinical usefulness for this modality include: difficulty in signal localization, low sensitivity (making large tissue volumes necessary), the necessity of water proton suppression for ^{1}H NMR, poor spectral resolution, and low numbers of quality *in vivo* MR spectrometers (11-13).

In these studies I have overcome (or avoided) these technical problems primarily by optimizing coil design and construction and by careful choice of the organs and pathologies to be studied. I have not expended much effort on developing new NMR techniques, endeavoring instead to apply and adapt existing techniques to new organ systems and pathologies.

Although the afore-mentioned technical problems are most often cited as the limiting factors, I consider the complexity of the biochemistry being monitored to be the main reason NMR has been slow to become a clinical tool. In each of the studies included in this dissertation, I have been frustrated by the present lack of a detailed biochemical understanding of the cellular responses involved in the processes being studied. Due to its fairly low sensitivity and resolution as well as other technical constraints, NMR spectroscopy has been unable to provide enough information to elucidate the biochemical basis for a pathologic condition to the point where more than a reasonable guess could be stated.

A biochemist/NMR spectroscopist is very reluctant to introduce clinical tests, such as the ones proposed herein, unless the underlying biochemical mechanisms are clearly understood. Also researchers in

this field tend to construct experimental protocols in such a manner that, while the biochemistry might be studied, the clinical applicability issue remains poorly addressed. From my experience as a medical laboratory technician and other medical experience, including very useful discussions with the medical doctors involved in these projects, I have gained the appreciation that this in-depth biochemical understanding is not a necessary prerequisite for the development of a useful diagnostic tool. My approach has been to attain as great an understanding of the physiology and biochemistry as possible and to develop and test hypotheses concerning the underlying biochemistry, but not to insist upon a complete understanding when assessing the ability of NMR spectroscopy to provide clinically useful information. This is a necessary approach given the present gaping holes in biochemical knowledge, especially for the organs and pathologies addressed in this thesis. These studies were designed specifically to study the feasibility of *in vivo* NMR spectroscopy and its effectiveness as a tool for the medical and clinical investigations of certain urologic pathologies. Additions to the existing biochemical knowledge were just bonuses, not the primary goals of these studies. I will discuss the biochemical rationale which forms the working hypotheses used to explain and justify both the results and the choice of specific metabolite ratios as indicators of viability, hormone sensitivity, spermatogenic status, etc.; but clear scientific proof of these hypotheses was never achieved, just supported by the data presented here and in the literature. This approach, although at times unsatisfying in a "pure science" sense, has allowed the assessment of NMR spectroscopy's applicability for studies of a variety of urologic

problems.

In choosing pathologies (and organ systems) for which NMR spectroscopy might be a useful investigative tool, one must assess not only the technical problems involved in obtaining spectra but also one must decide whether or not significant changes in the "steady-state" concentrations of the observable molecules might occur. Living cells often control their metabolic activity by regulating enzyme kinetics which can result in no perceptible change in the metabolites observed by NMR spectroscopy. Some studies have shown no significant changes in ^{31}P spectra, while organ (and cellular) function changed drastically (14-16). Events which will affect these observable metabolite concentrations include ischemia (caused by a myriad of factors), changes in enzyme concentration and/or iso-enzyme pattern (often hormonally induced) and changes in the regulation of metabolic pathways.

One area in which NMR spectroscopy has great potential to provide useful clinical information is in the determination of renal viability in cadaveric kidneys prior to transplantation. The need for a noninvasive technique to determine the metabolic health of these kidneys is clear. A transplant surgeon faces a dilemma every time a potentially transplantable organ is harvested. If the transplanted organ fails to function in the recipient, not only has a great deal of time and money been wasted but the patient may become immunized to a subsequent organ, thereby diminishing the prospects for a successful second transplant (17). On the other hand, if one discards every kidney for which there is any doubt of viability, many viable organs will be wasted. This is equally unacceptable given the present organ

shortages. Furthermore, even an extravagant discard practice will not prevent the occasional transplantation of nonviable kidneys. The resolution of this dilemma lies in the development of reliable methods of assessing renal viability in *ex vivo* kidneys.

Viability can be defined in a several different ways. For the transplant surgeon, the operational definition is simply that viability is the ability of an organ to support life or, at least, to function within acceptable limits in the recipient after transplantation. The biochemist and physiologist focus more on the intactness of organ (and cellular) structures and of biochemical pathways. In this thesis, I have primarily used the concept that viability is inversely related to the degree of ischemic injury to the kidney (18). Following this argument, one can quantify renal viability by quantifying the degree of ischemic injury. In the ischemic state, the concentrations of high energy phosphates (e.g. ATP) decrease while the concentrations of low energy phosphates (e.g. inorganic phosphate (Pi) and phosphomonoesters (PME)) increase. By monitoring the increase of low energy phosphates by ^{31}P NMR, one can quantify the degree of cellular ischemic damage. This, therefore, becomes a viability parameter which, after being calibrated with established invasive methods and post-transplantation function, can be used to predict the recoverability of renal function. These arguments are similar to those used in the design of many clinical lab tests and are, I feel, equally valid for the design of a ^{31}P NMR "lab test" for renal viability. Although one might wish to use a ratio of ATP/Pi, ATP concentrations in the cold-stored kidneys decrease to unmeasurable levels long before the cells are irreversibly damaged. Therefore, in these studies of

assessing viability in *ex vivo* kidneys, the PME/Pi ratio was chosen as an indicator of viability. Although both peaks can increase as a result of degradative processes, Pi accumulates much more rapidly and is also an end product of PME hydrolysis. After the onset of ischemia, catabolic reactions dominate and, as a result, the Pi concentration increases. The Pi increase relates to the rates of the reactions (affected by temperature and other factors) and by the duration of the ischemic state. If one could accurately measure the absolute cellular concentration of Pi by NMR, I feel this would be a useful viability indicator. Since one is limited to measuring relative concentrations by *in vivo* NMR, I have used the PME/Pi ratio because it follows (although inversely) the same behavior as the Pi alone and is easily measured.

In this dissertation are three chapters, each comprised of sets of experiments, designed to assess the utility of ^{31}P NMR as a means to measure renal viability in pre-transplant kidneys. The animal models used included rats (Chapter 3), dogs (Chapters 4 and 5) and humans (Chapter 5). The initial studies were done in rats because the goal was to determine if the PME/Pi ratio was an accurate indicator of the degree of ischemic damage (in both normothermic and hypothermic ischemia). In order to do this correctly, in a statistical sense, a large number of animals (>50) were required. This necessitated the use of rat kidneys for the initial ischemia (and cold storage) studies. The rat study showed that the PME/Pi ratio correlated well with the degree of renal ischemic damage. Ratios higher than 0.50 were indicative of reversible ischemic injury whereas ratios below 0.35 were found in all nonviable kidneys. The PME/Pi ratio also correlated well with electron microscopy studies of cellular damage. This had no

dependence on whether the cause was warm or cold ischemia. (For a discussion of the difference between warm and cold ischemia, see Chapter 2).

After the rat study showed statistical significance for the determination of ischemic damage by PME/Pi ratios, studies of the larger, easily transplantable canine kidney were initiated. The goals of these studies were to assess further the value of PME/Pi ratios as indicators of ischemic injury and to correlate these ratios directly with post-transplantation renal function. Included in the studies was the development of implanted coils and new surgical models, so kidney spectra could be obtained after transplantation both *in situ* and *ex vivo* (in which case the kidney was connected to the dog's circulatory system via two 1-meter-long plastic cannulas). The latter model allowed high quality spectra to be obtained, devoid of motion-induced line broadening and spectral contamination from other tissues. This model also allowed spectra to be obtained as the ischemic kidney was reperfused. When the kidneys were transplanted normally, at least an hour would elapse between reperfusion on the operating table and the initiation of the NMR studies. The canine studies demonstrated that PME/Pi ratios correlated significantly with post-transplantation recovery as well as with the degree of ischemia.

Since these canine studies supported the initial indications that ^{31}P NMR could be used to determine renal viability, studies of human kidneys prior to transplantation were initiated. Human kidneys were obtained from the Pacific Presbyterian Medical Center's transplant service (at UCSF, cold-stored kidneys are connected to a constant perfusion machine and were therefore unavailable for these studies).

The kidneys were maintained at 4^0 C in their sterile containers throughout the study. ^{31}P NMR spectra were obtained approximately 2 hours before transplantation (after between 6 and 44 hours of simple hypothermic storage). The PME/Pi ratios were then correlated with subsequent renal function in the recipient (no invasive determinations of renal viability are performed in clinical renal transplantation). The study of 16 human kidneys showed that PME/Pi ratios were indicative of renal recoverability in the clinical setting.

The above studies showed that PME/Pi ratios could be used to assess the viability of ischemic kidneys. It is still unclear, however, if this technique will ever become widely used. Its cost and its inability to address immunologic problems (which are usually a greater concern) may preclude its routine clinical use, but ^{31}P NMR could become a very useful tool for research into new organ preservation techniques and new preservation solutions. Presently, researchers assessing the efficacy of a new technique depend on the success of transplantation (which can be affected by factors other than viability) and invasive biopsy methods for determining renal viability. A noninvasive method such as NMR could increase the accuracy and, perhaps, reduce the number of animals (and cost) of such studies.

Since NMR could assess renal viability in the pre-transplantation kidneys, a logical extension of these studies was to study the utility of this modality in determining post-transplantation viability. The non-invasive evaluation of a nonfunctioning transplant is often a major problem (19). The inadequacies of existing diagnostic modalities can necessitate invasive procedures, such as renal biopsies, to differentiate the possible causes (i.e. acute tubular necrosis, immunologic rejection,

vascular insufficiency or ureteral obstruction (19). Chapter 6 contains a study assessing the ability of ^{31}P NMR to monitor the viability of renal transplants. The canine kidneys (both autografts and allografts) were transplanted to a lower abdominal subcutaneous pocket (devoid of overlying muscle). The spectra were obtained using a surface coil placed over the kidney with only 1 cm of skin and subcutaneous tissue between. Although the ^{31}P NMR spectra were useful in determining viability, no differences were noted between severely rejected kidneys and vascularly compromised kidneys. It appears that both thrombosis and severe rejection result in cellular ischemia which had the same effect on the ^{31}P NMR spectra despite its ultimate etiology. Thus, although ^{31}P NMR is useful in determining the metabolic "health" of renal cells, this technique showed little promise in differentiating the causes of cell injury.

The pre-transplantation setting is not the only situation in which determinations of renal viability would be useful. Renal obstruction with subsequent hydroureteronephrosis is a common clinical problem, especially in congenital obstruction, silent stone obstruction and in cancer patients with retroperitoneal or pelvic metastases. It is important that the severity of the renal damage be assessed so one can determine whether corrective surgery will benefit the patient. In the case of bilateral obstruction, it is essential to determine which kidney has the better chance of recovery. Studies of chronic obstruction of the urinary tract are few; however, they agree that the duration of the obstruction directly influences the time course of recovery of renal function after release of chronic obstruction(20, 21). This information is usually not available at the time when the surgeon

must decide on the appropriate treatment for hydronephrosis, be it repair or nephrectomy. Technetium-99m labelled dimercaptosuccinic acid (Tc-DMSA) renography has been used to predict renal recovery after release of chronic obstruction (22). The uptake of Tc-DMSA, however, is dependent upon the integrity of the renal tubular cells and blood flow, and can indicate no renal function in kidneys which later recover.

Since ^{31}P NMR can assess the cellular metabolic state independent of blood flow or tubular function, its utility in the determining renal viability for partially and completely obstructed kidneys was studied (Chapter 7). The results from this study were far less promising than those of assessing viability in the cold-stored kidneys. Localization was now a major problem. The sensitive volume of a surface coil includes large volumes of subcutaneous muscle which dominate the ^{31}P spectra. This problem was overcome by using surgically implanted NMR coils so that the coils' sensitive volumes included only renal parenchyma. Although implanted coils provided good spectral localization, local tissue reaction and infection were serious complications. Also, the results indicated that the renal damage was caused by local ischemia resulting in the death and sloughing off of a minority of cells at any one time. This renal injury was not an equally severe, organ-wide insult as was the case for the isolated, pre-transplantation kidneys. Therefore, the spectra being obtained from a large number of cells showed only minor changes after obstruction, although size and renal function diminished greatly. Another major complication in this study was the heterogeneity of kidney cell types. The death of certain cells in the nephrons can

cause a complete loss of function (one definition of nonviability), while many other cells may be viable and may dominate the ^{31}P spectrum, making it indistinguishable from the control spectrum. Despite these problems, a significant decrease in ATP/Pi ratios was noted over three weeks of complete obstruction, roughly paralleling the decrease in Tc-DMSA uptake. Therefore, although much more research is required, there may be some clinical utility for ^{31}P NMR when an assessment of global metabolic health is desired.

The kidney is not the only urologic organ for which determinations of cellular viability are important. A clinical need also exists for a noninvasive technique to monitor cellular metabolism in male reproductive organs. Section II contains ^{31}P NMR studies of testicular ischemia, the status of spermatogenesis and fertility.

Assessment of testicular disease must often rely on an invasive surgical approach. In spite of encouraging reports from sonographic and nuclear medicine studies, surgical exploration remains the primary means of diagnosing testicular torsion (23). Similarly, despite numerous investigations involving hormonal assays and cytologic or biochemical analysis of ejaculate, difficulties persist in determining the cause of male infertility, and invasive procedures such as testicular biopsy are ultimately required. To avoid unnecessary surgical exposure of the testis, and because testicular biopsies may contribute to infertility (by increasing the serum titers of antispermatozoal antibodies) (24, 25), an accurate, noninvasive method to assess the vascular integrity and function of testicular tissue needs to be explored.

Chapter 9 contains studies designed to assess the utility of ^{31}P NMR in determining the degree of ischemic damage and the status of spermatogenesis in canine and primate testicles. In this study, the first well-localized ^{31}P NMR spectrum of an *in situ* testicle was obtained. The spectra were characterized by a very prominent PME peak which was shown to reflect high concentrations of phosphocholine, phosphoserine and phoshoethanolamine, which are involved in the synthesis of membrane phospholipids. As was the case for renal ischemia, PME/Pi ratios were found to be indicative of ischemic injury (although the calibration was different due to the much higher baseline PME intensity in the testicle). It appears that this ratio could be used as an indicator of testicular viability for the clinical evaluation of testicular torsion.

When canine and primate testicles were subjected to hormonally-induced suppression of spermatogenesis, a significant decrease in PME/ATP and PME/phosphodiesters (PD) ratios was observed. From these results it appears that the relative concentrations of these phosphorus metabolites is under hormonal control. In the absence of normal hormonal stimulation, the synthesis of the phospholipid precursors which comprise the PME peaks appears to decrease, presumably via control by the Sertoli cell, which serves as a "nurse" cell for the developing germ cells. The observed increase in PD concentration is probably indicative of the organ shrinkage caused by cell atrophy and death which resulted in an increase in phospholipid degradation products including the phosphodiesters. In the phospholipid breakdown process, phosphodiesters are further degraded to yield phosphomonoesters.

This may explain why the decrease in the PME peak is not larger than was observed after suppression of spermatogenesis. Although little PME is being synthesized for membrane synthesis, a substantial concentration arises from the phospholipid degradation associated with cellular atrophy. This unfortunately limits the sensitivity and usefulness of this technique since the cessation of hormonally controlled phospholipid synthesis affects two metabolic pathways; one resulting in decreased PME concentration and the other increased PME concentration. Although the increase of PD was associated with decreased spermatogenesis in this study, it would be difficult in a clinical situation to rule out the possibility of the PD peak arising from epididymal spectral contributions, resulting in a false diagnosis. Nevertheless, a significant decrease in PME/ATP ratios appears to be a good indicator of hormonally-mediated suppression of spermatogenesis.

In addition to the intactness of spermatogenesis, further maturation of the sperm is also required for male fertility (26). In the epididymis, the sperm gain motility (27, 28). If the epididymis does not provide the proper environment for this to occur, functional infertility will result. A previous study had indicated that ^{31}P NMR could be used to assess epididymal function by monitoring the seminal concentration of glycerophosphocholine (29). This phosphodiester is secreted in high concentrations by the epididymis (28). Chapter 10 contains a ^{31}P NMR study of thirty semen samples from normal volunteers, infertility patients, and vasectomy patients. This study supported the contention that low seminal GPC concentrations are indicative of poor motility (or vasectomy). However, false positives

among the vasectomy group indicated that other glands can contribute GPC to the seminal fluid; consequently limiting the accuracy of this as a fertility test.

The final section (Section III) consists of NMR studies of the prostate and rat prostatic cancer. These studies also have demonstrated possible urologic applications for *in vivo* NMR techniques. Chapter 12 describes a study of androgen sensitivity in rat prostate cancer using high resolution ^{1}H MR imaging, ^{23}Na MR imaging and ^{31}P NMR spectroscopy. Dunning rat prostate tumors from both hormone-sensitive and hormone-resistant sublines were implanted in the flanks of male Copenhagen rats (30, 31). Baseline ^{31}P MR spectra showed a significantly higher phosphocreatine (PCr)/ATP ratio in the hormone-sensitive cancers than in the hormone-resistant cancers. Following androgen deprivation therapy in the hormone-sensitive tumors, PCr levels decreased substantially by three days. PCr/ATP ratios in the treated tumors were significantly lower than in the sham-operated controls by one week after treatment and remained so for the rest of the study. The spectral differences in the treated cancers preceded the change in growth rate by at least two weeks. These changes in relative PCr changes reflect changes in cellular bioenergetics. Enzyme assay studies of rat prostate cancer have shown that the concentration and isoenzyme pattern of several important enzymes, including creatine kinase (CPK), are under hormonal control (32). These enzymic changes appear to affect PCr/ATP ratios which can then be monitored by ^{31}P MRS. Therefore ^{31}P MRS may become a useful technique for the detection of hormone-sensitivity, consequent selection of treatment, and in the monitoring

of androgen deprivation therapy, provided localized ^{31}P spectra from the prostate are obtained.

In chapter 13 a transrectal probe for ^{1}H imaging and ^{31}P MR spectroscopy of the prostate gland is described. The probe is covered with plastic and consists of an insertable portion containing a rf coil and a handle containing a tuning and matching circuit. Using this transrectal probe, high resolution ^{1}H MR images and the first ^{31}P spectra of the canine prostate were obtained. Serial alterations in prostate size and changes in the phosphomonoesters to ATP ratio following orchiectomy (removal of the testes) were also studied. Transrectal images of the prostate appear to be superior to conventional whole body coil images and may have important clinical applications in staging and therapy of prostate cancer. Present methods for screening, staging and imaging prostatic cancer are less than optimal, although conventional MRI has shown great promise for prostate cancer staging (7, 33-35). A method to enhance prostate image quality is highly desirable to the practicing clinician. The advantages of high resolution images of the prostate gland could include better differentiation of peripheral and central zones, better delineation of capsular integrity, seminal vesicles and periprostatic fat and venous anatomy. Such images may improve both detection and staging of prostate cancer, help plan the surgical approach and enhance the ability to determine efficacy of hormonal and radiation therapy. Further, a technique to monitor prostatic cellular metabolism and bioenergetics may be beneficial in two additional ways: 1) The altered biochemistry of neoplastic cells could be observed. 2) The metabolic "health" of both normal and cancerous prostatic cells could

be monitored during therapy, yielding valuable information on the efficacy of the specific treatment involved. Studies of human prostates are presently being initiated, and soon the clinical applicability of this use for *in vivo* NMR will be better assessed.

Although none of the urologic applications contained in this dissertation have attained clinical use, all (except for the case of ureteral obstruction) are now being studied in humans using investigative whole-body MR units. The work contained in this dissertation has generated useful information as to the cellular metabolic response to the pathologies studied. Even if no routine clinical use is ever realized for the techniques contained in this thesis, I feel these studies are important both for medical research purposes and for widening the scope of (and generating interest in) studies of the clinical applicability for *in vivo* NMR techniques.

References

1. James TL, Margulis AR eds: Biomedical Magnetic Resonance. Radiology Research and Education Foundation, San Francisco, 1984.
2. Higgins CB, Hricak H: Magnetic Resonance Imaging of the Body. Raven Press, New York, 1987.
3. Morgan CJ, Hendee WR: Introduction to Magnetic Resonance Imaging. Multi-Media Publishing, Denver, 1984.
4. Young SW: Nuclear Magnetic Resonance Imaging: Basic Principles. Raven Press, New York, 1984.
5. Hricak H: Genitourinary system (kidneys, adrenal glands, and pelvis). In: James TL, Margulis AR, eds. Biomedical Magnetic Resonance. Radiology Research and Education Foundation, San Francisco, 1984; 381-396.
6. Hricak H: MRI of the Genitourinary Tract. In: Budinger TF, Margulis AR, eds. Medical Magnetic Resonance Imaging and Spectroscopy. Society of Magnetic Resonance in Medicine, Berkeley, CA 1986; 202-211.
7. Hricak H, Dooms GC, Jeffrey RB, Avallone A, Jacobs D, Benton WK, Narayan P, Tanagho EA: Prostatic carcinoma: Staging by clinical assessment, CT and MR imaging. Radiology 1987; 162: 331-336.
8. Bionetti PR, Lee JK, Ling D, Catalona CSJ: Clinical stage B prostate carcinoma: Stagiing with MR imaging. Radiology 1987; 162: 325-329.

9. Hricak H, Terrier F, Demas GE: Renal allografts: Evaluation by MR imaging. Radiology 1986; 159:435-441.

10. Geisinger MA, Risius B, Jordan ML, Zelch MG, Novick AC, George CR: Magnetic resonance imaging of renal transplants. AJR 1984; 143:1229-1234.

11. James TL: Technical obstacles hinder spread of MR spectroscopy. Diagnostic Imaging, 1986; 8:218-221.

12. Weiner MW: NMR spectroscopy for clinical medicine: Animal models and clinical examples. In: Cohen SM ed. Physiological NMR Spectroscopy: From Isolated Cells to Man. The New York Academy of Sciences, New York, 1987; 287-299.

13. Matson GB, Weiner MW: MR spectroscopy in vivo: Principles, animal studies, and clinical applications. In: Stark DD, Bradley WG, eds. Magnetic Resonance Imaging. C.V. Mosby Co., St. Louis, 1988; 201-228.

14. Balaban RS, Koretsky A, Katz L: NMR investigations of cellular energy metabolism. In: Cohen SM, ed. Physiological NMR spectroscopy: From Isolated Cells to Man. New York Academy of Sciences, New York, 1987; 48-53.

15. Chance B, Leigh JS, Clark BJ, Maris J, Kent J, Nioka S, Smith D: Control of oxidative metabolism and oxygen delivery in human skeletal muscle: A steady state analysis of the work/energy cost transfer function. Proc Natl Acad Sci USA, 1985; 82: 8384-8388.

16. Kushmerick MJ, Meyer RA: Chemical changes in rat leg muscle by phosphorus nuclear magnetic resonance. Am J Physiol 1985; 248: C542-549.

17. Fahy GM: Viability concepts in organ preservation. In: Toledo-Pereyra LH, ed. Basic Concepts in Organ Procurement, Perfusion, and Preservation for Transplantation. Academic Press, New York, 1982; 121-158.

18. Farber JL, Chien KR, and Mittnact SJ: The pathogenesis of irreversible cell injury in ischemia. AM. J. Pathol. 1981; 102: 27-31.

19. Dubovsky EV, Logie JR., Diethelm AG, Et AL,: Comprehensive evaluation of renal function in the transplanted kidney. J Nucl Med 1975;1115-1120.

20. Klahr S.: Pathophysiology of obstructive nephropathy. Kidney Int. 1983; 23:414-426.

21. Buttner M, Brown l, Wieland MF, and Erdman E.: Renal function and (Na^+ and K^+) - ATPase in chronic unilateral hydronephrosis in dogs. J. Urol 1986; 135:185-190.

22. McDougal WA, Flanagan RC: Renal functional recovery of the hydronephrotic kidney predicted before relief of obstruction. J. Urol. 1981; 18: 440-442.

23. Ransler CW III, Allen TD: Torsion of the spermatic cord. Urol Clin North Am 1982; 9:245-250.

24. Guazzieri S, Lembo A, Ferro G, et al.: Sperm antibodies and infertility in patients with testicular cancer. Urology 1985; 26:139-142.

25. Gorden DL, Barr AB, Herrigel JE, Paulsen CA: Testicular biopsy in man. I. Effect upon sperm concentration. Fertil Steril 1965; 16:522-530.

26. Simmons FA. Medical progress. Human infertility. NEJM 1956; 255:1140-1146.

27. Mann T, and Mann CL. Male reproductive function and semen. New York, Springer-Verlag, 1981.

28. Turner TT. On the epididymis and its function. Invest. Urol. 1979; 16:311.

29. Arrata WSM, Tyler B, and Corder S. The role of phosphate esters in male fertility. Fertil and Steril 1978; 30:329.

30. Vigneron DB, Hricak H, Narayan P, Nunes L, Moseley M, James TL: Detection of the biochemical response of prostate cancer to androgen deprivation by P-31 MRS. Abstracts of the Sixth Annual Meeting of the Society of Magnetic Resonance in Medicine, p 36, 1987.

31. Vigneron DB, Hricak H, James TL, Jajodia PB, Nunes L, Narayan P: Androgen sensitivity of rat prostate cancer studied by ^{31}P NMR spectroscopy, ^{1}H MR imaging and ^{23}Na MR imaging. Magn. Reson. in Med. (submitted).

32. Hall M, Silverman L, Wenger AS, Mickey DD: Oncodevelopmental enzymes of the Dunning rat prostatic adenocarcinoma. Cancer Research 1985; 45:4053-4059.

33. Ling D, Lee JK, Meiken JP, Balte DM et al.: Prostatic carcinoma and benign prostatic hyperplasia: The ability of MR imaging to distinguish between the two diseases. Radiology 1986; 155:103.

34. Byron PJ, Butler HE, Nelson AD, Lipuma JP, et al.: Magnetic Resonance imaging of the prostate. AJR 1986; 146:543-548.

35. Phillips ME, Kneget HY, Sprectar LE, Arger PH et al.: Prostate disorders: MR imaging at 1.5 T. Radiology 1987; 164:386-392.

SECTION I : RENAL VIABILITY

Chapter 2: Introduction to Renal Viability Studies.

The studies contained in this section assess the potential of ^{31}P NMR spectroscopy in the determination of renal viability. This technique was studied for applicability in three separate, clinically-significant situations: 1) pre-transplantation viability of cold-stored kidneys; 2) post-transplantation viability; and 3) renal viability after ureteral obstruction.

As discussed in chapter 1, an accurate noninvasive technique to monitor viability in the pre-transplant setting would be significant for both clinical practice and transplantation research. Presently no such technique exists. The most widely used clinical test of organ viability, yet one of the least definitive, is vascular resistance (1). In order to assure good conditions of perfusion, the perfusion pressure is routinely monitored for all continually perfused hypothermic kidneys, therefore, this is a free noninvasive index of organ viability that requires no extra effort. This test can be useful to screen out some vascularly compromised kidneys, but most nonviable organs demonstrate normal vascular resistance (2). Assays of the compounds which diffuse into the perfusate have shown that the presence of certain large proteins is indicative of cellular damage, yet accurate quantitation is not possible and this method is not considered to be sensitive enough to determine renal viability routinely (1). Another noninvasive technique is the determination of surface pH using a surface electrode. This is limited in that only very few cortical cells

are monitored. Also, studies have shown that low pH does not seem to be a causative factor in ischemic injury, and pH correlates poorly with recoverability (3, 4).

Only invasive tests are presently available to monitor accurately renal cellular integrity. Mitochondrial matrix stability, measured by electron microscopy, assesses the structural integrity of renal cells. Intracellular adenine assays, obtained by freeze extraction of renal tissue, have shown that high adenine nucleotide concentrations correlate with intact metabolic pathways. Both these techniques have been used to predict renal viability (5-8). However, since both these techniques require surgical biopsies, they are not practical for clinical transplantation or clinical estimation of viability (9). If one could perform these cellular tests in a noninvasive manner, a clinically useful viability test would result. A noninvasive method to study the structural integrity of subcellular structures is not plausible, but *in vivo* NMR spectroscopy allows intracellular levels of adenine nucleotide and other compounds important to cellular energetics to be monitored noninvasively.

Studies have shown that irreversible uncoupling of mitochondrial respiration is primarily responsible for renal cell necrosis under ischemic conditions (7). The uncoupling of mitochondrial respiration is predominantly due to depletion of cytosolic adenine nucleotides for both warm and cold ischemia although the mechanisms and rates are different for the two cases (10). In the case of warm ischemia, the depletion of ATP and ADP results from the cessation of mitochondrial oxidative phosphorylation (i.e. lack of production of high energy phosphates due to the absence

of oxygen) with continued utilization of these compounds in pathways vital to cellular function. During cold storage, this mechanism also occurs but at a much slower rate, since cellular energy usage is greatly reduced at low temperatures. Some preservation techniques which perfuse cold-stored kidneys with oxygen-rich preservation solutions have been tested (1, 9, 11). This idea is based on the finding that the enzymes involved in oxidative phosphorylation (unlike those involved in glycolysis) retain substantial function at 4° C (7). However, these techniques have failed to increase storage times. The production of ATP in the mitochondria is coupled to cytosolic utilization by means of a translocase enzyme in the mitochondrial membrane. This enzyme is temperature sensitive and a great reduction in its function occurs below 18° C (12). It is this lack of adequate transportation of ATP out of the mitochondria which causes the uncoupling of energy production and energy utilization in hypothermic renal cells. The loss of adenine nucleotides have been shown by freeze-extraction assays to predict accurately the degree of post-transplantation tubular necrosis and consequently renal viability (13).

In the studies contained in this section, ^{31}P NMR was used to monitor the relative concentrations of intracellular adenine nucleotides and other phosphorus-containing metabolites especially inorganic phosphate in order to predict renal viability. In the ischemic state, the concentrations of high energy phosphates (e.g. ATP) decrease while the concentrations of low energy phosphates (e.g. inorganic phosphate (Pi) and phosphomonoesters (PME)) increase. By monitoring the increase of low energy phosphates by ^{31}P NMR, the degree of cellular ischemic damage was assessed. This, therefore,

becomes a viability parameter closely related to the established, yet invasive, adenine nucleotide assay, but it can be obtained without any destruction of renal cells.

The studies included in the following three chapters were not the first ones employing ^{31}P NMR to study cold-stored, ischemic kidneys. In the late 1970's and early 1980's, Oxford university's *in vivo* NMR research group, directed by Dr. George Radda, applied ^{31}P NMR spectroscopy to the assessment of the metabolic state of isolated, ischemic kidneys (14-18). The initial studies employed the rat kidney model and followed ^{31}P spectral changes over a 25 hour period (14-16). They found a rapid decrease of ATP spectral intensities, becoming unobservable within 1.5 hours of cold storage. Inorganic phosphate concentrations increased most rapidly initially and continued to accumulate throughout the 25 hour study. Intracellular pH was measured by determining the chemical shift of the Pi peak relative to a methyl triethylphosphonium-iodide standard contained in a glass capillary, and then using calculations similar to the method of Moon and Richards (19). In hypothermic ischemia, during which glycolytic pathways are shut down, the pH decreased to between 6.6 and 6.7 within 4 hours and remained constant for the rest of the 25 hour study. In the case of warm ischemia, in which glycolysis with resulting lactic acid production can occur, the pH decreased more to between 6.3 and 6.4 within 40 minutes and remained constant for the remainder of the 3 hour study. The published accounts of this work and of the subsequent human studies (18) concluded that ^{31}P NMR could be useful for assessing renal viability, but no practical indicator of metabolic viability was proposed.

These researchers concentrated on pH as an indicator of renal viability, but this is impractical for four reasons: 1) since they had no intracellular reference peak the measurements are suspect due to magnetic susceptibility effects and difficulties in accurately correlating Pi chemical shift to pH; 2) for both warm and cold ischemia, pH was shown to become constant long before irreversible damage usually occurs; 3) one study showed an intracellular pH dependence on the pH of the preservation solutions used (17); and 4) pH has been shown not to be a causative factor in renal ischemic damage (3, 4, 7, 10).

Our studies described in the first 3 chapters were designed specifically to develop a protocol to quantitate renal ischemic injury by measuring ^{31}P NMR spectral intensity ratios. These experiments were designed to determine: 1) which compounds would be observable by ^{31}P NMR during prolonged hypothermic storage; 2) whether ratios of peak intensities changed in a manner reflecting the duration and degree of ischemia; 3) if the ratios correlated well with renal function after reperfusion.

Chapter 6 contains a study using ^{31}P NMR to assess viability in post-transplantation kidneys. The determination of *in situ* viability is far more complicated than was the case for the isolated kidneys. Published NMR studies of this nature are rare and not conclusive as to the utility of this technique (20, 21, 22). Noninvasive evaluation of a nonfunctioning transplanted kidney is presently lacking (23). Despite current diagnostic modalities, invasive procedures (such as renal biopsy) may be required to differentiate the possible causes (i.e. acute tubular necrosis, rejection, vascular insufficiency or ureteral obstruction) of a nonfunctioning transplanted kidney.

Therefore, new noninvasive methods to monitor organ metabolism and viability are needed. Though renal function is closely associated with viability, the lack of function does not necessarily preclude cellular viability; thus renal viability must be assessed on a cellular level in a nonfunctioning kidney. As has been previously stated, NMR can monitor intracellular metabolic status independent of function and thereby may be useful to assess renal metabolic status and to predict renal recoverability.

In chapter 7, another study to assess the viability of *in vivo* kidneys is described. In this case, however, the insult was ureteral obstruction. Obstructive nephropathy, in itself, is not particularly difficult to diagnose, but determining the extent of renal damage and the ability of the kidney to recover after corrective surgery is much more difficult(24, 25). Previous investigations into the effects of ureteral obstruction on the kidney have focused mainly on determinations of renal function, renal hemodynamic changes, histologic parameters and rates of oxygen consumption (26-33). Most of these studies have employed acute experimental protocols and only a few have studied chronic partial and complete ureteral obstruction (26, 27). These studies have shown that prolonged ureteral obstruction causes destruction of nephrons, progressive renal atrophy and, ultimately, renal insufficiency.

Techniques to predict renal recoverability, to date, have been based on determining the remaining renal function in the obstructed kidney. Radionuclide scintigraphy of technetium-99m-dimercapto-succinic acid (Tc-DMSA) uptake has been shown to reflect the functioning cortical tubular mass of *in situ* kidneys (34). Studies

employing Tc-DMSA scintigraphy to measure renal tubular function in obstructed kidneys have shown this technique to be useful in predicting renal functional recovery after surgical repair (35, 36). The uptake of such radiopharmaceuticals, however, depends not only on the functional integrity of renal cortical cells but also on renal blood flow. Although substantial radiotracer uptake is predictive of adequate post-release renal function, the lack of radionuclide uptake may not necessarily preclude renal viability. NMR, on the other hand, can assess the cellular metabolic state independent of blood flow or function. The study presented in Chapter 7 was designed to investigate the effect of chronic partial and complete obstruction on intracellular renal metabolism as determined by ^{31}P NMR and to compare ^{31}P NMR findings with renal tubular function as measured by *in vivo* Tc-DMSA scintigraphy.

References

1. Fahy GM: Viability concepts in organ preservation. In: Toledo-Pereyra LH ed. Basic Concepts in Organ Procurement, Perfusion, and Preservation for transplantation. Academic Press New York, 1982; 121-158.
2. Foreman J: Prediction of viability of rabbit kidneys preserved by hypothermic perfusion. Cryobiology 1975; 12:231-237.
3. Ljunggren B, Norberg K, Siesjö BK: Influence of tissue acidosis upon restitution of brain energy metabolism following totaal ischemia. Brain Res 1974; 77:173-186.
4. Nemoto EM, Frinak S: Brain tissue pH after global brain schemia and barbiturate loading inrats. Stroke 1981; 12:77-82.
5. Trump BF, Mergner WJ, Kahng MW, Saladino AJ: Studies of the subcellular pathophysiology of ischemia. Circulation, 1976; 53(suppl. 1): 17.
6. Humes HD and Weinberg JM: Alterations of renal tubular cell metabolism in acute renal failure. Mineral Electrolyte Metab. 1983; 9:290.
7. Feinberg H: Energetics and mitochondria. In: Organ Preservation: Basic and Applied Aspects. Edited by Pegg DE, Jacobsen IA, and Halasz NA. Lancaster: MTP Press Limited, 1982; 3-15.

8. Calman KC: The prediction of organ viability. I. An hypothesis. Cryobiology, 1974; 11:1 .

9. Grundman R: Fundamentals of preservation methods. In: Toledo-Pereyra LH ed. Basic Concepts in Organ Procurement, Perfusion, and Preservation for transplantation. Academic Press New York, 1982; 93-120.

10. Southard JH, Senzig KA, Hoffman RM, and Belzer FO: Energy metabolism in kidneys stored by simple hypothermia. Transplant. Proc. 1977; 9:1535-1547.

11. Calman KC, Quin RO, and Bell PRF: Metabolic aspects of organ storage and prediction of organ viability. In Organ Preservation .Ed. Pegg DE , Lancaster: MTP Press, 1982; 113-119.

12. Pfaff E, Heldt HW, Klingenberg M: Adenine nucleotide translocation of mitochondria, kinetics of the adenine nucleotide exchange. Eur J Biochem 1969; 10: 484-491.

13. Fischer JH, Schmidt IH, Kulus D, Isselhad W.: Renal viability testing during preservation by metabolic parameters. In Organ Preservation. Ed. Pegg DE , Lancaster: MTP Press, 1982; 113-119.

14. Sehr PA, Radda GK: A model kidney transplant studied by phosphorus nuclear magnetic resonance. Biochem Biophys Res Com 1977; 77:195.

15. Sehr PA, Bore PJ, Papatheofanis J, Radda GH: Non-destructive measurement of metabolites and tissue pH in

the kidney by ^{31}P nuclear magnetic resonance. Br J exp Pathol 1979; 60:632-641.

16. Bore PJ, Sehr PA, Chan L, Thulborn KR, Ross BD, Radda GK: The importance of pH in renal preservation. Transplant Proc 1981; 13:707-708.

17. Sehr P, Bore P, Tulborn K, Papatheofanis I, Chan L, Radda GK: Tissue pH changes in renal preservation. In: Organ Preservation: Basic and Applied Aspects. Edited by Pegg DE, Jacobsen IA, and Halasz NA. Lancaster: MTP Press Limited, 1982; 109-112.

18. Chan L, French ME, Gadian DG, Morris PJ, Radda GK, Bore PJ, Ross BD, Styles P: Study of human kidneys prior to transplantaton by phosphorus nuclear magnetic resonance. In: Organ Preservation: Basic and Applied Aspects. Edited by Pegg DE, Jacobsen IA, and Halasz NA. Lancaster: MTP Press Limited, 1982; 113-119.

19. Moon RB, Richards JH: Determinations of intracellular pH by ^{31}P Nuclear magnetic resonance. J Biol Chem 1973; 248: 7276-7280.

20. Grist TM, Kneeland JB, Jesmanowicz A, Froncisz W, Flamig DP, Hyde JS: Techniques for localized *in vivo* human proton and P-31 spectroscopy: Application to kidney metabolism in renal transplant recipients. Radiology 1986; 161(P):148.

21. Kensora TG, Shamash F, Oh H, Smith MB: Measurement of phosphate metabolism in the transplanted human kidney

by 31-P NMR. Sixth Annual Mtg Soc Magn Res Med 1987; 1:188.

22. Shapiro JI, Haug CE, Weil R III, Chan L: ^{31}P Nuclear magnetic resonance study of acute renal dysfunction in rat kidney transplants. Mag. Reson. in Med. 1987;5:346-352.

23. Dubovsky EV, Logie JR., Diethelm AG, Et AL,: Comprehensive evaluation of renal function in the transplanted kidney. J Nucl Med 1975;1115-1120.

24. Buerkert J, Klahr S: Obstructive nephropathy. In: Massry SG, Glasscock RJ: Textbook of Nephrology. Williams and Wilkins Publishers, 1983; Vol. 2, p. 6.237-6.256.

25. Rudnick MR, Bastl CP, Elfinbrin IB, Nasins RG: The differential diagnosis of acute renal failure. (In) Brenner BM, Lazarus JM (eds.). Acute Renal Failure. W.B. Saunders Co., 1983; p. 176-222.

26. Klahr S: Pathophysiology of obstructive nephropathy. Kidney Int. 1983; 23:414-426.

27. Buttner M, Brown L, Wieland W-F, Erdman E: Renal function and ($Na^+ + K^+$) - ATPase in chronic unilateral hydronephrosis in dogs. J Urology 1986; 135:185-190.

28. Vaughan ED Jr., Sorenson EJ, Gillenwater JY: The renal hemodynamic response to chronic unilateral complete ureteral occlusion. Invest Urol 1970; 8:78-90.

29. Moody TE, Vaughan Ed Jr., Gillenwater JY: Relationship between renal blood flow and ureteral pressure during 18 hours of total unilateral ureteral occlusion. Invest Urol 1975;13:246-251.

30. Dal Canton A, Corradi A, Stanziale R, Maruccio G, Migone L: Effects of 24-hour unilateral ureteral obstruction on glomerular hemodynamics in rat kidney. Kidney Int 1979; 15:457-462.

31. Hsu CH, Kurtz TW, Rosenzweig J, Weller JM: Intrarenal hemodynamics and ureteral pressure during ureteral obstruction. Invest Urol 1977; 14:442-445.

32. Lyrdal F, Olin T: Renal blood flow and function in the rabbit after surgical trauma. Scand J Urol Nephrol 1975; 9:161-168.

33. Panko WB, Beamon CR, Middleton GW, Gillenwater JY: Effects of obstruction on renal metabolism: Renal tissue metabolite concentration after a-ketoglutarate infusion. Invest Urol 1978; 15:331-339.

34. Taylor A Jr: Quantitation of renal function with static imaging agents Sem Nucl Med 1982; 12:330-344.

35. Kawamura J, Hosokawa S, Yoshida O: Renal function studies using ^{99m}Tc - dimercaptosuccinic acid. Clin Nucl Med 1979; 4:39-46.

36. McDougal WS, Flanigan RC: Renal functional recovery of the hydronephrotic kidney predicted before relief of the obstruction. Invest Urol 1981; 18:440-442.

Chapter 3: Assessment of Renal Viability in Ischemic Rat Kidneys by ^{31}P NMR Spectroscopy

Purpose

To determine if the use of ^{31}P NMR is feasible and practical for determinations of renal viability prior to transplantation, a prospective study was designed, in which intracellular phosphorus metabolite levels were correlated with variable amounts of warm (20^{o}-$37^{o}C$) renal ischemia times and subsequent cold ($4^{o}C$) storage time in the rat kidney. Metabolite ratios derived from ^{31}P NMR spectra were also correlated with electron microscopic findings and post-ischemia (warm) renal function.

Materials and Methods

Variable Warm and Cold Ischemia Studies

Mature male Sprague-Dawley rats (180 to 250 grams) were anesthetized with intraperitoneal injection of pentobarbitol (40 mg/kg-body weight) for all studies. Surgical exposures were made via a midline transperitoneal incision from xyphoid to genitalia. Rats whose kidneys were removed for NMR studies (N=25) previously had their aorta cannulated with a 24-gauge angiocatheter (just above the iliac bifurcation), which was secured with 5-0 silk suture. The inferior vena cava was vented and the animals were exsanguinated. The thorax was simultaneously opened through the anterior diaphragmatic wall

and the suprarenal aorta and inferior vena cava were immediately clamped. Sixty milliliters of 4°C sterile lactated Ringer's solution with 5% dextrose (pH 5.0) was delivered through the aortic cannula. The kidneys were removed after specific warm ischemia times and kept in simple cold storage in 10mm NMR tubes at 4°C. The rats were divided into four groups which were subjected to warm ischemia of a duration of: 0 minutes (N=7), 20 minutes (N=8), 60 minutes, and 120 minutes before flushing and simple hypothermic storage. ^{31}P NMR spectra were obtained for all kidneys, without interrupting continuous cold storage, at intervals of approximately 2, 24, 48 and 72 hours after cold renal flushing. Tissue samples from the kidneys were obtained immediately after each NMR experiment for electron microscopic ultrastructure analysis.

Renal Function and Survival Studies

A separate group of rats was studied for the effects of varying amounts of warm ischemia on subsequent renal function and survival (N=30). In this group, the right ureter was isolated and ligated with 5-0 dexon ties, followed by systemic heparinization with 300 units aqueous heparin. The left renal vascular pedicle was isolated and clamped for the same durations of warm ischemia as was described in the previous section (0 minutes, 20 minutes, 60 minutes, and 120 minutes). After the set length of ischemia time had elapsed, the vascular clamps were removed and perfusion of the kidneys immediately resumed in all rats (as observed by restoration of normal color). The abdomen was then closed. Blood samples were acquired from rat tail veins for serum creatinine levels (by colorimetric alkaline

picrate analysis) at 72 hours for rats with 0 to 60 minutes of ischemia and at 24 hours for rats with 120 minutes of ischemia.

^{31}P NMR Methods

At the end of the warm ischemia period, the kidneys were flushed with cold perfusate and immediately placed in 10 mm NMR tubes and stored at 4^{o} C for the remainder of the study. A sealed capillary tube containing 1 M methylenediphosphoric acid (MDPA; Sigma), buffered to a pH of 9.0, was placed in each MRS tube as a chemical shift reference standard. The ^{31}P NMR was obtained at 97.6 MHz on a home-built spectrometer using a 5.6 Tesla superconducting magnet with a 7.6 cm bore (Cryomagnet Systems) and a Nicolet 1180/293B data system. The spectra were obtained from the Fourier transform of 500 acquisitions with an interpulse delay of 2 seconds and a tilt angle of 45^{o}. When compared with spectra obtained with a delay of 10 seconds, no change in peak intensity was observed; indicating no T1 saturation effects. Chemical shifts were referenced (in ppm) to the MDPA peak, and the peak assignments of Koretsky et al. were used (1). All peak intensity ratios were obtained with the Nicolet computer line fitting program. In this linefitting routine, the parameters (shape, width, amplitude and position) of computer-generated lines were altered until coincidence with the experimental signal was optimized and the absolute intensity of the difference spectrum (experimental minus calculated) was minimized. From the peak areas, the phosphorus metabolite ratios were calculated. Statistical analysis was done with the unpaired Student's *t* test.

Electron Microscopy

Immediately upon removal of the kidneys, 1-mm thick shavings of the renal cortex and medulla were dropped in 5 ml of 2 percent glutaraldehyde, and 0.1 M sodium cacodylate, pH 7.4, at 4° C. After 24 hours the tissue fragments were rinsed, post-fixed in two percent osmium tetroxide for one hour and then embedded. Ultrathin sections were cut from each block, stained with two percent uranyl acetate and lead citrate, and examined in a Philips EM-201 microscope. Proximal tubular epithelial cells were examined for evidence of ischemic damage. The criteria used for EM ultrastructural staging was as follows: Stage 1 -- No evidence of intracellular damage. The nuclei and mitochondria are completely normal. No evidence of ischemic damage. Stage 2 -- Mild ischemic damage. Some condensation of mitochondrial matrix and mild mitochondrial swelling noted. Stage mostly associated with reverible changes. Stage 3 -- Moderate ischemic damage associated with irreversible changes. Frequent floculent densities in inner compartment of mitochondria with disruption of cell membrane noted. Stage 4 -- Gross cell death with intracellular calcifications and karyolysis.

Results

^{31}P NMR spectra showed measurable phosphomonoester (PME) and nicotinic adenine dinucleotide (NAD) resonances throughout the first 50 hours of cold storage time in all kidneys studied. The NAD resonance may have contributions from both the oxidized and the reduced forms of both NAD and NADP. The ^{31}P spectra gave no

evidence of ATP or ADP in the ex vivo cold-stored kidney; thus, the contributions from alpha-ATP or alpha-ADP to the NAD resonance are negligible. The inorganic phosphate (Pi) chemical shift which corresponded to a pH of approximately 7.1 decreased only slightly to approximately 6.9 during the 72 hours of cold-storage. A time-dependent decrease in the PME/Pi ratio (Figure 5) and in the NAD/Pi (Figure 6) ratio was found over the 72 hours of cold perfusion. All groups were significantly ($p<0.05$) different from each other at approximate scanning times of 2, 24, and 48 hours (table 1) which helped establish a separate but parallel decay curve of NAD/Pi and PME/Pi ratios (Figures 5 and 6).

Renal function studies of solitary functioning post-ischemic kidneys and subsequent survival revealed no difference in serum creatinine between the 0 and 20 minute ischemic groups; both had an average serum creatinine concentration of 0.6 mg/dl. However, at 72 hours the 60 minute ischemic group had significantly elevated ($p<0.05$) creatinine levels (2.1 mg/dl) as compared with kidneys subjected to less ischemia. In the 120 minute ischemia group, no rat survived for more than 48 hours (N=9) and all serum creatinine levels were measured 24 hours after the ischemia. The average serum creatinine level for this group was 4.7mg/dl. The 4 week survival for rats whose kidneys experienced 60 minutes or less of ischemia was 100 percent (Table 1). Non-fatal azotemia associated with the 60 minute ischemia group corresponded to an NAD/Pi ratio of 0.17 (standard error(SE)=0.06) and a PME/Pi ratio of 0.45 (Figures 5 and 6).

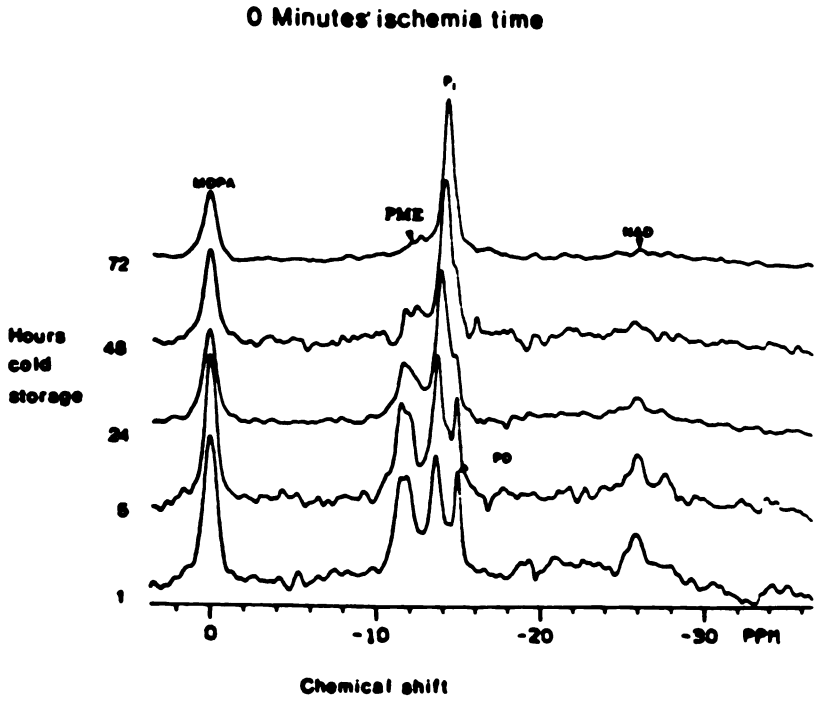

Figure 1. Serial ^{31}P NMR spectra from cold-stored rat kidneys subjected to negligible warm ischemia. Note the relative increase in Pi peak intensities with time. Peak assignments are as follows: MDPA = methylene diphosphonate standard, PME = phosphomonoesters, Pi = inorganic phosphate, PD = phosphodiesters, NAD = nicotinic adenine dinucleotide.

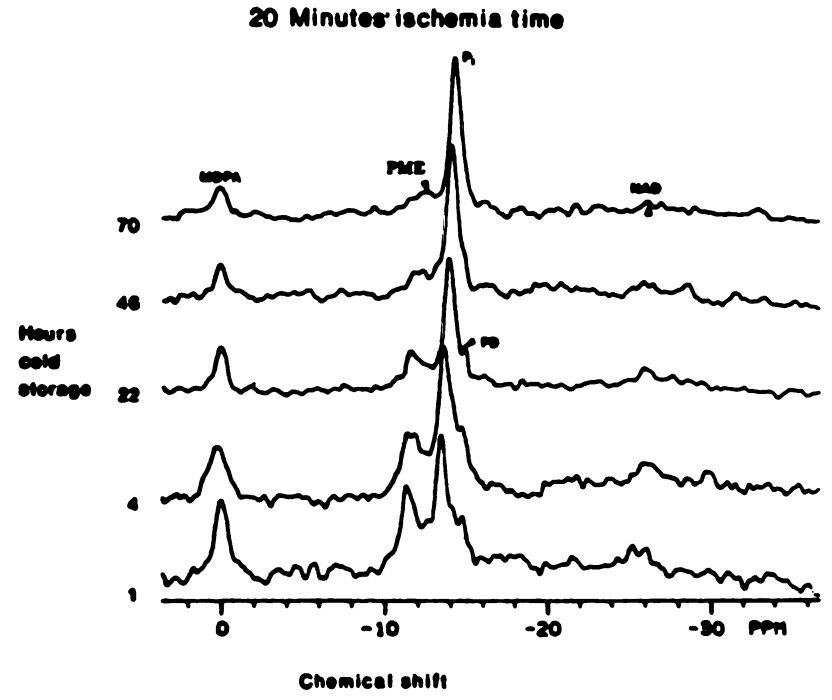

Figure 2. Serial ^{31}P NMR spectra from rat kidneys subjected to 20 minutes of warm ischemia prior to cold-storage. A similar pattern (as compared with Figure 1.) of spectral changes was observed, however initial PME/Pi ratios were significantly lower.

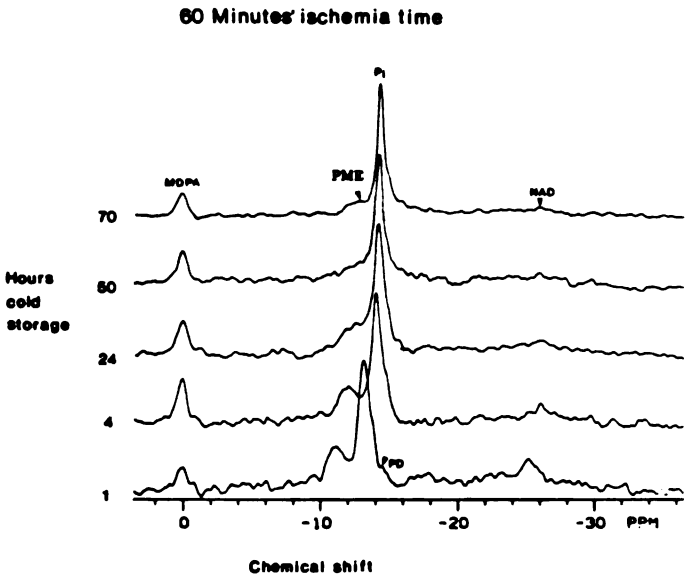

Figure 3. Serial ^{31}P NMR spectra from rat kidneys subjected to 60 minutes of warm ischemia prior to cold-storage. Initial relative peak intensities of PME and NAD were much lower than for kidneys subjected to less warm ischemia. Within 24 hours of hypothermic ischemia, NAD was nondectable and the PME peak was only barely measurable.

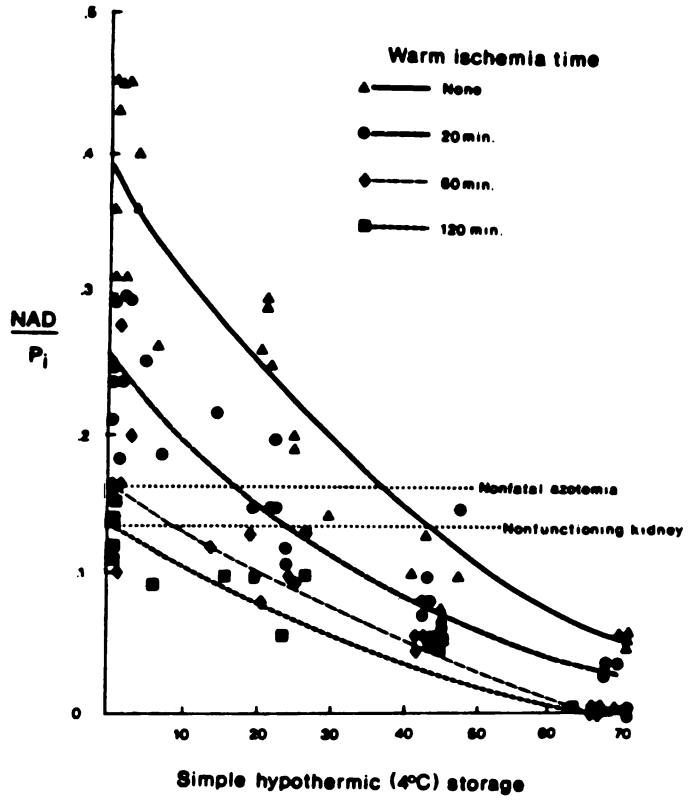

Figure 4. Graphic display of the repsonse of renal NAD/Pi ratios to various durations of warm ischemia and subsequent hypothermic storage.

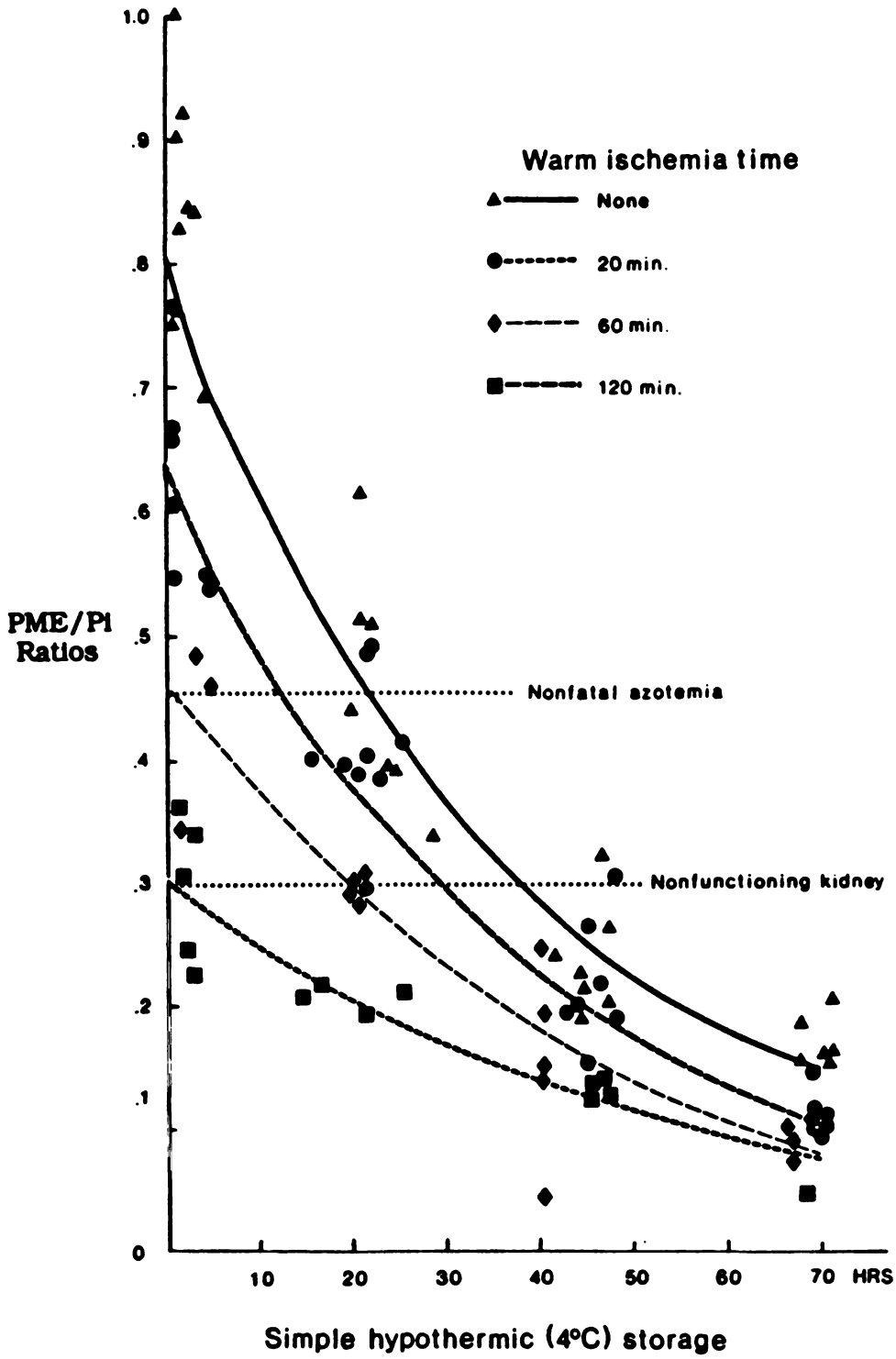

Figure 5. Graphic display of the repsonse of renal PME/Pi ratios to various durations of warm ischemia and subsequent hypothermic storage.

Table 1 Comparison of PME/Pi ratios and Electron Microscopy with Post-Ischemic Renal Function

Warm Ischemia Time (Minutes)	PME/Pi Ratios[1]	EM Stage[2]	Survival at 4 Wks.	Serum Creatinine
0	0.80	1	100%	0.6 mg/dl
20	0.63	2	100%	0.6 mg/dl
60	0.45	3	100%	2.0 mg/dl
120	0.30	4	0%	4.7 mg/dl

[1]All groups are significantly different ($p<0.005$) from each other.

[2]Criteria for EM Ultrastructural staging: Stage 1 - No evidence of intracellular damage. The nuclei and mitochondria are completely normal. Stage 2 - Mild ischemic damage. Some condensation of mitochondrial matrix and mild mitochondrial swelling noted. Stage 2 is mostly associated with reversible changes. Stage 3 - Moderate ischemic damage associated with irreversible changes. Frequent floculent densities in inner compartment of mitochondria with disruption of cell membrane noted. Stage 4 - Gross cell death with intracellular calcifications and karyolysis.

Table 2 Comparison of EM Staging With Various Warm and Cold Ischemia Times

EM Staging*	Warm Ischemia Time (Minutes)	Hypothermic Storage Time (Hours)
1	0	0
1	0	4
2	0	24
3	0	48
3	0	72
2	20	0
2	20	24
3	20	48
4	20	72
3	60	0
3	60	4
4	60	24
4	60	48
4	60	72
4	120	0

*For Staging Criteria see Table 1.

Electron microscopic findings were also correlated with the amount of ischemia and cold storage time (Table 2). Established irreversible ischemic cell damage findings (2) corresponded to an PME/Pi ratio of 0.45 (table1).

Discussion

As discussed in Chapter 2, a modality capable of safely and accurately determining renal viability is presently lacking, and would be of great value to clinicians and transplantation researchers alike (3-5). Such a technique must assess cellular metabolic integrity since macroscopic and vascular characteristics are not accurate indicators of renal viability for *ex vivo* kidneys (3, 6). A useful viability indicator must accurately reflect the loss of cellular bioenergetic status. This viability parameter can then be correlated (and calibrated) with irreversible damage as measured by an invasive biopsy method and post-surgical recoverability.

In this study ^{31}P NMR is proposed as a method to accomplish noninvasive determinations of renal viability by measuring intracellular metabolite concentration ratios and then calibrating these ratios with established viability parameters. Although it has been known for several years that ^{31}P NMR can be used to measure relative intracellular concentrations of metabolites vital to cellular energy metabolism, its clinical applicability is presently very limited (7-9). A major reason for this is that the ^{31}P spectra of living tissues are not significantly affected by a large variety of pathologies even though organ function might be destroyed. Constant metabolite ratios under

such conditions can be be brought about in two ways: 1) the cellular response is such that the steady-state concentrations of these metabolites are not significantly altered even though reaction kinetics (i.e. metabolic work) may have decreased to a point where cellular function is compromised; and 2) when the percentage of cells affected at any point in time is small, spectral contributions from unaffected cells dominate, causing organ viability to be inaccurately assessed. ^{31}P NMR can be a useful tool to assess the renal injuries induced in this study since none of the above scenarios occurred. During renal ischemia, steady-state concentrations of the metabolites monitored by ^{31}P NMR (most notably ATP, Pi, and phosphomonoesters including AMP) were not maintained, and large changes in the ^{31}P spectra were observed. In this study the renal artery was either completely occluded or severed, resulting in global ischemia which affected every renal cell. Therefore, the changes in ^{31}P spectra did accurately reflect the cellular response to the complete ischemia studied.

In this study PME/Pi ratios demonstrated a good correlation with the degree of renal ischemic damage. When correlated with the survival studies (and serum creatinine levels), ratios higher than 0.50 were found to be indicative of reversible ischemic injury whereas ratios below 0.35 were found in all nonviable kidneys. The PME/Pi ratio also correlated well with electron microscopy studies of cellular damage. This had no dependence on whether the cause was warm or cold ischemia. Although the NAD/Pi ratio also demonstrated a good correlation to the degree of ischemic damage, the low relative concentration of NAD made this ratio more difficult to measure accurately than the PME/Pi peak. Consequently, the PME/Pi ratio was

chosen as an indicator of viability. Although both PME and Pi resonances can increase as a result of degradative processes, Pi accumulates much more rapidly and is also an end product of PME hydrolysis. After the onset of ischemia, catabolic reactions dominate and, as a result, the Pi concentration increases. The intracellular Pi accumulation relates directly to rates of these catabolic reactions (affected by temperature and other factors) and to the duration of the ischemic state. If one could accurately measure the absolute cellular concentration of Pi by NMR, I feel this would be a useful viability indicator. Since relative concentrations are more easily measured by *in vivo* NMR, I have used the Pi/PME ratio because it follows roughly the same behavior as the Pi alone.

Previous studies (non-NMR) have shown that 45 minutes of warm ischemia is equivalent to 24 hours of cold storage in terms of cellular damage (2, 10-12). The EM studies presented in this chapter support this assertion as well. The fact that PME/Pi ratios were the same in both cases further supports the validity of using this ratio to monitor renal viability.

Although more studies are required to determine the accuracy of this technique, it appears from this investigation that ^{31}P NMR is well suited for the noninvasive assessment of renal viability in isolated kidneys. The technique was fast, consistent, noninvasive and had no adverse effects on the kidneys. From this study, however, one can only draw conclusions about cold-storage of bisected rat kidneys. Further studies are required to determine whether the PME/Pi ratio is useful in determinations of renal viability in intact kidneys of other species (most importantly humans). Also, in this study PME/Pi ratios

were not correlated directly with post-transplantation renal function. The experiments presented in the next two chapters were designed to address these deficiencies.

References

1. Koretsky AP, Wang S, Murphy-Boesch J, Klein MP, James TL, Weiner MW: ^{31}P NMR spectroscopy of rat organs , in situ, using chronically implanted radiofrequency coils. Proc. Natl. Acad. Sci. 80: 7491, (1983).
2. Venkatachalam MA, Bernard DB, Donohoe JF, Levinsky NG: Ischemic damage and repair in the rat proximal tubule: differences among the S_1, S_2, and S_3 segments. Kidney Int. 14:31 (1978).
3. Fahy GM: Viability concepts in organ preservation. In: Toledo-Pereyra LH ed. Basic Concepts in Organ Procurement, Perfusion, and Preservation for transplantation. Academic Press New York, 1982; 121-158.
4. Goldszer RC, Strom TB, Tilney NL: Acute renal failure associated with renal transplantation. In: Acute Renal Failure. Edited by B.M. Brenner and J.M. Lazarus. Philadelphia: W.B. Saunders, chapter 21, pp555-566, 1983.
5. Kootstra G: Organ preservation. Transplant. Proc. 1984; 16:185.
6. Calman KC: The prediction of organ viability. I. An hypothesis. Cryobiology, 1974; 11:1.
7. Nunnally RL: In vivo monitoring of metabolism with nuclear magnetic resonance spectroscopy. Semin. Nucl. Med., 1983; 13:377.

8. James TL: Technical obstacles hinder spread of MR spectroscopy. Diagnostic Imaging, 1986; 8:218-221.

9. Weiner MW: NMR spectroscopy for clinical medicine: Animal models and clinical examples. In: Cohen SM ed. Physiological NMR Spectroscopy: From Isolated Cells to Man. The New York Academy of Sciences, New York, 1987; 287-299.

10. Jacobsen IA, Pegg DE: Kidney. In: Organ Preservation for Transplantation. Edited by AM Karrow Jr., and DE Pegg. New York: Marcel Dekker, Inc., p 553-575, (1981).

11. Southard JH, Senzig KA, Hoffman RM, Belzer FO: Energy metabolism in kidneys stored by simple hypothermia. Transplant. Proc. 9: 1535 (1977).

12. Calman KC, Quinn RO, Bell PRF: Metabolic aspects of organ storage and prediction of organ viability. In : Organ Preservation. Edited by D.E. Pegg. Edinburgh: Churchill Livingstone, p. 225, 1973.

Chapter 4: Assessment of Renal Preservation by ^{31}P NMR: Biopsy Studies of Isolated Canine Kidneys Before and After Transplantation

Purpose

The previous studies with rat kidneys demonstrated the utility of PME/Pi ratios, derived by ^{31}P NMR, as a noninvasive indicator of renal viability in isolated kidneys (1, Chapter 2). The purpose of this study was to determine whether PME/Pi ratios could accurately reflect the metabolic energy status in canine kidneys during warm and cold ischemia and after transplantation. Although technical constraints dictated the use of renal biopsies, the study was designed to simulate the peri-transplant setting in order to test further the utility of this method for biomedical determinations of renal viability.

Materials and Methods

Twenty-five adult mongrel dogs (20 to 25 kg) were anesthetized with acepromazine, ketamine and pentobarbitol, and the kidneys were exposed by a midline abdominal incision. Before dissection of the renal vessels, 20 mg. of furosemide and 500 ml lactate were administered intravenously. A total of thirty-three canine kidneys were subjected to various amounts of ischemia: 12 kidneys served as well perfused *in situ* controls, 6 *in situ* kidneys were ischemic (by renal pedicle clamping) for 45 minutes, and 15 kidneys were removed, flushed with cold Downes' solution (2), cold stored for 24

hours and then transplanted into recipient dogs. Renal transplantations were performed, after left nephrectomy, by end-to-end anastomosis of the left renal vessel stumps in all dogs. Renal viability, characterized by adequate perfusion and function, was directly assessed by the presence or absence of urine production in each kidney.

Renal Biopsy Specimens

All biopsy specimens were standardized: wedge biopsies of two to three cm^3 of renal corticomedullary tissue. Tissue was taken *in vivo*, after 45 minutes of warm ischemia and after four hours of reperfusion, and after 24 hours of *ex vivo* cold storage and after 4 hours of reperfusion post-transplantation. After biopsy, renal tissue specimens were immediately cooled to 4°C in flush solution and studied by ^{31}P NMR spectroscopy.

^{31}P NMR Spectroscopy

Tissue specimens were kept in 10 mm NMR tubes at 4°C during the entire cold storage time (including NMR studies). A sealed capillary tube containing 1 M methylene diphosphonic acid (MDPA; Sigma), buffered to pH 9.0, was placed in each NMR tube as a reference standard. The ^{31}P NMR was performed at 97.6 MHz on a home-built spectrometer with a 5.6 Tesla superconducting magnet with a 7.6 cm diameter bore (Cryomagnet System; Indianapolis, IN) and a Nicolet 1180/293B data system. The spectra were obtained from the Fourier transform of 400 acquisitions with parameters chosen to prevent saturation. Chemical shifts were referenced to the

MDPA resonance, and the peak assignments described by Koretsky et al (3) were used. All peak intensity ratios were obtained by using the Nicolet line fitting program. Statistical analysis was performed with the unpaired Student's t test (results are expressed as mean ± S.D.).

Results

The spectra from the controls show high PME/Pi ratios from an *in vivo* biopsy (Figure 1). All 12 kidneys exhibited a high PME/Pi ratio, with a mean of 0.87 ± 0.12. Excellent urine production was noted in all controls intraoperatively.

Spectra of kidneys subjected to 45 minutes of warm ischemia showed a PME/Pi ratio of 0.50 ± 0.12 (Figure 2). After four hours of reperfusion, the mean PME/Pi ratio was 1.02 ± 0.07 (Figure 2). Regeneration of PME/Pi was accompanied by substantial urine production in the post-reperfusion period.

Eight transplanted kidneys exhibited excellent reperfusion; manifested by organ firmness and urine production within 10 minutes after anastomosis. Seven transplanted kidneys were soft and showed inadequate reperfusion (associated with a complete lack of urine production) secondary to hemorrhage (N=2), hypotension (N=2), and thrombosis (N=3). The inadequately reperfused transplants failed as a result of technical and anastomotic defects, but they were included in this study to show the further relationship of PME/Pi changes with greater ischemia. Representative spectra in Figure 3 reveal that after 24 hours of hypothermic storage, the PME/Pi ratio fell to approximately 0.50. With adequate perfusion for 4 hours, the PME/Pi

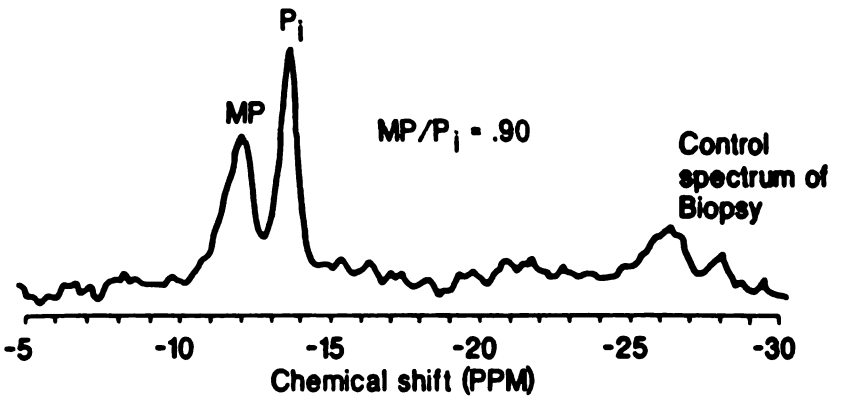

Figure 1. ^{31}P NMR spectra of control *in vivo* canine kidney biopsy. Peak assignments are as follows: MP = phosphomonoesters (designated PME in text), Pi = inorganic phosphate, PD = phosphodiesters. Chemical shifts are expressed as parts per million (ppm) relative to MPDA (not shown).

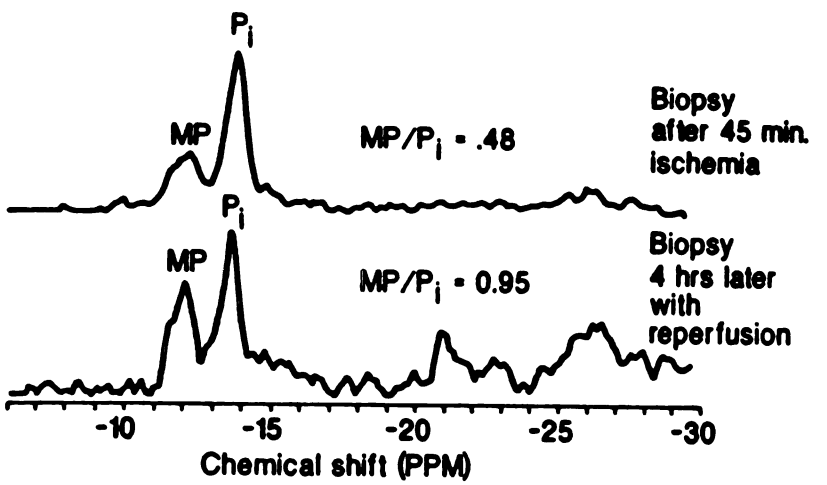

Figure 2. ^{31}P NMR spectra of canine kidney biopsy after 45 minutes of warm ischemia and 4 hours of subsequent reperfusion. Peak assignments are the same as in Figure 1.

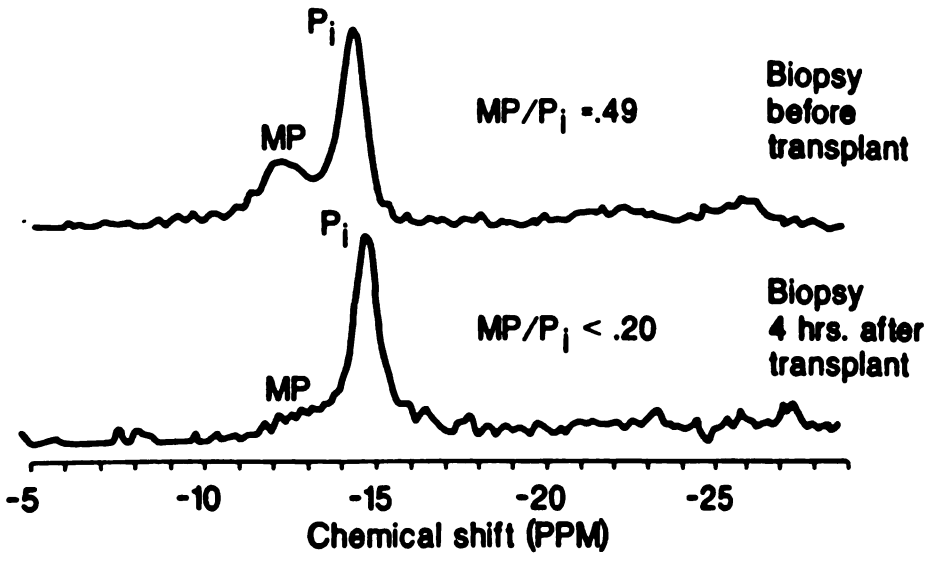

Figure 3. ^{31}P NMR spectra of canine kidney biopsy after 24 hours of hypothermic storage and 4 hours of subsequent adequate perfusion (successful transplant; urine production resumed). Peak assignments are the same as in Figure 1.

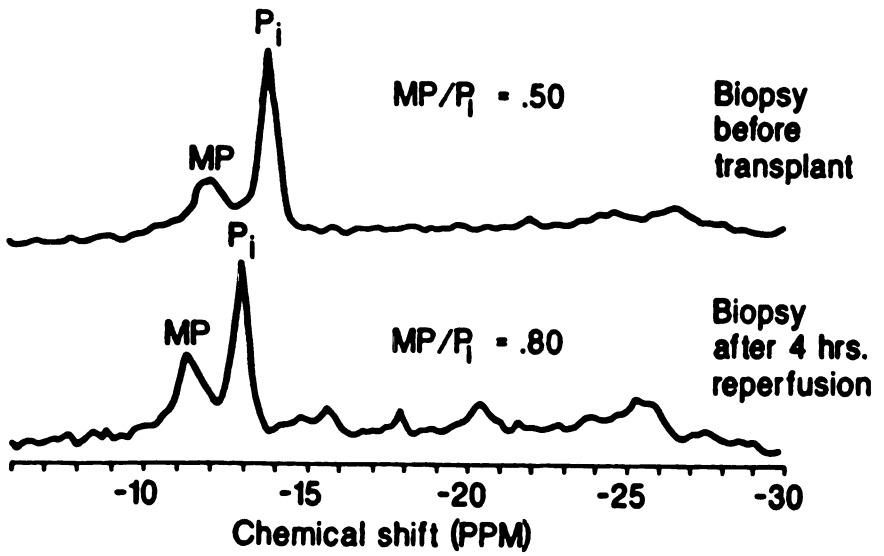

Figure 4. ^{31}P NMR spectra of canine kidney biopsy after 24 hours of hypothermic storage and 4 hours of subsequent inadequate perfusion (unsuccessful transplant; no urine production). Peak assignments are the same as in Figure 1.

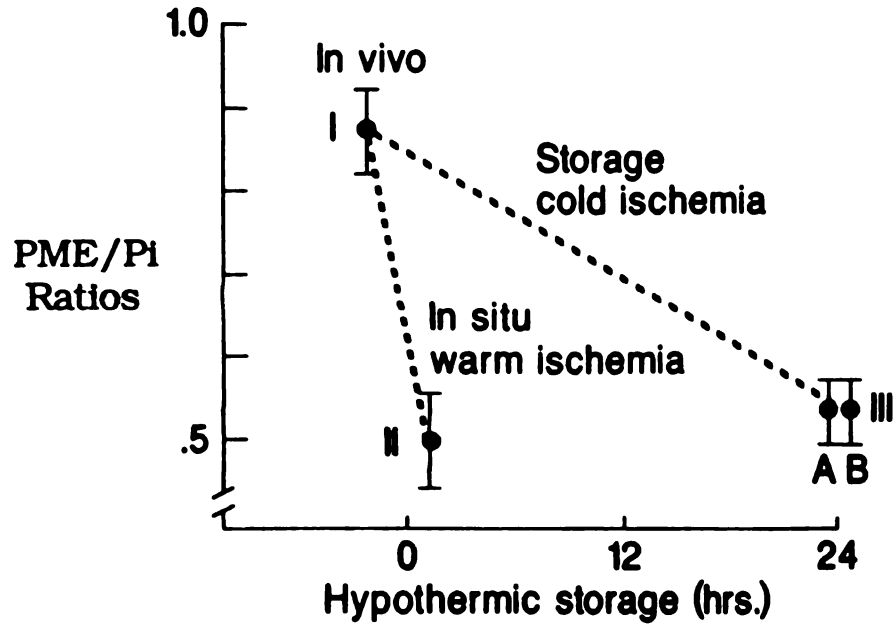

Figure 5. Graphic display of the changes in renal PME/Pi ratios with duration of normothermic and hypothermic ischemia.

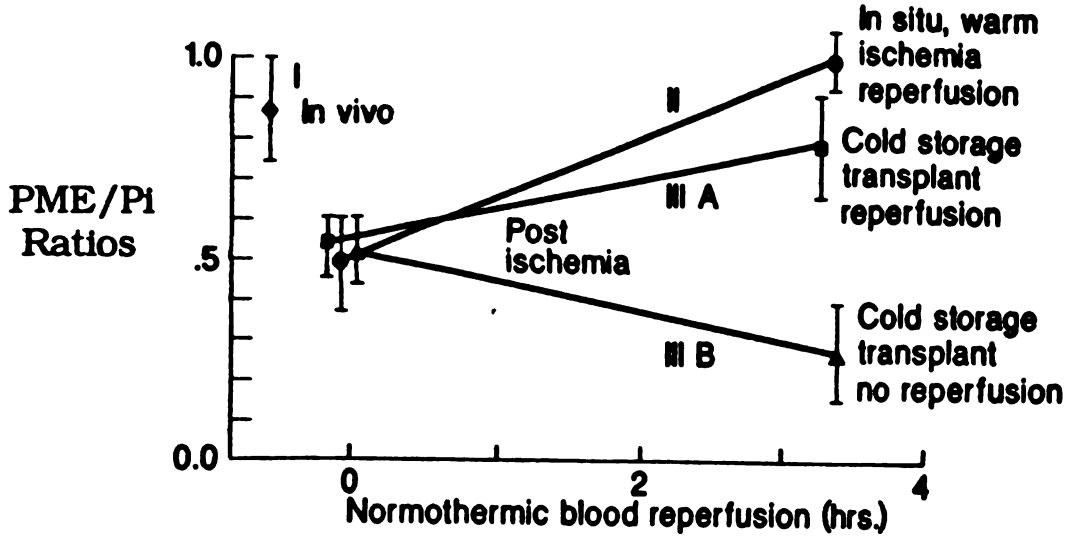

Figure 6. Graphic display of the changes in renal PME/Pi ratios before and after 4 hours of reperfusion following either 45 minutes of warm ischemia or 24 hours of hypothermic storage.

ratio returned to control levels with evidence of regeneration of ATP and other metabolites. Collectively, the eight successful transplant kidneys had a mean PME/Pi ratio of 0.54 ± 0.08 after 24 hours of cold storage ischemia; this ratio increased to 0.88 ± 0.15 after 4 hours of reperfusion. However, in the seven kidneys which were not adequately perfused, the mean PME/Pi ratio decreased from 0.56 ± 0.08 after 24 hours of cold storage to 0.28 ± 0.12 4 hours after transplantation (Figure 4).

Plotting the results of all 33 kidneys, we found that, after each period of ischemia, the PME/Pi ratio in all groups decreased to approximately 0.50 (Figure 5), with no significant difference noted among these groups. After adequate reperfusion, the PME/Pi ratios returned to normal values (associated with adequate urine production), with no significant differences from control levels; after inadequate perfusion, PME/Pi ratios decayed significantly ($p<0.001$) to nonviable levels (Figure 6).

Discussion

Prior to this study, ^{31}P NMR had not been used to study renal metabolism pre- and post-transplantation. However, Sehr and Radda studied a rat surgical model that approximated a renal transplant (4). In their preparation an intact rat kidney was cold-stored for 1 hour and then perfused by blood mechanically pumped through plastic cannulas from a live assist rat. In their study, ATP reappeared in the ^{31}P NMR spectra within 30 minutes of reperfusion, yet did not return

to control levels. This may have been due to inadequacies in the cannulated-kidney surgical model used by these investigators.

Like Sehr and Radda, we were limited to small sample volumes due to magnet constraints. However, the transplant model we selected was more similar to clinical transplantation. The plastic cannulas, essential to model of Radda and Sehr, can cause microemboli which adversely and irregularly affect reperfusion (5-7). Although we were forced to use invasive biopsies, we had more confidence in our transplant model (especially as to reproducibility) than in the model selected in the previous study.

One goal of this study was to determine if the PME/Pi ratio reflected the return to normal metabolic energy status after renal transplantation. Previous studies have shown that four hours of reperfusion is adequate for the restoration of normal cellular metabolism after 24 hours of cold perfusion. The results of our study demonstrated that the PME/Pi ratios do return to normal values after transplantation. Restoration of normal PME/Pi values were also found for kidneys reperfused after 45 minutes of warm ischemia. Both these results lend further support to the hypothesis that the PME/Pi ratio can be used as an accurate viability indicator.

The validity of this technique was also supported by the behavior of renal PME/Pi ratios during both warm and cold ischemia. The mean PME/Pi ratio after 45 minutes of ischemia was the same as that measured after 24 hours of hypothermic storage (0.50 ± 0.12 and 0.54 ± 0.08 respectively). Since several studies have shown that the degree of ischemic damage is roughly the same in the two cases (8-10), the

results of this study indicate that PME/Pi ratios reflect bioenergetic status despite the type of ischemic insult.

When PME/Pi values obtained in this study are compared with the values presented in the last chapter, no species dependency is found for this ratio during renal ischemia. For example after 24 hours of cold ischemia the mean PME/Pi ratio for rat kidneys was 0.48 $\pm$ 0.14 which is not significantly different from the value determined for canine kidneys under the same conditions (0.54 $\pm$ 0.08). This lack of species dependency (especially if it holds true for humans as well) bodes well for accurate calibrations of this ratio using (and for) any animal model.

In summary, the results of this study support the conclusion of the previous chapter ehich entailed ischemic rat kidneys, that PME/Pi ratios can be used as an accurate indicator of renal viability. This study (in conjunction with the previous study) demonstrated no species dependency between rats and dogs as to renal PME/Pi ratios for a range of ischemia times both warm and cold. It was also shown that PME/Pi ratios in canine renal biopsies return to normal values within four hours after transplantation. Although no conclusions can be drawn as to the utility of ^{31}P NMR in the post-transplantation setting, it appears to be a useful tool for pre-operative assessment of renal viability.

References

1. Bretan PN Jr., Vigneron DB, James TL, Williams RD, Hricak H, Juenemann K-P, Yen TSB, Tanagho EA:

Assessment of renal viability by phosphorus-31 magnetic resonance spectroscopy. J. Urol., 1986;135:866.

2. Downes G, Hoffman R, Huang J, Belzer FO: Mechanism of action of washout solutions for kidney preservation. Transplantation, 1973;16:46.
3. Koretsky AP, Wang S, Murphy-Boesch J, Klein MP, James TL, Weiner MW: ^{31}P NMR spectroscopy of rat organs, *in situ*, using chronically implanted radiofrequency coils. Proc. Natl. Acad. Sci. USA 1983;80:7491.
4. Sehr PA, Radda GK, Bore PJ, Sells RA: A model kidney transplant studied by phosphorus NMR. Biochem. Biophys. Res. Commun., 77:195, 1977.
5. Waugh WH, Kubo T: Development of an isolated perfused dog kidney with improved function. Am J Physiol 1969; 217:277.
6. Nizet A: The isolated perfused kidney: possibilities, limitations and results. Kidney Int. 1975; 7:1.
7. Rosenfeld S, Sellers AL, Katz J: Development of an isolated perfused mammalian kidney. Am J Physiol 1959; 196:1155.
8. Southard JH, Senzig KA, Hoffman RM, Belzer FO: Energy metabolism in kidneys stored by simple hypothermia. Transplant. Proc. 1977;9:1535.
9. Calman KC, Quinn RO, Bell PRF: Metabolic aspects of organ storage and prediction of organ viability. In : Organ

Preservation. Edited by D.E. Pegg. Edinburgh: Churchill Livingstone, p. 225, 1973.

10. Fahy GM: Viability concepts in organ preservation. In: Toledo-Pereyra LH, ed. Basic Concepts in Organ Procurement, Perfusion, and Preservation for Transplantation. Academic Press, New York, 1982; 121-158.

Chapter 5: ^{31}P NMR Assessment of Renal Viability in Intact Canine and Human Isolated Kidneys

Purpose

The purpose of the present study is to develop further ^{31}P NMR techniques to assess renal viability. The experiments were specifically designed to: 1) verify the reliability of the PME/Pi ratio as a viability parameter in intact canine and human kidneys; 2) develop NMR coil technology to allow spectroscopic monitoring of canine and human cadaveric kidneys before and after transplantation; and 3) compare the results from implanted and surface coils for post-transplantation renal spectroscopy.

Methods

Canine Studies

Fifteen adult mongrel dogs (20 to 25 kg) were anesthetized with acepromazine, ketamine and pentobarbital, and the kidneys were exposed by a midline abdominal incision. Before dissection of the renal vessels, 20 mg. of furosemide and 500 ml of lactated Ringers solution with 5% dextrose were administered intravenously. Eighteen canine kidneys were subjected to various renal preservation maneuvers:

1) Four normal, well-perfused *in situ* kidneys monitored by an implanted MRS coil.

2) Four *ex vivo* kidneys were immediately attached to vascular cannulas and normothermically perfused, with concurrent monitoring by MRS surface coils.

3) After nephrectomy, four kidneys were immediately cold-flushed with 4^{0} C hyperosmolar lactated Ringer's solution with 5% dextrose and placed in simple hypothermic storage for 24 hours. These kidneys were then transplanted into recipient dogs primed with 40 mg. of methylprednisolone intravenously. Renal transplantations were performed with vascular cannulas, and the kidneys were then monitored using MRS surface coils.

4) Six kidneys were removed, immediately cold flushed with hyperosmotic lactated Ringer's solution and placed in simple hypothermic storage for up to 72 hours. During storage, the kidneys were monitored with NMR surface coils, and renal microcirculation was studied concurrently in two kidneys by nuclear scintigraphy.

Human Studies

Cadaveric kidneys (N=16), provided by Dr. Geoffrey Collins at the Pacific Presbyterian Medical Center, were studied by ^{31}P NMR within 12 hours of harvesting. Post-operative renal function was followed in recipient patients.

^{31}P NMR Studies of Cold-Stored Kidneys

Intracellular phosphorus metabolites were monitored by ^{31}P NMR in whole canine and human kidneys using a home-built, tune-switched MRS coils. Spectra were obtained at 35 MHz on a GE CSI-I spectrometer with a 2-Tesla, 30 cm (horizontal bore),

superconducting magnet. The H_2O proton resonance was used to shim the magnetic field prior to the acquisition of ^{31}P spectra. The spectra were obtained from the Fourier transforms of 400 acquisitions. All peak intensity ratios were obtained using the GE line-fitting program. Statistical analysis was performed using the unpaired Student's *t* test (results expressed as mean $\pm$ S.D.).

^{31}P NMR Studies Using Implanted Coils

The canine kidneys were mobilized and a two-turn, 5-cm diameter ^{31}P NMR coil was placed around the midsegment of the kidney (Figure 1). This coil obtained spectra from approximately 70 cm^3 of isolated renal tissue. The coil leads were brought out through the midline abdominal incision. Before spectroscopy an inflatable cuff was placed around the renal pedicle to induce variable amounts of reversible arterial occlusion. The dog was then placed inside the magnet bore and the kidney was positioned in the center of the magnetic field. Spectra were obtained during normal blood perfusion, during warm ischemia of up to 45 minutes, and during 2-4 hours of reperfusion.

^{31}P NMR Studies of Cannulated kidneys

To assess the spectral contributions of adjacent tissues and fluids, solitary well-perfused kidneys were studied 50 to 100 cm away from the dog's body. Two 100-cm-long (4-mm diameter) perfusion cannulas were connected to the lower aspects of the dog's aorta and inferior vena cava and used to cannulate the renal artery and vein (Figure 2). This surgical model also allows the spectral changes

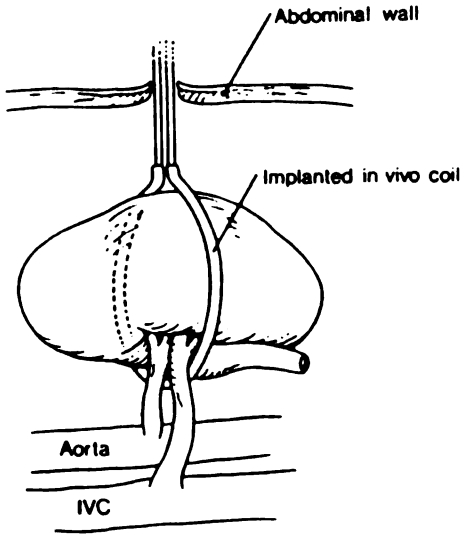

Figure 1. *In vivo* canine kidney with impanted coil.

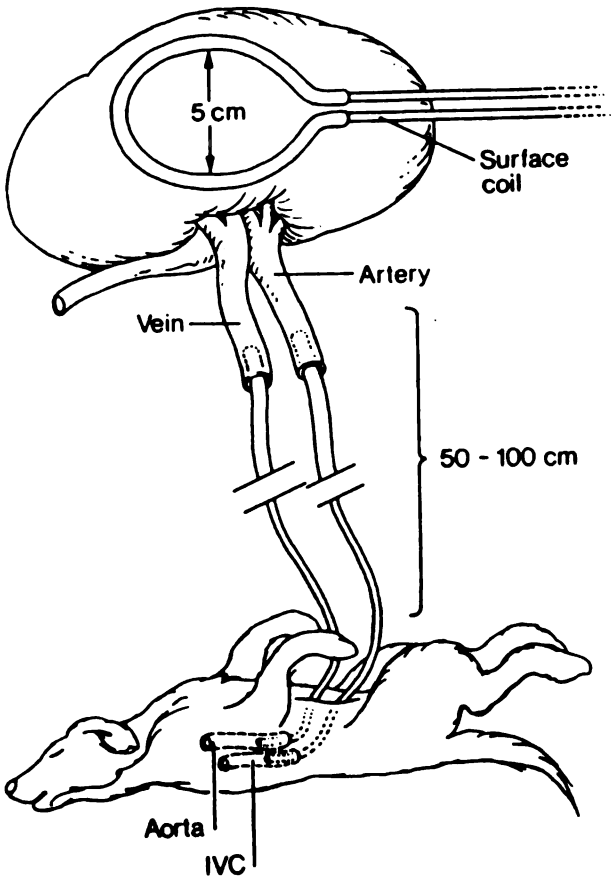

Figure 2. Normothermic blood perfusion apparatus for ^{31}P NMR spectroscopy of extracorporeal canine kidney.

immediately after reperfusion to be monitored by ^{31}P NMR in kidneys subjected to both warm and cold ischemia.

Warm ischemia: Four canine kidneys were removed, cold-flushed to prevent clotting and then connected to the perfusion cannulas within 10 minutes. The kidney was placed in a plastic holder and positioned above a 5 cm-diameter tune-switched (tuneable to either ^{31}P or ^{1}H frequencies) surface coil (Fig. 2). This coil arrangement allowed both accurate shimming and ^{31}P spectra to be obtained from approximately 35 cm^2 of renal tissue. Spectra were obtained during normothermic perfusion, 45 minutes of ischemia (induced by clamping the cannulas) and during one to four hours of reperfusion.

Cold Ischemia: Four canine kidneys were removed, cold-flushed and placed in hypothermic storage for 24 hours before connection to the perfusion apparatus. These dogs were primed with 40 mg. of methylpredisolone intravenously. Spectra were obtained after 24 hours of cold storage and during the four hours of normothermic reperfusion.

Isotopic Microcirculation Studies

Four canine kidneys were removed, cold-flushed and kept at 4°C for up to 72 hours. During this period ^{31}P NMR-monitoring of these intact kidneys was accomplished using surface coils external to the cold-storage containers. The proportion of cortical and medullary renal microcirculation patency was studied concurrently in two kidneys during hypothermic storage by direct infusion into the renal artery of 0.1 to 5 mCi of technetium-99m-labelled macroaggregated

albumin (Tc-MAA) in 10 ml of flush solution at 1, 24, 48 and 72 hours. This technique has been used previously to assess the integrity of renal cortical medullary microcirculation in cold-stored kidneys in an attempt to determine ischemic damage and renal viability (1-3). The renal Tc-MAA was imaged with a Siemans Pho-Gamma IV scintillation camera and the cortical medullary distribution of the albumin particles was assessed visually and by computer analysis. Cortical microcirculation was expressed as a percentage of the total renal circulation.

Human Cadaveric Kidneys

After flushing with Collins 2 solution immediately after harvesting, cadaveric kidneys were studied by ^{31}P NMR during simple hypothermic storage within sterile containers using an external 5 cm-diameter surface coil. Spectra were obtained without removal from or disruption of the sterile storage container or interruption of hypothermia. Total NMR study time was 30 minutes per kidney. The kidneys, when transplanted had 18- to 43-hour storage times. Post-operative renal function was assessed by measuring serum creatinine levels and total urine output in the recipient patients 3 days after transplantation surgery. Postoperative day#3 was chosen so that early rejection would not interfere with viability as measured by renal function.

Results

Representative spectra from *in situ* kidneys showed a complete

loss of visible adenosine triphosphate (ATP) within 45 minutes of warm ischemia, although PME/Pi ratios were still measureable (Figure 3). After 45 minutes of ischemia this ratio decreased from its normal value of 1.0 to 0.50. Thirty minutes of warm ischemia resulted in only a 40% decrease in this ratio. After three hours of reperfusion, the PME/Pi ratio returned to its normal value.

Spectra from the *ex vivo* cannulated kidneys were similar to those obtained for *in situ* kidneys (Figure 4.) Upon attachment to the perfusion apparatus, immediate urine production was noted in all kidneys. The PME/Pi ratios returned to normal after reperfusion. After several hours, however, this ratio along with ATP levels decreased gradually.

Representative spectra of the reperfused kidneys after 24 hours of cold-storage demonstrated the regeneration of ATP and restoration of the control PME/Pi ratio. However, this ratio and ATP levels showed a marked decrease after 3 hours.

Microcirculation studies with Tc-MAA revealed no correlation with viability during 72 hours of hypothermic storage (table 1). The decay rates of PME/Pi ratios in the six canine were consistent with each other and with results obtained in rats in a previous study (4).

The spectral resolution was much better when the *ex vivo* cannulated model was used since motion due to breathing was absent and therefore B_0 homogeneity was also much better. The control *in situ* kidney spectra demonstrated a much higher Pi peak than did the spectra of isolated kidneys. Therefore, it appears that the fluid surrounding the implanted coil contributed to the observed spectra.

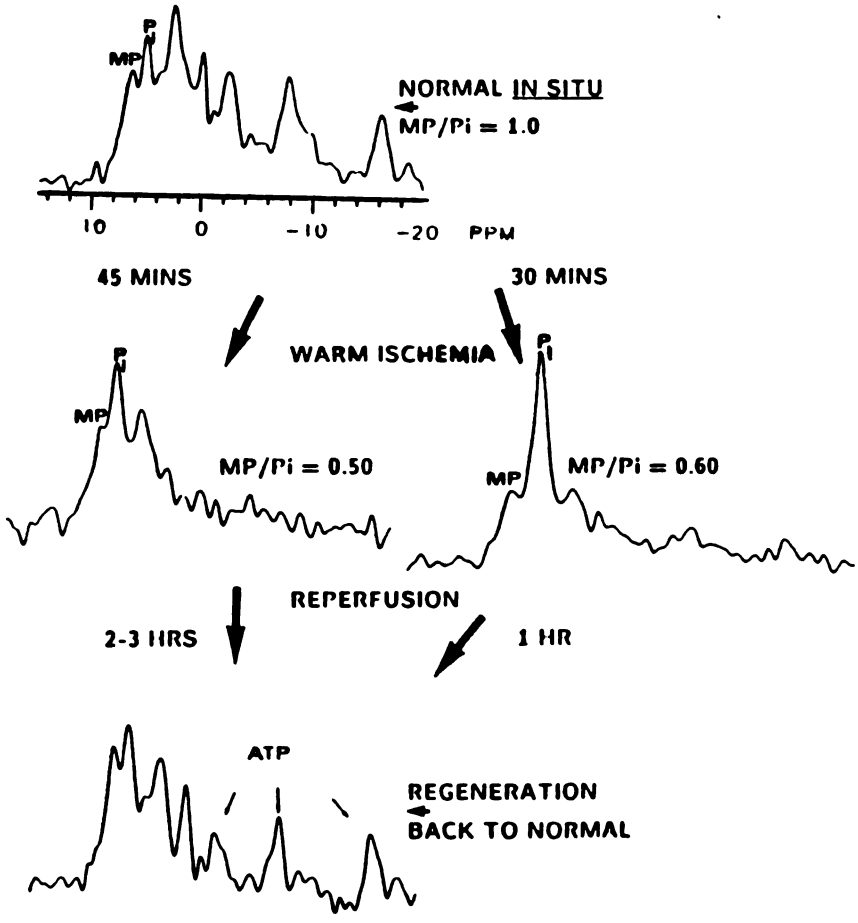

Figure 3. Serial ^{31}P NMR spectra of *in situ* canine kidney subjected to warm ischemia. Peak assignments are as follows: MP = phosphomonoesters (designated PME in text), Pi = inorganic phosphate, ATP = adenine triphosphate (with some contributions from other mobile nucleoside triphosphates)

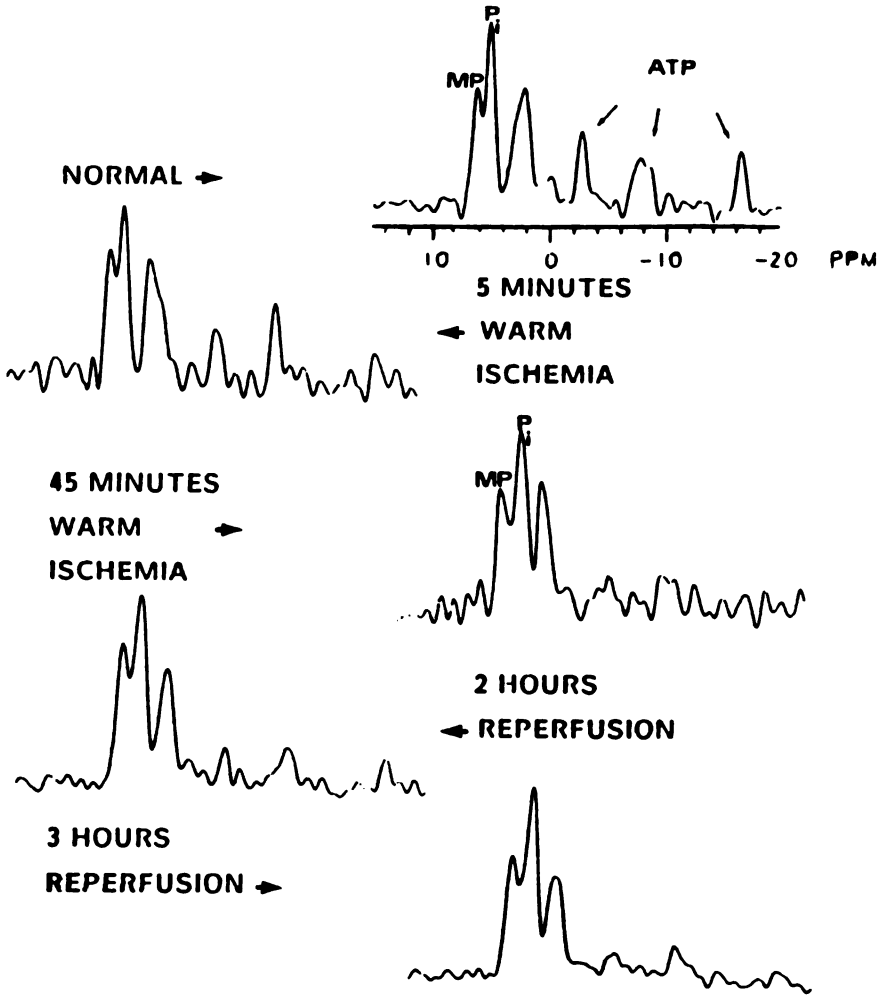

Figure 4. Serial ^{31}P NMR spectra of extracorporeal canine kidney subjected to warm ischemia. Peak assignments are same as in figure 3.

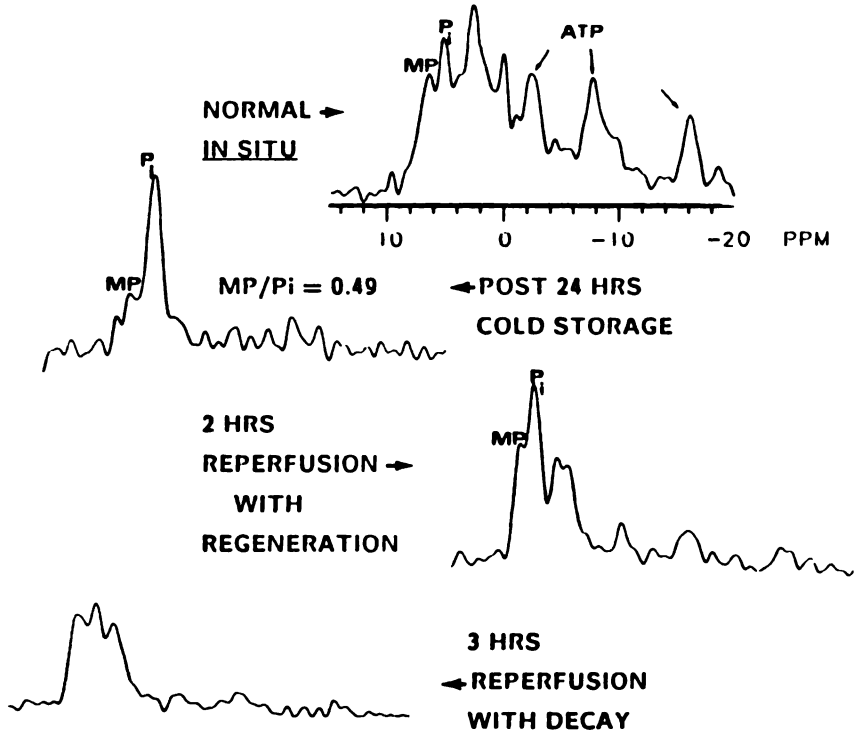

Figure 5. Serial ^{31}P NMR spectra of extracorporeal transplanted canine kidney. Peak assignments are same as in figure 3.

Table 1 Comparison of PME/Pi Ratios with Scintigraphic Determinations of Renal Microcirculation

Cold-storage Time (hours)	PME/Pi Ratios*	TC-MAA % Uptake†
1	1.03 ± 0.06	49.5 ± 9.3
24	0.55 ± 0.04	38.8 ± 2.1
48	0.20 ± 0.01	38.9 ± 3.4
72	0.13 ± 0.01	46.5 ± 4.5

* All PME/Pi ratios were significantly different from each other ($p<0.01$).

† Renal cortical microcirculation expressed as a percentage of the total renal circulation. No significant differences were noted between values.

Table 2 Comparison Between PME/Pi Ratios in Cold-Stored Human Kidneys and Post-Transplantation Renal Function

Viability	PME/Pi Ratios*	Post-transplant 3rd Day Urine Output (ml)	Decrease in Serum Creatinine (mg/dl)
Non-viable n=3	0.37 ± 0.2	<200	None
Viable n=13	0.85 ± 0.08	1,584 ± 693	5.2 ± 3.1†

\- Significant differences ($p<0.05$) were found between non-viable and viable kidneys for all three parameters.

* All PME/Pi ratios were measured by ^{31}P NMR spectroscopy within 3 hours before transplantation.

† Pre-transplantation, 8.6 ± 5.2; post-transplantation, 3.4 ± 2.1.

A total of 16 cadaveric kidneys with adequate follow-up in the recipient patients were studied (table 2). Of these kidneys, three were noted to have low PME/Pi ratios (0.37 ± 0.2) and demonstrated oliguria (<200 ml/day) and azotemia (serum creatinine 9.1 ± 3.0 mg/dl) on post-transplant day #3. The other 13 kidneys had high PME/Pi ratios (0.85 ± 0.08) associated with a urinary output of 1,584 ± 693 ml/day on post-transplant day #3 and a drop in serum creatinine from the preoperative level of 8.6 ± 5.2 mg/dl to 3.4 ± 2.1 mg/dl. Thus, these 13 kidneys were all verified as viable.

Discussion

Although correlations have been drawn between renal viability and the preservation of renal cortical microcirculation (1-3), the results of the present study suggest that Tc-MAA scintigraphy cannot routinely differentiate between viable and nonviable kidneys (Table 1). Therefore, this technique was of no use in the assessment of cadaveric transplant viability during hypothermic storage, and correlations of PME/Pi ratios with this parameter were of little value in assessing the utility of ^{31}P NMR in the pre-transplant determination of renal viability. While both cell swelling (4-6) and vasoconstriction can hinder renal cortical blood flow, the latter, being temporary, does not have a quantifiable relationship with renal viability, which may explain the lack of correlation with progressive ischemic injury. Our results are in agreement with studies that indicate the usefulness of renal perfusion characteristics only lies in screening out wildly aberrant organs since most nonviable kidneys do not show abnormal vascular resistance (7, 8).

In this study, PME/Pi ratios measured for intact canine kidneys responded to both warm and cold ischemia identically to those found for canine and rat renal biopsies (Chapters 3 &4; 9,10). These results lend further support to the accuracy of this method for noninvasive determinations of renal viability and demonstrated the validity of the previous experiments which used renal biopsies instead of intact organs.

The two experimental models employed for ^{31}P spectroscopic monitoring of PME/Pi ratios in post-transplant canine kidneys performed adequately, but each had inherent advantages and difficulties. When a surface coil was used to monitor the extracorporeal kidneys perfused via cannulas, the resulting spectra were higher in signal-to-noise and spectral resolution (than for the other model) due to improved magnetic field shimming for the motionless isolated kidneys. Also, spectra could be obtained immediately before and after reperfusion using this model, instead of the requirement at least 30 minutes between spectral acquisition and surgical manipulations using the other model. The one drawback of this model was that the plastic tubing induced thrombosis and consequently renal parenchymal damage after approximately 2-4 hours of reperfusion. This deficiency, inherent in such perfusion models, has also been reported by other investigators (4-6, 11-13). The implanted coil model did not suffer from this problem, but organ motion associated with respiration created problems for magnetic field shimming, resulting in poorer spectral resolution. Also, fluid would sometimes collect around the kidney and the implanted coil resulting, in some cases, in elevated spectral Pi peaks.

The ^{31}P NMR study of human kidneys prior to transplantation demonstrated an excellent correlation between PME/Pi ratios and post-surgical renal function (Table 2). This study also demonstrated that ^{31}P NMR spectra with sufficient spectral resolution and signal-to-noise ratio could be easily obtained within 30 minutes per kidney without interrupting hypothermic storage or altering organ sterility. Although experimental manipulations of ischemic human kidneys were not possible for obvious reasons, it did appear from the ^{31}P NMR spectra obtained in this study that the decrease in PME/Pi ratios with ischemic duration was similar in degree to that measured for both canine and rat kidneys (Chapters 3-5; 9, 10). This not only lends strong support for the accuracy of the PME/Pi ratio as a viability indicator, but also indicates that calibrations of this ratio with the degree of ischemic damage (and with post-transplant recoverability) performed in animal studies can be used for clinical studies as well.

During this ^{31}P NMR study of human kidneys, certain, albeit rare, clinical situations occurred which demonstrated the medical benefits which this powerful technique could offer if it was readily available to renal transplantation services. Four kidneys were suspected of parenchymal damage and nonviability. Of these, a pair had been harvested from a 12-year-old meningomyelocele patient with a history of urinary tract infections. Usually such kidneys would have been discarded. However, one was found to have a normal (>0.75) PME/Pi ratio as well as demonstrating normal renal parenchyma in MR images. This kidney was transplanted and demonstrated excellent function in the recipient patient. The other kidney, however, was found to have a relatively low PME/Pi ratio (less than 0.50) and was

discarded after MRI revealed moderate dilation of the renal pelvis and ureter and appreciable thinning of the cortex. These findings were verified by gross examination and were consistent with gross reflux and scarring. In a second pair of kidneys, bilateral megaureters were noted during harvesting, but MR images revealed normal parenchyma without calyceal dilation and normal PME/Pi ratios (0.85) were measured. Subsequently, these kidneys functioned well after transplantation. Thus organ wastage was prevented by utilizing MRI and MRS to assess the degree of renal damage.

Although the studies contained in this chapter were not extensive enough in a numerical sense for a clear determination of the accuracy of this technique, they strongly demonstrate the potential of ^{31}P NMR for the clinical determination of pre-transplant renal viability. As the proliferations of clinical MR instruments capable of rapidly providing ^{31}P NMR spectra of cadaveric kidneys continues, the number of studies similar to those presented in this chapter should increase. From these studies a better understanding of the accuracy and applicability of this technique should develop, resulting, I hope, in a clinical utility for the unique information provided by ^{31}P NMR-monitoring of renal metabolite levels.

References

1. McNay JL, Abe Y: Pressure-dependent heterogeneity of renal cortical blood flow in dogs. Circ Res1970;27:571.

2. Miller HC, Alexander JW, Nathan P: Effect of warm ischemic damage on intrarenal distribution of flow in preserved kidneys. Surgery 1972; 72:193.

3. Anaise D, Asari H, Atkins H, Oster Z, Waltzer W, Pollack W, Bachvaroff RJ, Rappaport FT: A noninvasive approach to the assessment of organ viability after kidney preservation in dogs. Transplant Proc 1984; 16:164.

4. Dunn RN, Merkel FK, Roseman D, Haklin M, English K: Is normothermic preservation an alternative to hypothermic preservation? In: Organ Preservation: Basic and Applied Aspects. Edited by Pegg DE, Jacobsen IA, Halasz NA MTP Press, Lancaster 1982; p 273.

5. Waugh WH, Kubo T: Development of an isolated perfused dog kidney with improved function. Am J Physiol 1969; 217:277.

6. Nizet A: The isolated perfused kidney: possibilities, limitations and results. Kidney Int. 1975; 7:1.

7. Fahy GM: Viability concepts in organ preservation. In: Toledo-Pereyra LH ed. Basic Concepts in Organ Procurement, Perfusion, and Preservation for transplantation. Academic Press New York, 1982; 121-158.

8. Foreman J: Prediction of viability of rabbit kidneys preserved by hypothermic perfusion. Cryobiology 1975; 12:231-237.

9. Bretan PN Jr., Vigneron DB, Hricak H, Juenemann K-P, Williams RD, Yen TSB,Tanagho EA, James TL: Assessment

of renal viability by ^{31}phosphorus magnetic resonance spectroscopy. J Urol 1986; 135:866.

10. Bretan PN Jr., Vigneron DB, Hricak H, Juenemann K-P, Williams RD, Tanagho EA, James TL: Assessment of renal preservation by phosphorus-31 magnetic resonance spectroscopy: *in vivo* normothermic blood perfusion. J Urol 1986.
11. Wijk J van der, Rijkmans BG, Kootstra G: Six-day kidney preservation in a canine model: Influence ofa one-to-four-hour *ex vivo* perfusion interval. Transplantation 1983; 35:408.
12. Kulatilake AE: Isolated perfusion of canine and human kidneys. Br J Surg 1967; 54:877.
13. Rosenfeld S, Sellers AL, Katz J: Development of an isolated perfused mammalian kidney. Am J Physiol 1959; 196:1155.

Chapter 6: Assessment of Canine Renal Transplant Viability by ^{31}P NMR spectroscopy

Purpose

The experiments presented in the preceding three chapters established the utility of ^{31}P NMR for determining viability in isolated *ex vivo* kidneys. The purpose of this study was to evaluate the use of metabolite ratios derived by ^{31}P NMR in determining *in situ* post-transplantation renal viability. To accomplish this canine kidneys were transplanted to a subcutaneous pocket so that surface coil ^{31}P NMR spectra could be obtained noninvasively with only minor spatial localization difficulties. The ^{31}P NMR results were subsequently compared to established methods of scintigraphically assessing renal function (1).

Methods

Fourteen adult beagles (15 to 20 kg) were anesthetized with acepromazine, ketamine, and pentobarbital by a protocol approved by the Institutional Committee on Animal Research. The right kidneys were exposed by a midline abdominal incision. Before dissection of the renal vessels, 20 mg of furosemide and 500 cc of lactated Ringer's solution with 5 percent dextrose were administered intravenously.

Kidneys were then removed and immediately cold-flushed with 4^{o} C Collins solution. Renal transplantation was performed by anastomosis to the right common iliac or femoral vessels, with the

kidneys placed in a right lower abdominal subcutaneous pocket. Two groups of transplants (N=10) were autografts so that control spectra and spectra of vascularly compromised kidneys could be obtained without the possibility of immunologic rejection. The occurrence of vascular thrombosis in five autografts was the result of anastomosis to the iliac vessels, requiring the kidney to be brought through a window in the external oblique muscle, causing tension of the renal pedicle. This was prevented in the other autografts and in the allografts (N=4) by either fixing the kidney in place or by anastomosis to the femoral vessels. The allografts were performed so that the spectral effects of rejection could be studied.

All kidneys were transcutaneously monitored intermittently 2-3 times per week during the first week post-transplantation by ^{31}P NMR using a 5 cm surface coil. Some (N=2) functioning kidneys were monitored up to 2 months post-transplantation. Radioisotope renograms were performed after all NMR studies. Renal biopsies were taken at the time of the final ^{31}P-NMR spectroscopy experiments. Statistical analysis was performed with the unpaired student *t* test (results are expressed as mean $\pm$ S.D.).

^{99m}Tc-DTPA Renal Flow and Function

Post-transplant renal flow and function was measured by nuclear scintigraphy using ^{99m}Tc-DTPA (Diethylenetriaminepentaacetic acid) and in a few instances with ^{99m}Tc-DMSA (Dimercaptosuccinic acid). Scintigraphic data were obtained subsequent to each NMR study for direct comparisons. Protocols followed all HEPC (Human and Environmental Protection Committees) guidelines. After intravenous

injection, *in vivo* flow scintigraphy was performed by 3-second scintiphotos for 1 minute, followed by 2-minute sequential scintiphotos for the next 30 minutes in the case of Tc-DTPA, or a single scintiphoto at 4 hours in the case of Tc-DMSA. Renal flow and function was evaluated qualitatively in each case from the scintiphotos.

Histologic Studies

Tissue specimens were obtained from all groups at autopsy and correlated with the findings from ^{31}P NMR and radioisotope renogram studies performed just prior to sacrifice. Tissues were immediately fixed in 10% neutral buffered formalin and subsequently embedded in paraffin. The tissue sections were stained with hematosylin and eosin.

^{31}P NMR Spectroscopy

Spectra were obtained at 35 MHz on a General Electric (CSI-II) spectrometer/imager with a 2-Tesla, 30-cm (horizontal bore) superconducting magnet. Intracellular phosphorus metabolites were monitored transcutaneously by ^{31}P NMR from a 5-cm-diameter surface coil. The spectra were obtained from the Fourier transforms of 200 to 400 acquisitions with a pulse length of 40 microsec, a sweepwidth of 2000 Hz and 4 K data points.

Chemical shifts were referenced (in part per million [ppm] to the phosphocreatine peak and the peak assignments described by Koretsky et al. were used (2). All peak intensity ratios were obtained with the GE line-fitting program.

Transcutaneous localization of the kidney for coil placement was accomplished by palpation. In cases of questionable placement of

surface coils because of postoperative edema, the kidney was localized by ultrasound.

Results

All renal transplants were accomplished without difficulty and intraoperatively all kidneys produced urine.

Good correlation was noted between transplant ^{31}P NMR spectra and renal function, perfusion and overall viability as measured by scintigraphy and histology (Table 1).

Spectra (Figure 1) from the normal control transplants show characteristic ATP, PME, PD and Pi peaks. All control kidneys had excellent flow and function as well as viability, as verified by radioisotope studies (Figure 2) and biopsy evaluation; likewise, ^{31}P NMR-derived PME/Pi (1.32$\pm$0.23) and ATP/Pi (0.90$\pm$0.36) ratios were high. In contrast, all vascularly-compromised autografts demonstrated lack of blood flow and function with Tc-DTPA (Figure 2), histologic evidence of severe ischemia, and gross evidence of venous or arterial thrombosis. Compared to controls, significantly ($p<0.005$) less viability was noted in these kidneys as monitored by low PME/Pi (0.58$\pm$0.30) and ATP/Pi (0.20$\pm$0.13) ratios (Figure1).

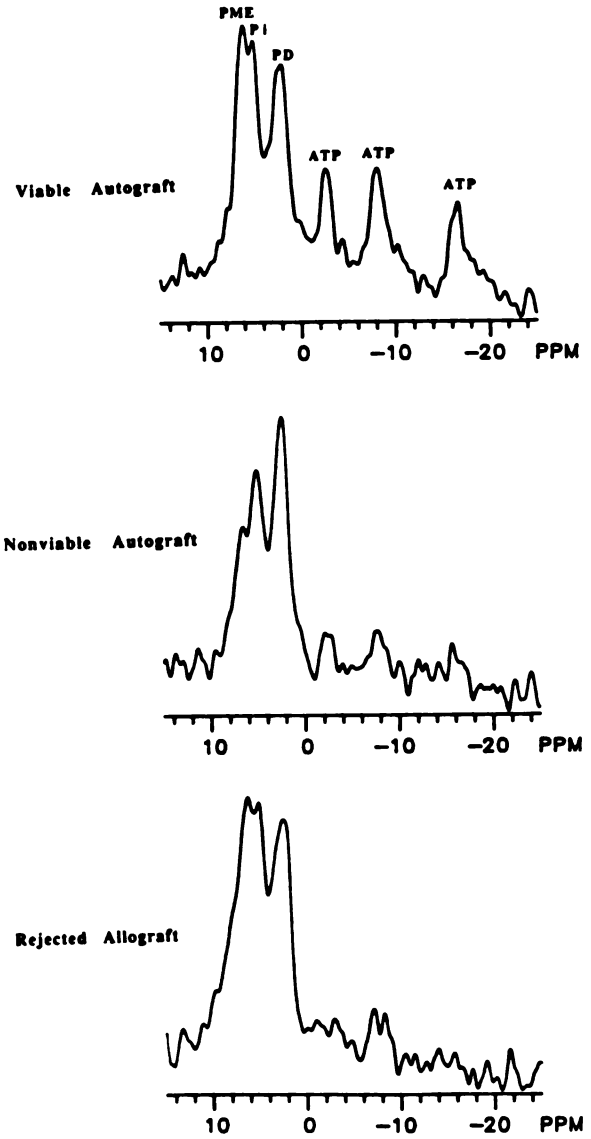

Figure 1. Serial ^{31}P-NMR spectra of viable autograft (A), nonviable ischemic autograft (B), and rejected allograft (C) in *in situ* canine renal transplants with characteristic ATP, PME (phosphomonoesters), PD (phosphodiester) and Pi (inorganic phosphate) peaks.

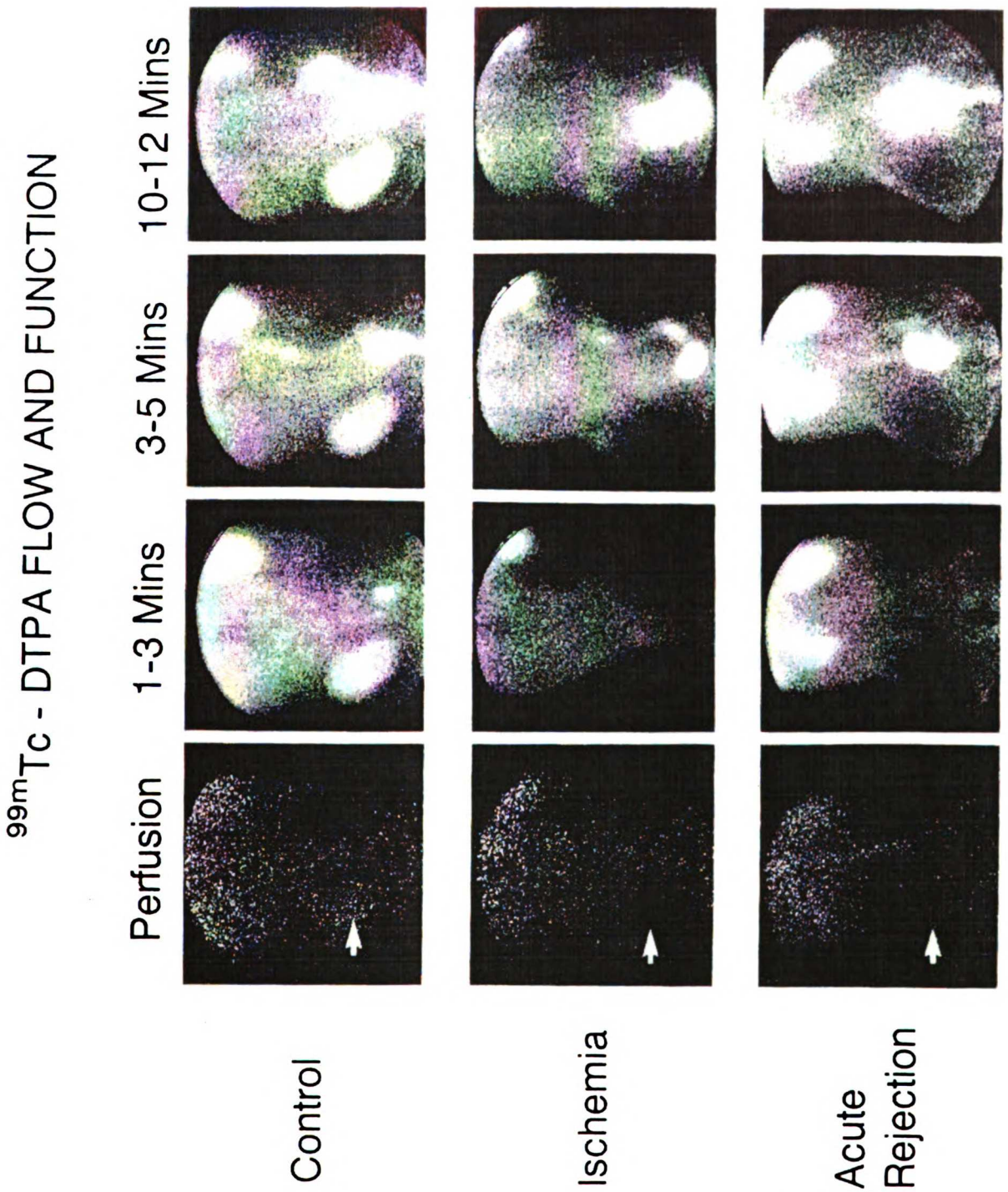

Figure 2. ^{99m}Tc-DTPA renal flow and function studies of normal functioning controls, nonfunctioning ischemic and rejected canine renal transplants. The control study shows prompt perfusion (arrow) to the transplant whereas the ischemia and acute rejection studies show markedly reduced perfusion. Subsequent radiotracer uptake is likewise much worse in the latter two instances. Native kidney uptake and excretion of the radiotracer are present in each study.

TABLE 1
CANINE RENAL ^{31}P NMR CHANGES ASSOCIATED WITH TRANSPLANT VIABILITY

	GROUP	N	^{31}P NMR PME/PI	^{31}P NMR ATP/PI	^{99m}Tc DTPA Renogram	Histology
I.	Autografts Controls	(5)	1.32±0.23	0.90±0.36	Normal	Normal
II	Autografts Nonviable	(5)	0.58±0.30*	0.20±0.13*	No flow or function	Nonviable with severe ischemic changes
III	Allografts	(4)	0.24±0.22*	0.10±0.01*	No flow or function	Acute rejection

*$p < 0.005$ compared to controls

Rejecting kidneys were noted to have absent blood flow by cortical function scintigraphically. Severe vascular damage also was associated with the acute rejection. PME/Pi (0.24±0.22) and ATP/Pi (0.10±0.01) ratios were also significantly ($p<0.005$) Figure 1) less compared to controls, reflecting nonviability. No statistical difference in PME/Pi or ATP/Pi ratios was observed between vascularly compromised and rejected kidney groups.

Discussion

Impaired function in a transplanted kidney may be caused by a variety of processes such as acute tubular necrosis, rejection, cyclosporin toxicity, vascular thrombosis, or ureteral obstruction. The kidney can recover from all of these complications if the metabolic integrity of a sufficient portion of renal cortical and medullary cells is maintained. This chapter presents studies of transplanted kidneys which were either normal in function or completely nonfunctional as a result of vascular thrombosis or acute rejection, respectively. NMR was demonstrated to correlate well with these levels of dysfunction.

NMR parameters denoting renal transplant viability in rats, canines, and humans, have been defined for kidneys during pretransplant hypothermic storage (3-8). It has been shown that ^{31}P NMR preoperative evaluation of cold-stored cadaveric kidneys could differentiate viable from nonviable kidneys -- a finding that can prevent unnecessary waste of organs in clinical transplantation (5,6).

In the present study, ^{31}P NMR was shown to assess intracellular metabolic integrity in individual canine kidneys in situations similar to

the clinical post-operative renal transplant setting in humans. Loss of metabolic integrity is reflected by significant decreases in the ATP/Pi and PME/Pi ratios. Normally functioning transplanted kidneys (as verified by radioisotope flow and function studies) were associated with high ATP/Pi and PME/Pi ratios. Conversely, complete renovascular compromise caused ischemic damage which was reflected by significant decreases in both ATP/Pi and PME/Pi peaks. Similar NMR changes were, however, seen in animals with severe rejection. No significant difference was noted between ^{31}P spectra of autografts with vascular thrombosis and spectra from the rejected allografts. This is probably due to the fact that the cells responded similarly to the ischemic insult, regardless of its cause. Our results also demonstrate similar Pi chemical shift for rejected and ischemic renal transplants, indicating parallels in intracellular pH changes in both cases. This conflicts with results published by Shapiro et al, who found differing Pi chemical shifts for kidneys subjected to ischemia and rejection insults (9). Their three rejected kidneys demonstrated normal intracellular pH and near-normal levels of ATP. This would suggest a minor degree of rejection without global ischemia. In our study, the rejection was severe, resulting in extensive ischemia demonstrated by absence of ATP levels. Therefore, when severe vascular rejection occurs, the resulting ischemia appears to be indistinguishable from thrombotic ischemia.

Whereas PME/Pi ratios were useful for the determination of pre-transplant viability, the ATP/Pi ratios appear to be more useful for the assessment of post-transplantation renal viability. Although PME may represent a precursor energy storage pool for ATP in the kidney, the

exact relationship between these two metabolites is not currently defined; further investigations may clarify their specific interactions in the kidney. Inorganic phosphate is the catabolic product of many reactions. Its concentration increases as cellular bioenergetic status decreases. The increased Pi concentration is probably the main factor affecting the decrease in PME/Pi and ATP/Pi ratios. Metabolite ratios derived from ^{31}P NMR spectra were indicative of renal viability in all kidneys studied (Figure 1), supporting its value in a clinical transplantation setting.

Currently, it is possible to use the same instrument for MRI and NMR (with surface coil). Renal transplant patients can therefore be assessed easily by both imaging and spectroscopy for renal viability. More studies are clearly needed to expand upon these observations, but, at present, it would appear that NMR lacks the specificity to discriminate between severe ischemia and acute rejection.

References

1. Hattner RS, Engelstad BL, Dae MW: Radionuclide evaluation of renal transplants. In: Nuclear Medicine Annual 1984, Freeman, L.M., and Weissman, H.S., eds. Raven Press, New York, 1984, pp 319-342.
2. Koretsky AO, Wang S, Murphy-Boesch J, Klein MP, James TL, Weiner MW: ^{31}P-NMR spectroscopy of rat organs *in situ* using chronically implanted radiofrequency coils. Proc Natl Acad Sci 1983;80:7491.
3. Bretan PN, Vigneron DB, Hricak H, et al: Assessment of renal viability by phosphorus-31 magnetic resonance spectroscopy. J Urol 1986;135:866-871.
4. Bretan PN, Vigneron DB, Hricak H, et al: Assessment of renal preservation by ^{31}P-MRS - in vivo normothermic blood perfusion. J Urol 1986;136:1356-1359.
5. Bretan PN, Vigneron DB, Hricak H, et al: Assesment of clinical renal preservation by ^{31} P-MRS. J Urol, 1987;137:146.
6. Bretan PN, Vigneron DB, Hricak H, et al: Human cadaveric renal viability assessed by ^{31}P-MRS. Proceedings of the Society of Magnetic Resonance in Medicine, Montreal, Canada, 1986, pp 1025-1026.
7. Sehr PA, Bore PJ, Papatheofanis J, Radda GH: Non-destructive measurement of metabolites and tissue pH in the kidney by ^{31}P nuclear magnetic resonance. Br J Exp Pathol 1986;60:632.

8. Sehr PA: A model kidney transplant studied by phosphorus nuclear magnetic resonance. Biochem Biophys Res Commun 1977; :195.

11. Shapiro JJ, Haug CE, Weil R III, Chan L: 31P nuclear magnetic resonance study of acute renal dysfunction in rat kidney transplants. Magn Res in Med 1987;5:346-352.

Chapter 7: The Renal Effects of Complete and Partial Ureteral Ischemia Studied by ^{31}P NMR and Tc-DMSA Scintigraphy

Purpose

In vivo ^{31}P NMR was evaluated as a technique to study the effects of partial and complete ureteral obstruction on the porcine kidney in comparison with renal tubular function as determined by Tc-99m-dimercaptosuccinic acid (Tc-DMSA) scintigraphy.

The purposes of the present study were: 1) to investigate the effect of chronic partial and complete obstruction on intracellular renal metabolism as determined by ^{31}P NMR spectroscopy; and 2) to compare the ^{31}P NMR findings with renal tubular function as measured by *in vivo* Tc-DMSA scintigraphy.

Materials

Animals

For the partial ureteral obstruction experiments, 10 weaned Yucatan micropigs (10.5-14.0 kg) were divided into 2 groups: sham-operated controls (n=4) and obstructed animals (n=6). For the complete obstruction experiments, 17 weaned piglets (7-10 kg) were divided into sham-operated control (n=5) and obstructed (n=12) groups. Micropigs and piglets were chosen as our experimental animals because of their convenient size and, more importantly,

because of the structural and functional similarities of the porcine kidney to the human (1).

Surgical Procedure

Anesthesia was induced in all animals with an intramuscular injection of a mixture of ketamine (22 mg/kg) and xylazine (2 mg/kg) preceded by 0.05 mg/kg atropine, and was maintained with an inhalant anesthetic (1-2% halothane). One kidney from each animal was exposed through a flank incision, and a radiofrequency (rf) coil was placed on the surface of the kidney and fixed in the retroperitoneal space with 2-0 dexon sutures. The wire ends of the coils were brought through a subcutaneous tunnel to the skin on the dorsal aspect of the animal and placed in a subcutaneous pocket. For the partial obstruction experiments, the ureter of all animals (controls and experimental) was isolated, but in the 6 experimental animals a 2-cm, longitudinally slit piece of silicone 16 (5 mm inner-diameter) French tubing was wrapped around a small segment of the middle portion of the ureter. Each end of the slit was then secured with a suture (2). This tubing restricted the ureters to a maximum outer diameter of 5 mm for a length of 2 cm. For the complete ureteral obstruction experiments, the ureter of the 12 experimental animals was ligated at the junction of the proximal one-third and distal two-thirds of the ureter. All animals were maintained on an antibiotic regimen of 30 mg/kg Di-Trim (40mg Trimethoprim and 200 mg Sulfadiazine) intramuscularly once a day for 5 days postoperatively. Presence of hydronephrosis was confirmed by ultrasound after the first week of the study.

Just before sacrifice, 3 control animals were anesthetized, the renal pedicle was isolated and an inflatable cuff was placed around the renal artery to induce ischemia while the kidney was being studied by ^{31}P-NMR.

Coils

Two-turn, 2-cm-diameter copper wire coils, with a 75 pf ceramic chip capacitor soldered near the loops, were affixed to a 3 cm square acrylic plate (3 mm thick) with silicone cement. Copper tape was placed on the backside (away from the coil) of the acrylic square to provide a radiofrequency shield so that spectral contributions from adjacent tissues were negated. The shield, coil and capacitor were then coated with silicone sealant and allowed to dry. The coils were autoclaved before implantation.

^{31}P NMR Spectroscopy

^{31}P NMR spectra were obtained at 2T in a GE CSI-II spectrometer at 24 hours postoperatively, at 1 and 3 weeks of partial ureteral obstruction, and at 1, 2 and 3 weeks of complete ureteral obstruction. Anesthesia was induced and maintained in all animals during spectroscopy experiments as described above. Just before each experiment, the coil wires were pulled out of the subcutaneous pocket and soldered to a balance-matched tuning circuit (3). The animals were positioned in an acrylic cradle and put into the 30-cm-diameter bore of the spectrometer. Before ^{31}P spectral acquisition, the magnetic field homogeneity was optimized by shimming on the water

proton signal until the water proton line-width was 30 Hz or less. A one-pulse experiment with pulse duration of 30 μs, interpulse delay of 3 sec, acquisition time of 512 msec and 200-400 acquisitions, was employed. Exponential line broadening of 20 Hz was used. The GE line-fitting computer program was used to fit each peak of the spectrum to measure peak areas. In this linefitting routine, the parameters (shape, width, amplitude and position) of computer-generated lines were altered until coincidence with the experimental signal was optimized and the absolute intensity of the difference spectrum (experimental minus calculated) was minimized. From the peak areas, the phosphorus metabolite ratios were calculated. The phosphodiester peak can have contributions from urinary inorganic phosphate since its chemical shift is similar to that of the phosphodiesters due to the low pH of the urine (4).

Tc-DMSA Studies

Radioisotopic evaluation of relative renal cortical tubular function was carried out with Tc-DMSA in all animals preoperatively and at weeks 1 and 3 for partial obstruction and weeks 1, 2, and 3 for complete obstruction. Approximately 2 mCi Tc-DMSA was injected intramuscularly and *in vivo* quantitative scintigraphy was performed 4 hours later using a Siemens Pho-Gamma IV scintillation camera with a low-energy all-purpose collimator. These scintiphotos were stored on a DEC 11/34 computer for subsequent region-of-interest quantification over both kidneys after background subtraction. Renal uptake was

expressed as the percentage of total renal function measurable on the obstructed side {[obstructed/(obstructed + nonobstructed)] x 100}.

Pathology

At the conclusion of the study, kidneys from all animals were removed at autopsy and submitted for gross and microscopic histologic evaluation. On gross inspection, kidneys were evaluated for size, parenchymal thickness, presence of scar tissue and dilation of the pelvocaliceal system. The tissues were fixed in 10% neutral buffered formalin and subsequently embedded in paraffin. Tissue sections were then stained with hematoxylin and eosin and submitted for histologic evaluation.

Results

The ^{31}P NMR spectra obtained using the implanted coil method were reproducible and characterized by a small phosphocreatine peak, thus indicating little spectral contribution from adjacent muscles. After subjecting 3 kidneys to complete ischemia by inflating the occluding cuff around the renal artery, all ATP peaks decreased rapidly and were not observable within 5 minutes, demonstrating that the kidney was the source of the high energy phosphorus metabolites observed in the ^{31}P MR spectra.

Partial Ureteral Obstruction

Figure 1 shows representative ^{31}P NMR spectra of control animals and animals after 24 hours, 1 week and 3 weeks of ureteral

obstruction. Table 1 shows selected ATP/Pi ratios during this period of chronic partial ureteral obstruction. The ATP/Pi ratio remained essentially unchanged in the control group during the 3-week experimental period, increasing insignificantly. This ratio did not change significantly during the first week of ureteral obstruction in the experimentally obstructed animals. It did decrease slightly by the third week of the study, but this decrease was not statistically significant. The PD/ATP ratios, although slightly elevated in the obstructed group, did not change significantly in either the controls or the experimental animals.

Table 2 shows relative renal function as evaluated by Tc-DMSA. The total renal tubular function on the operated side in the control animals before coil implantation represents maximum values. In all the controls, the 5-6% reduction observed after coil placement may be due to gamma ray attenuation by the implanted coils, by greater interposed tissue, or by a combination of these factors. The obstructed kidneys showed slightly but not significantly decreased Tc-DMSA uptake at the end of the 1st week, and major functional impairment by the 3rd week of partial ureteral obstruction, when the 74% decrease was highly significant ($P<.0005$).

Macroscopic observations at sacrifice showed that the obstructed kidneys were enlarged, the renal pelves were dilated, the calyces were dilated and blunted, and the renal parenchyma was thinned to approximately 50% of normal. The ureteral lumina were patent, but with a substantial decrease in diameter, indicative of incomplete ureteral obstruction.

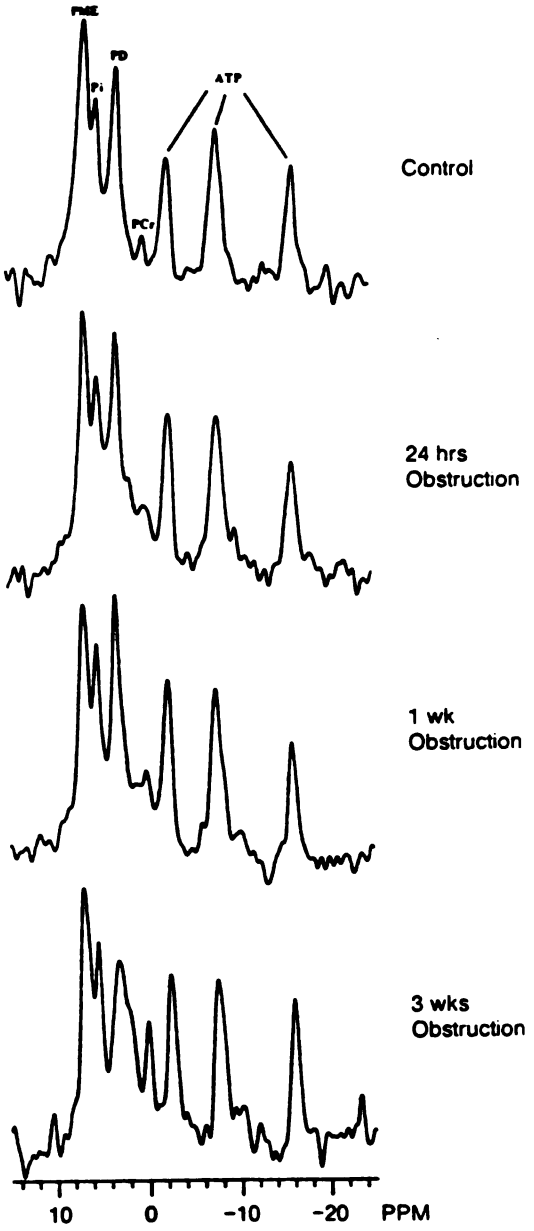

Figure 1. Representative *in vivo* P-31 NMR spectra of control porcine kidneys, and kidneys following 24 hour 1 week and 3 week partial ureteral obstruction. Peak assignments are as follows: PME, phosphomonoesters; Pi, intracellular inorganic phosphate; PD, phosphodiesters with contributions from urine Pi; PCr, phosphocreatine (at 0 ppm); ATP, adenosine triphosphate (with possible contributions from other nucleoside triphosphates).

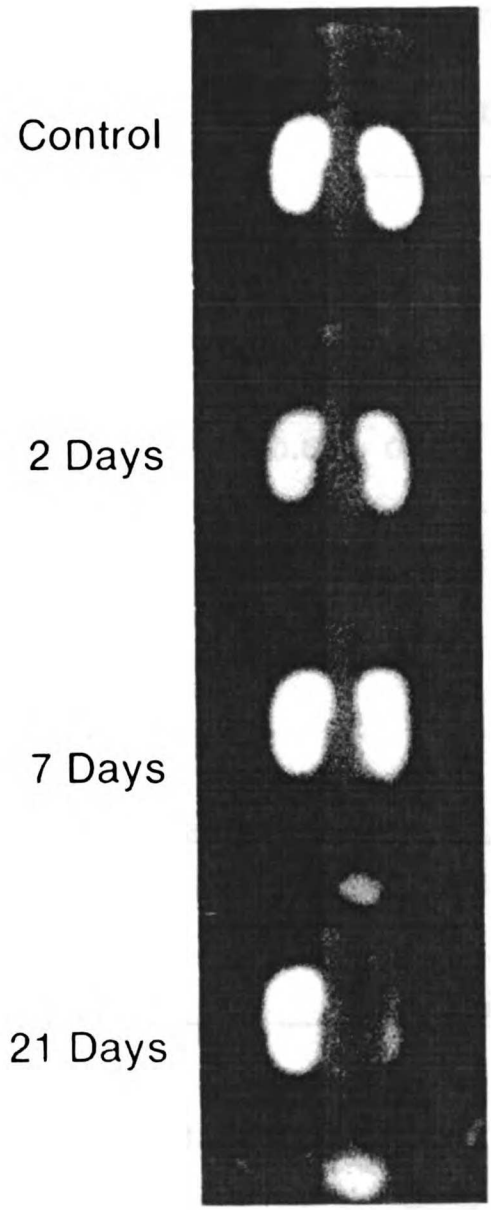

Figure 2. Tc-DMSA scintiphotos showing progressively diminished renal function after partial ureteral obstruction.

TABLE 1: KIDNEY ATP/Pi RATIOS WITH PARTIAL URETERAL OBSTRUCTION

TIME*	CONTROLS	OBSTRUCTED	% DIFFERENCE
24 Hours	0.71 ± 0.07	0.75 ± 0.19	+6
1 Week	0.73 ± 0.22	0.79 ± 0.26	+8
3 Weeks	0.79 ± 0.29	0.64 ± 012	-19

*After coil implantation

Values are mean ± SEM,

TABLE 2: RELATIVE Tc-DMSA UPTAKE DURING CHRONIC PARTIAL URETERAL OBSTRUCTION

Group	TC-99m-DMSA (%)
Preobstructed	50.2 ± 2.2 (n=10) *
1 wk Control	45.6 ± 2.0 (n=4)
Obstructed	39.6 ± 7.9 (n=6)
3 wk Control	44.0 ± 3.0 (n=4)
Obstructed	12.7 ± 1.0 (n=5) **

* Values are mean ± SEM,

** p<.0005 (Student's t-test) between control and obstructed groups

Complete Ureteral Obstruction

Serial MR spectra and Tc-DMSA images from kidneys before and after obstruction are shown in Figures 3 and 4. Values for ATP/Pi ratios and percent uptake of Tc-DMSA are shown in Tables 3 and 4, respectively.

ATP/Pi ratios for the control animals decreased 1 week after coil implantation to 84.1% (standard error (SE)=6.3%) of initial values and remained at this level for the remaining 2 weeks. Animals with ureteral obstruction showed a significant decrease in the ATP/Pi ratio to 69.8% (SE)=3.2%) of their initial values during the 1st week following obstruction; after 2 weeks, this ratio had decreased to 59.1% (SE=3.0%); and after 3 weeks, this ratio was 49.5% (SE=3.4%). Over the 3-week period of ureteral obstruction, ATP/Pi ratios decreased roughly in parallel with the decrease of renal function as determined by Tc-DMSA uptake (Figure 5).

Following ureteral ligation, Tc-DMSA uptake by the obstructed kidney, as a percentage of the total renal uptake, decreased to 39.7 $\pm$ 4.1% at 2 days, 17.3 $\pm$ 5.8% at 1 week, 5.1 $\pm$ 0.91% at 2 weeks and 2.0 $\pm$1.0% at 3 weeks (Figures 4, 5). Renal blood flow, assessed qualitatively in the Tc-DMSA arterial bolus pattern at 2 days and 3 weeks, also revealed deterioration of vascular perfusion during this period.

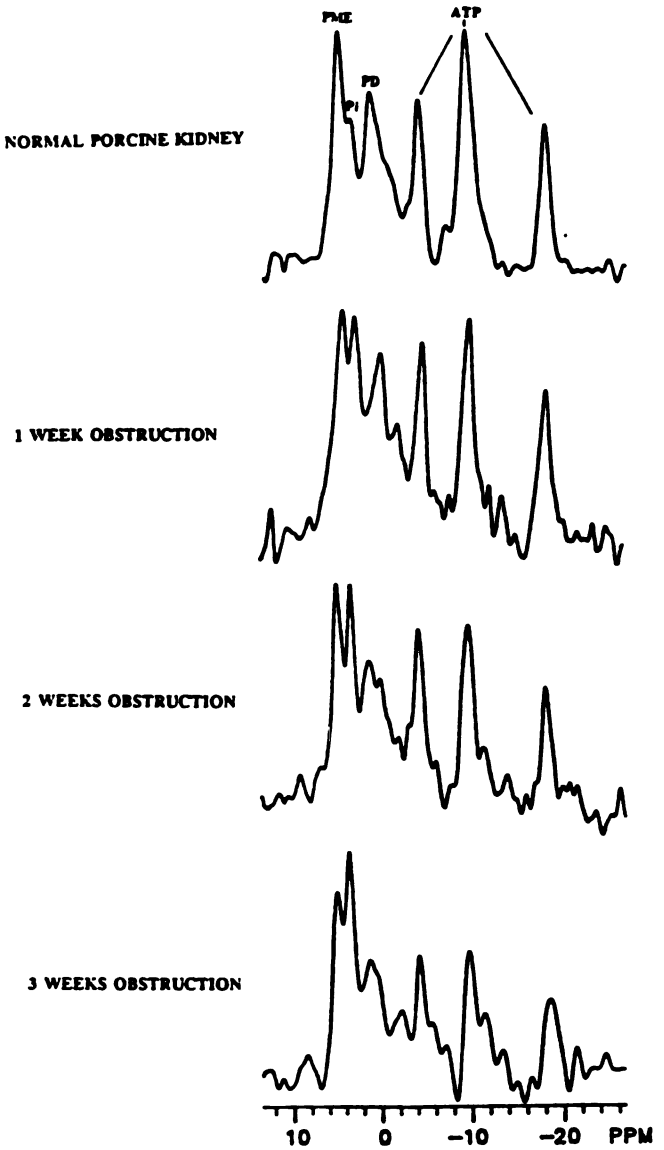

Figure 3 Representative ^{31}P NMR spectra of normal porcine kidneys and kidneys subjected to 1 week, 2 weeks and 3 weeks of complete unilateral ureteral obstruction. The same abbreviations as in Figure 1 were used. Note the relative decrease in ATP peak intensities with increasing duration of obstruction.

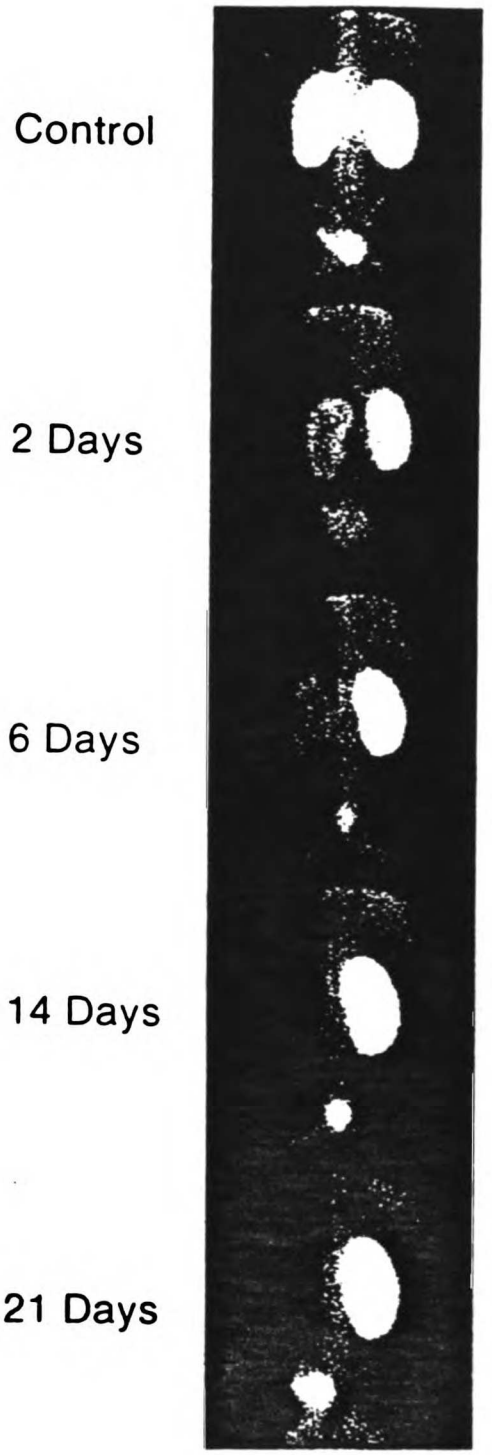

Figure 4. Tc-DMSA scintiphotos demonstrating progressively diminishing renal tubular function following complete ureteral obstruction on the left.

TABLE 3: KIDNEY ATP/Pi RATIOS WITH COMPLETE URETERAL OBSTRUCTION

TIME*	CONTROLS	OBSTRUCTED	% DIFFERENCE
24 Hours	1.27 ± 0.12	1.31 ± 0.12	3
1 Week	0.98 ± 0.07	0.91 ± 0.09	- 7
2 Weeks	0.97 ± 0.06	0.68 ± 0.05	- 30
3 Weeks	1.07 ± 0.15	0.61 ± 0.04	- 43

*After coil implantation

Values are mean ± SEM

TABLE 4: RELATIVE Tc-DMSA UPTAKE DURING COMPLETE URETERAL OBSTRUCTION

GROUP	PERCENTAGE UPTAKE [a]
Controls	44.0 ± 1.2
Obstructed for 2 days	39.7 ± 4.1
Obstructed for 1 week	17.3 ± 5.8*
Obstructed for 2 weeks	5.1 ± 0.9*
Obstructed for 3 weeks	2.0 ± 0.0*

[a] Mean ± standard error

* Statistically significant from pre-obstructed group ($p < 0.001$)

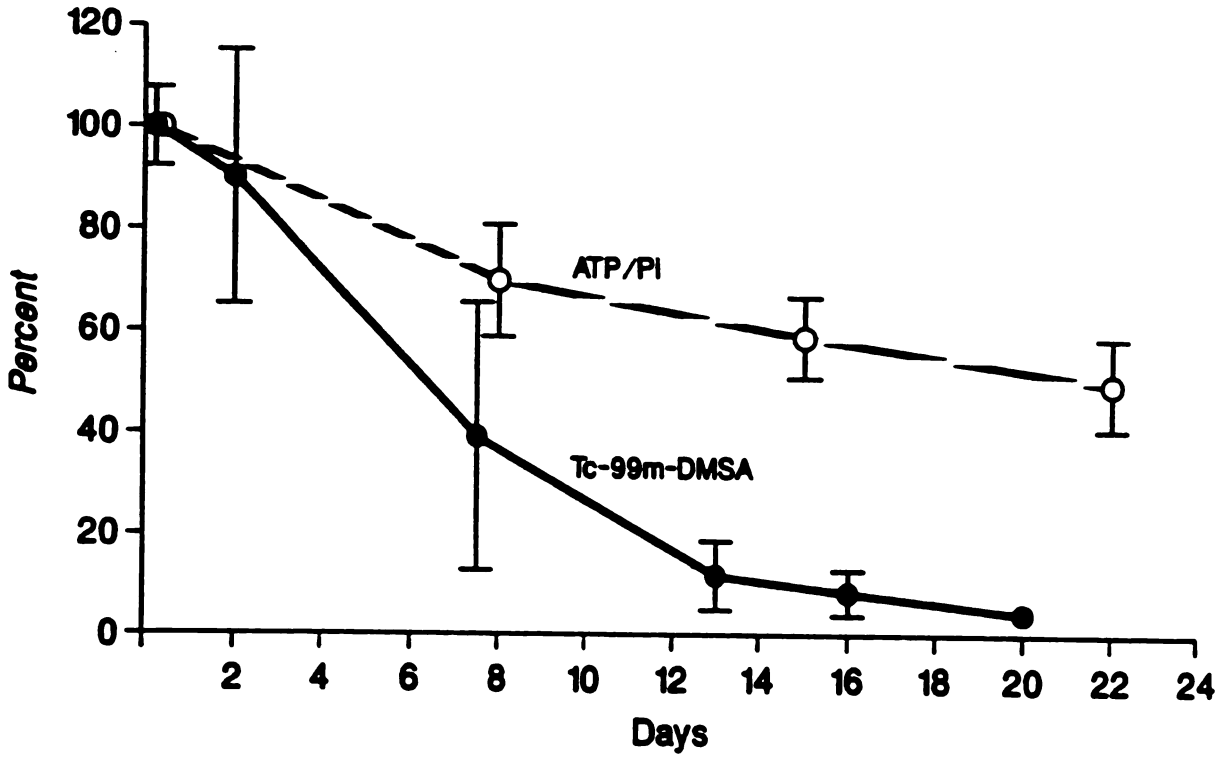

Figure 5. Graphic display of the decrease over time of Tc-DMSA uptake and ATP/Pi ratios: both shown as percentage of initial values.

Gross and histologic examination of control kidneys upon sacrifice revealed completely normal renal cortex, medulla and collecting system. Severe hydronephrosis, consisting of pelvocalyceal dilatation, cortical thinning and evidence of hylanization, was observed in the obstructed kidneys. Their parenchyma contained connective tissue, necrotic distal tubules, proximal tubules with marked atrophy and small oval glomeruli.

Discussion

The impairment of renal function during obstructive nephropathy is manifested by: a) inability of the kidney to concentrate urine; b) decreased capability of acid excretion; and c) eventually decreased renal blood flow, glomerular filtration rate (GFR) and tubular function (5). In the present experiments, the effect of obstruction on renal function was accompanied by certain ^{31}P NMR changes. Secondary reduction of renal blood flow causes renal ischemic changes, thus reducing the ATP/Pi ratio in the obstructed kidney. The dilated intrarenal collecting system of the obstructed kidney allowed a larger urinary volume to be detected by the sensitive volume of the coil, resulting in prominent PD resonance peaks containing substantial contributions from urinary inorganic phosphate (Figure1). Intracellular Pi also seems to accumulate in renal obstruction and appears as a prominent peak in the spectrum of the obstructed kidney, separable from urinary Pi by virtue of the pH-dependent chemical shift.

The bioenergetic state of the kidney, as determined by these selected ^{31}P NMR-derived metabolite ratios, demonstrated only minimal alteration during the 3 weeks of partial ureteral obstruction. A possible explanation for this observation is that the pathophysiologic changes observed in acute, complete ureteral obstruction that result in ischemia and necrosis of renal cells occur only gradually with partial obstruction and, therefore, create a less dramatic renal insult over a 3-week period. Persistent complete obstruction led to a progressive decline in the ATP/Pi ratio, which decreased to 50% of the pre-obstructed level by 3 weeks. This indicates that the ischemic insult is more rapid in onset and more widespread in extent if the obstruction is complete rather than partial.

Relative renal tubular function as evaluated by Tc-DMSA, however, did show a marked and progressive deterioration with partial chronic ureteral obstruction (Table 2). The discrepancy between the ^{31}P NMR and Tc-DMSA data may be explained by the fact that, although the Tc-DMSA uptake depends on renal blood flow and functional integrity of renal tubular cells, ^{31}P NMR spectra will show little or no change in the ATP/Pi ratio as long as viable tissue predominates in the sensitive volume of the coil. The very gradual spread of necrosis through the renal parenchyma may allow impairment or even death and sloughing off of tubular cells without significantly changing the ATP/Pi ratio determined from a large volume of cells. Both renal blood flow (6-13) and functional integrity of renal tubular cells deteriorate in obstructive nephropathy (14, 15). The observations of Wilson (16) after 2 to 4 weeks of partial ureteral obstruction suggest impaired sodium reabsorption. However, since these changes are less

prominent in partial ureteral obstruction, renal cells may still be viable as identified by ^{31}P NMR. With chronic incomplete obstruction, the renal cells may lose their functional properties while retaining those metabolic activities necessary for survival. Although ^{31}P NMR may predict renal viability during obstructive nephropathy, it still remains to be elucidated whether the potential for renal recoverability will correlate with the ^{31}P NMR findings.

It has been suggested that Tc-DMSA uptake may give erroneously high values in the presence of ureteral obstruction because of activity excreted into the urine and accumulated in the renal pelvis (17, 18). However, scintigraphy permited visualization of the renal pelvis in all animal studies, and in no animal was significant pelvic tracer observed at any time after obstruction.

The rate of deterioration in renal cortical tubular function after partial ureteral obstruction is significantly slower than we and others (19, 20) have reported with complete ureteral obstruction. Although this appears to be an eminently reasonable observation, there are in fact few studies in the literature that document changes in renal function after partial ureteral obstruction. Wilson (16) has reported histologic and micropuncture observations in hydronephrotic rats after 2-4 weeks of partial ureteral obstruction, including deterioration of single nephron filtration rate to 76% of normal and of obstructed kidney glomerular filtration rate to 18% of normal. Post-obstructive recovery only approached 46% of normal GFR in the experimental kidney. Stecker et al. (21) found a similar degree of depression of GFR in dogs with a partially ligated ureter. Clearly, the degree and duration of partial obstruction will substantially affect the extent of

functional deterioration. It is extremely difficult to produce an animal model with a fully controllable degree of partial obstruction, as seen in the considerable variability among the individual animals in the present study and as reported by Wilson (16). Nevertheless, the model of partial obstruction reported here in the pig should be extremely important in providing a suitable diversity of degrees of hydronephrotic dysfunction for comparison of NMR with Tc-DMSA regarding their ability to predict functional recoverability.

Partial obstruction produced results that differed from those found for complete obstruction. During 3 weeks of complete obstruction, the ATP/Pi ratio decreased by a factor of 2, whereas the present study demonstrated only a 20% drop after 3 weeks of partial ureteral obstruction. On the other hand, Tc-DMSA uptake dropped by a factor of 25 (to 2% of total renal function) in complete ureteral obstruction but only by a factor of 4 (to 13% of total function) in partial ureteral obstruction. Clearly, renal tubular function, as measured by Tc-DMSA, is quite sensitive to pathophysiologic changes consequent upon obstruction, while the organ-averaged cellular bioenergetic state (ATP/Pi) is not nearly as strongly affected. Therefore, it appears that although ^{31}P NMR could predict post-surgical renal recovery in the transplant setting (22-26) where all cells were exposed to similar ischemic stresses, the utility of this technique in predicting post-surgical recovery for obstructed kidneys is much less clear. After 3 weeks of complete obstruction, only 2% of the total renal tubular function was detected by Tc-DMSA uptake, whereas ^{31}P NMR demonstrated a substantial ATP concentration, indicating a large proportion of viable cells. ^{31}P NMR is limited in that this technique

cannot differentiate between cell types, whereas Tc-DMSA uptake depends on the integrity of vascular perfusion and tubular cells specifically. In this study, the functional integrity of cortical tubular cells as measured by Tc-DMSA scintigraphy decreased much more rapidly after ureteral obstruction than did the organ-averaged bioenergetic status as monitored by ^{31}P NMR. Therefore, it is possible that functional viability and cellular viability are not as closely related for the obstructed kidney as they are for the ischemic pre-transplant kidney.

Nevertheless, there may well be cases where the unique information provided by ^{31}P NMR spectroscopy could be useful in the clinical investigation of ureteral obstruction. For this use, however, the technical aspects of the methodology still need to be improved for application to the clinical setting, because low sensitivity and difficulty in spatial localization for ^{31}P NMR will not currently permit accurate assessment of a small or atrophied kidney in a fully noninvasive procedure. Improvements in spatial localization will be particularly important for the evaluation of fetal and neonatal hydronephrosis, where early surgical intervention may be critical.

References

1. Swindle MM. Comparative anatomy of the pig. Charles River Tech Bull. Wilmington, Massachusetts 1987.
2. Tanagho EA: Surgically induced partial urinary obstruction in the fetal lamb. I. Technique. Invest Urol 1972;10(1):19-24.
3. Murphy-Boesch J, Koretsky AP: An *in-vivo* NMR probe circuit for improved sensitivity. J Mag Res 1984;54:526-532.
4. Koretsky AP, Wang S, Murphy-Boesch J, Klein MP, James TL, Weiner MW: ^{31}P NMR spectroscopy of fat organs, *in situ*, using chronically implanted radiofrequency coils. Proc Natl Acad Sci USA 1983;80:7491-7495.
5. Brenner and Rector: **The Kidney**. Vol II. Philadelphia: W.B. Saunders 1981, pp. 2026-2044.
6. Vaughan ED Jr., Sorenson EJ, Gillenwater JY: The renal hemodynamic response to chronic unilateral complete ureteral occlusion. Invest Urol 1970;8(1):78-90.
7. Moody TE, Vaughan Ed Jr., Gillenwater JY: Relationship between renal blood flow and ureteral pressure during 18 hours of total unilateral ureteral occlusion. Invest Urol 1975;13:246-251.
8. Dal Canton A, Corradi A, Stanziale R, Maruccio G, Migone L: Effects of 24-hour unilateral ureteral obstruction on glomerular hemodynamics in rat kidney. Kidney Internatonal 1979;15:457-462.

9. Hsu CH, Kurtz TW, Rosenzweig J, Weller JM: Intrarenal hemodynamics and ureteral pressure during ureteral obstruction. Invest Urol 1977; 14; 442-445.

10. Lyrdal F, Olin T: Renal blood flow and function in the rabbit after surgical trauma. *Scand* J Urol Nephrol 1975;9:161-168.

11. Stecker JF Jr, Vaughan ED Jr, Gillenwater JY: Alteration in renal metabolism occurring in ureteral obstruction *in vivo*. Surg Gynecol Obstet 1971;133:846-848.

12. Kerr WS Jr: Effect of complete ureteral obstruction for one week on kidney function. J Appl Physiol 1954;6:762-772.

13. Kerr WS Jr: Effects of complete ureteral obstruction in dogs on kidney function. Am J Physiol 1956;184:521-526.

14. Gillenwater JY, Westervelt FB Jr, Vaughan ED Jr, Howards SS: Renal function one week after release of chronic unilateral hydronephrosis in man. Kidney International 1975;7:179-186.

15. Better OS, Arieff AI, Massry SG, Kleeman CR, Maxwell MH: Studies on renal function after complete unilateral ureteral obstruction of three months' duration in man. Am J Med 1973;54:234-240.

16. Wilson DR: Micropuncture study of chronic obstructive nephropathy before and after release of obstruction. Kidney International 1972;2:119-130.

17. Bingham JB, Maisey MN: An evaluation of the use of ^{99}Tc-m-dimercaptosuccinic acid (DMSA) as a static renal imaging agent. Brit J Radiol 1978;51:599-607.

18. De Maeyer P, Simons M, Oosterlinck W, De Sy WA: A clinical study of ^{99m}Technetium dimercaptosuccinic acid uptake in obstructed kidneys: Comparison with the creatinine clearance. J Urol 1982;128:8-9.

19. Taylor A Jr, Lallone R: Differential renal function in unilateral renal injury: Possible effects of radiopharmaceutical choice. J Nucl Med 1985;26:77-80.

20. Schelfhout W, Simons M, Oosterlinck W, De Sy WA: Evaluation of ^{99m}Tc-dimercaptosuccinic acid renal uptake as an index of individual kidney function after acute ureteral obstruction and desobstruction. An experimental study in rats. Eur Urol 1983;9:221-226.

21. Stecker JF Jr, Gillenwater JY: Experimental partial ureteral obstruction. I. Alteration in renal function. Invest Urol 1971;8:377-385.

22. Bretan PN Jr., Vigneron DB, James TL, Williams RD, Hricak H, Juenemann K-P, Yen TSB, Tanagho EA: Assessment of renal viability by ^{31} phosphorus magnetic resonance spectroscopy. J Urology 1986;135:866-871.

23. Bretan PN Jr., Vigneron DB, Hricak H, Juenemann K-P, Williams RD, Tanagho EA, James TL: Assessment of renal preservation by phosphorus-31 magnetic resonance spectroscopy: *in vivo* normothermic blood perfusion. J Urology 1986;136:1356-1359.

24. Bretan PN Jr., Vigneron DB, Hricak H, Collins GM, Price DC, Tanagho EA, James TL: Assessment of clinical renal preservation by phosphorus-31 magnetic resonance spectroscopy. J Urology 1987;137:146-150

25. Hull WE, Pomer S, Vogt P: High-field 31P-NMR Analysis of Phosphate Metabolites in Excised Rat Kidney:Assessment of Preservation for Transplantation. Sixth Annual Mtg Soc Magn Res Med 1987;1:281.

26. Sehr PA, Radda GK, Bore PJ, Sells RA: A model kidney transplant studied by phosphorus nuclear magnetic resonance. Biochem. Biophys. Res. Comm. 1977; 77:195.

SECTION II: TESTICULAR METABOLIC INTEGRITY

Chapter 8: Introduction to Testicle and Semen Studies

The studies described in the previous section have shown that ^{31}P NMR can be used to assess renal cellular viability. In this section, the use of this technique has been extended to study testicular cellular viability and male fertility. As was true for the kidney, there often arise clinical situations for which determinations of testicular cellular metabolic competence are important for diagnosis, the choice of proper therapy, and for monitoring the response to the treatment.

One fairly clear-cut application of *in vivo* NMR is in the diagnosis of testicular torsion. This injury occurs when the spermatic cord and testis twist along their long axis causing first venous, then arterial obstruction, leading to ischemic necrosis of the testicle (1,2). The ease with which a diagnosis of testicular torsion is made depends greatly on the individual case. When acute scrotal pain is coincident with a high and transverse-lying testicle of an adolescent, the diagnosis of torsion is straight-forward (3). In many cases, however, it is difficult to rule out other causes of scrotal pain and the diagnosis can be very difficult to make (3).

Since patient history and a physical examination are often not adequate, several radiologic modalities have been evaluated for their ability to improve the diagnostic accuracy for testicular torsion. High-resolution ultrasound can provide excellent anatomical detail (4, 5) yet its role in diagnosing torsion appears to be minimal. Ultrasonography of clinical torsion at a time when testicular salvage was possible has

shown changes which were not significantly different from acute epididymo-orchitis (6). Although ultrasound is useful for visualizing the intrascrotal anatomy in patients who might be inadequately examined due to severe pain or a tense hydrocele, use of this modality is rarely helpful in identifying the need for immediate corrective surgery (7, 8). Doppler ultrasound also has not been accurate enough for routine clinical diagnosis of torsion (9-11). The most widely accepted imaging modality for the diagnosis of torsion is the testicular radionuclide scintiscan (12, 13). Decreased radionuclide uptake as compared to the other testicle indicates decreased perfusion (i.e. torsion). Although one study determined a 88% accuracy for scrotal scanning (14), there are drawbacks to the technique. Intermittent torsion, incomplete ischemia, technical inadequacies or mis-interpretation can cause false-negative results. False-positives also occur as a result of any hypovascular scrotal lesion such as an abscess, hernia, hydrocele, hematoma or tumor necrosis. Recently, clinical and experimental studies employing MRI have shown that this modality may allow visualization of spiral distortion of the fascial planes in the spermatic cord above the testis and of the anatomy of the lesion (3, 15). More studies are required before the accuracy of this technique is ascertained.

The diagnosis of testicular torsion can be obvious in some cases, but, in many instances, a diagnosis based on present techniques can be suggestive but not conclusive. Presently, the only universally accepted method to rule out torsion as the cause for an acutely painful scrotum is surgical exploration (16, 17).

The radiologic modalities, mentioned above, determine the presence of testicular torsion by observing anatomical abnormalities or the rate of blood perfusion at the time of the study. Although these techniques can be used to diagnose torsion and even to get a rough idea of its severity, they are indirect methods for determining the degree of cellular ischemic injury and consequently the recoverability of the testicle. NMR techniques are the only methods presently available to measure directly cellular bioenergetic status independent of blood flow or function. In the study presented in chapter 9, ^{31}P NMR spectroscopy was used in a manner very similar to that used to determine viability in the ischemic kidneys (Chapters 3-5). Using this technique the presence of testicular ischemia was very easy to observe due to the resulting absence of ATP resonances. In addition, the decrease of PME/Pi ratios was shown to be indicative of the severity of ischemic metabolic injury. Thus, NMR appeared to be much more informative than any other modality, since the cellular effects were directly measured. No other technique has as great a potential for determining the severity of the ischemic insult, which is the important factor in choosing the proper treatment of this malady. Experimental studies in canines have shown that both the duration and the degree of the torsion influence the severity of the injury (18). Although the techniques which monitor blood perfusion can assess the severity of the torsion at the time of the test (in the best cases), the duration of the torsion can not be directly determined, nor can one determine if the degree of torsion was constant over the duration of intrascrotal pain. Thus, NMR can provide information which cannot be obtained in any other noninvasive manner. There are, however,

drawbacks in implementation of this technique. These include availability of an appropriate MR instrument, time required (approximately 30 minutes), difficulties in placing the surface coil on a painful scrotum, and the difficulty of accurately calibrating PME/Pi ratios with the degree of recoverability. Extensive clinical testing is required to assess the clinical applicability of this promising technique.

The use of NMR in the detection of ischemia and cellular viability had precedence, but the study of the ^{31}P spectral effects of hormonal suppression of spermatogenesis was completely novel. No previous studies of this type exist in the literature. Major changes occur in gene-expression, enzyme concentrations and overall cellular activity after androgen deprivation in testicles. It was, therefore, reasonable to expect that ^{31}P spectral changes would reflect the biochemical alterations after the suppression of hormonal activation in the testes.

The clinical need for an accurate noninvasive method of assessing spermatogenesis on the cellular level is clear. Despite investigations involving hormonal assays and cytologic and biochemical analysis of ejaculate, invasive biopsies are often required to determine the presence and cause of male infertility (19). These biopsies are undesirable both because it is an invasive, tissue-destroying technique and because biopsies may contribute to infertility by increasing serum titers of antispermatozoal antibodies (20, 21). Chapter 9 contains a study of ^{31}P NMR spectral changes accompanying 6 weeks of hormonally induced suppression of spermatogenesis. This study was

designed to determine whether ^{31}P NMR could be useful as a noninvasive indicator of the status of spermatogenesis.

In chapter 10, another study designed to use ^{31}P NMR to assess male infertility is presented. In this study, however, the spectra were obtained from human ejaculates not testicular cells. A previous study indicated that ^{31}P NMR could be used to assess epididymal function by monitoring the seminal concentration of glycerophosphocholine (GPC)(22). This phosphodiester is secreted in high concentrations by the epididymis, where the sperm gain motility; becoming fully functional (23, 24). It is presumed that the lack of GPC is indicative of poor epididymal function resulting in non-motile sperm. The previous study did not include many infertility patients, and its conclusions were vague as to the accuracy of this test. Our study (chapter 10) does address the clinical applicability of this technique with thirty semen samples from normal volunteers, infertility patients and vasectomy patients.

References

1. Mikuz G: Testicular Torsion: Simple grading for histologic evaluation of tissue grading. Appl Pathol 1985; 3:134-139.
2. Ransler CW III, Allen TD: Torsion of the spermatic cord. Urol Clin North Am 1982; 9:245-250.
3. Workman SJ, Kogan BA: Old and new aspects of testicular torsion. Seminars in Urology 1988 (in press).
4. Krone KD, Carroll BA: Scrotal ultrasound. Radiol Clin North Am 1985; 23:121-139.
5. Hricak H, Lue T, Filly RA, et al: Experimental study of the sonographic diagnosis of testicular torsion. J Ultrasound Med 1983; 2:349-356.
6. Bird K, Rosenfield AT, Taylor KJW: Ultrasonography in testicular torsion. Radiology 1983; 197:527-534.
7. Arger PH, Mulhern CB, Coleman BG: Prospective analysis of the value of scrotal ultrasound. Radiology 1981; 141:763-766.
8. Fournier GR Jr, Laing FG, Jeffrey RB, et al: High resolution scrotal ultrasonography: Highly sensitive but non-specific diagnostic technique. J Urol 1985; 134:490-493.
9. Rodriguez DD, Rodriguez WC, Rivera JJ, et al: Doppler ultrasound versus testicular scanning in the evaluation of the acute scrotum. J Urol 1981; 125 343-346.
10. Haynes BE: Doppler ultrasound failure in testicular torsion. Ann Emerg Med 1984; 13:1103-1107.

11. Hardwick WC: Letter to the Editor re ref above. Ann Emerg 1985; 14:1243-1244.

12. Smith SP, King LR: Torsion of the testis: Techniques of assessment. Urol Clin North AM 1979; 6:429-443.

13. Holder LE, Melloui M, Chen D: Current status of radionuclide scrotal imaging. Semin Nucl Med 1981; 11:232-249.

14. Lutzker LG: The fine points of scrotal scintigraphy. Semin Nucl Med 1982; 12:387-393.

15. Landa HM, Gylys-Morin V, Mattery RF, et al: Early detection of testicular torsion by magnetic resonance imaging. Program of the Section on Urology, 56th Annual Meeting of the American Academy of Pediatrics, New Orleans LA, 1987;43.

16. Cranston DW, Moisey CU: The management of acute scrotal pain. Br J Surg 1983; 70:505-506.

17. Williamson RCN: Torsion of the testis and allied conditions. Br J Surg 1976; 63:465-476.

18. Sonda LP Jr, Lapides J: Experimental torsion of the spermatic cord. Surgical Forum 1961; 12:502-504.

19. Simmons FA. Medical progress. Human infertility. NEJM 1986; 255:1140-1146.

20. Guazzieri S, Lembo A, Ferro G, et al.: Sperm antibodies and infertility in patients with testicular cancer. Urology 1985; 26:139-142.

21. Gorden DL, Barr AB, Herrigel JE, Paulsen CA: Testicular biopsy in man. I. Effect upon sperm concentration. Fertil Steril 1965; 16:522-530.

22. Arrata WSM, Tyler B, and Corder S. The role of phosphate esters in male fertility. Fertil and Steril 1978; 30:329.

23. Mann T, and Mann CL. Male reproductive function and semen. New York, Springer-Verlag, 1981.

24. Turner TT. On the epididymis and its function. Invest. Urol. 1979; 16:311.

Chapter 9: Assessment of Canine and Primate Testicular Metabolic Integrity by ^{31}P NMR spectroscopy

Purpose

This study was designed to evaluate the utility of ^{31}P NMR spectroscopy in the assessment of acute testicular ischemia, vascular integrity, and spermatogenesis. The specific goals of this study were to determine: 1) the feasibility of MR surface coils for noninvasive, transcrotal localization of testicular ^{31}P NMR spectra, 2) the relationship between relative concentrations of phosphorus metabolites and acute testicular ischemia, and 3) if phosphorus metabolite ratios, in any way, reflect the status of spermatogenesis. To accomplish these goals, *in situ* canine and primate testicles were studied and the metabolite ratios derived from ^{31}P NMR spectra were correlated with the duration of complete ischemia and with established testicular histologic parameters.

Materials and Methods

Testicular Assessment

Eight adult, conditioned, mongrel dogs (20-25 kg) and two monkeys (Macaca cynomulgus, 6.5 kg) were anesthetized with acepromazine, ketamine, and/or pentobarbital. Subsequently, 16 canine and four primate testicles were subjected to various manipulations and monitored by ^{31}P NMR spectroscopy.

Normal, well-perfused, *in vivo* canine testicles (n=8) served as controls. A biopsy of each testicle was performed immediately after NMR spectroscopy for histologic correlation. To assess the contribution of overlying scrotal skin and dartos muscle to the testicular NMR spectra, a fully relaxed spectrum (TR=15 sec), obtained with the coil placed on the scrotum, was compared with a spectrum from a surgically exposed testicle in the same animal.

Complete warm ischemia was induced in eleven *in situ* canine testicles by clamping of the spermatic cord for up to 9.5 hours. ^{31}P NMR spectroscopy was performed sequentially during this period. Biopsies of selected testicles (n=4) were performed at 0, 2, 4, and 6 hours of testicular ischemia to correlate histologic changes with acute ischemia. In two testes subjected to 3 or 6 hours of warm ischemia, the spermatic cord clamp was released and the testicles were reperfused for 2.5 hours to assess post ischemic acute viability.

Spermatogenesis was suppressed in 4 canine and 4 primate testicles by weekly intramuscular injections of 0.5 mg estradiol benzoate and 400 mg testosterone enanthate dissolved in sesame oil; these compounds are known to be effective gonadotropin inhibitors in canines and humans (1, 2). To verify inhibition of pituitary gonadotropin feedback and suppression of spermatogenesis, biopsies of the testicles were performed after 4 and 6 weeks. Just before biopsy, ^{31}P NMR spectra were obtained for all testicles for correlation with histologic parameters.

Histology

Tissue specimens were obtained from all experimental groups. Control testicles were removed, and histologic examination was performed. Biopsy specimens were obtained from the canine testicles during the previously described ischemic periods. For testicles with suppressed spermatogenesis, biopsy was performed after 4 and 6 weeks of hormone treatment. All tissue specimens were immediately fixed in Zenker solution and subsequently embedded in paraffin. The tissue sections were stained with hematoxylin and eosin and viewed under magnification (x100). Specimens were examined by the pathologist without any knowledge of the clinical history of the animals. The tissues were assessed for the presence of any abnormalities, and the degree of spermatogenesis was rated according to the testicular biopsy score count (3, 4). Sections of seminiferous tubules were assigned a score according to the existence of the following conditions: 10 = complete spermatogenesis, perfect tubules; 9 = many spermatids present but disorganized spermatogenesis; 8 = only a few spermatozoa present; 7 = no spermatozoa but many spermatids present; 6 = only a few spermatids present; 5 = no spermatozoa or spermatids but many spermatocytes present; 4 = only a few spermatocytes present; 3 = only spermatogonia present; 2 = no germ cells but Sertoli cells present; 1 = no cells present in the tubules. A mean score was calculated from the sum of the scores of the individual tubules divided the total number of tubules observed (20 per specimen).

^{31}P NMR Spectroscopy

Spectra were obtained on a GE CSI-II spectrometer/imager with a 2T superconducting magnet with a 30 cm bore horizontal bore. Intracellular phosphorus metabolites from *in situ* canine and primate testicles were monitored with surface coils 1.5 cm (for canines) and 1.2 cm (for primates) in diameter, tuned to 34.6 MHz. The signal was localized to the testicles mainly via coil size and placement. A 180° pulse at the surface was used to negate any spectral contributions from scrotal muscle; this was merely an added precaution since studies with exposed testes demonstrated negligible contributions from the scrotum. Spectral contributions from muscles and/or epididymis would be readily apparent owing to large increases in phosphocreatine (PCr) and phosphodiester (PD) peaks, respectively. Adjustments of coil size or placement eliminated these undesirable contributions.

The acquisition parameters routinely used were a 180° pulse at the surface (10-15 microseconds), 256 acquisitions, 2K data points, a sweepwidth of $\pm$2000 Hz, and a 3 sec interpulse delay. Fully relaxed spectra (delay of 15 sec) were also obtained to obtain the T1 saturation factors due to the 3 second interpulse delay. All ratios were then corrected by these saturation factors.

Chemical shifts were referenced in parts per million (ppm) to the PCr peak. All peak intensity ratios were obtained using the GE line-fitting routine.

Statistical analysis of the data was performed with the unpaired Student *t* test.

Results

Spectra (Figure 1) from the normal control *in situ* canine testicles show characteristically high adenosine triphosphate (ATP) (with some possible contributions from other nucleoside triphosphates) and phosphomonoesters (PME) peaks and much smaller inorganic phosphate (Pi), PD, and PCr peaks. All control testicles had biopsy scores of 10. We found no differences between the localized testicular NMR spectra obtained from *in situ* canine testicles and those from surgically exposed testicles in the same animals (Figure 2).

Spectra with muscle contributions were easily recognized due to the much greater PCr concentration in muscle than in the testis. Also, spectra with epididymal contributions demonstrated a very large PD peak due to the great abundance of glycerophosphocholine in epididymal tissues. Correct coil size and placement resulted in negligible contributions from these tissues.

Spectra (Figure 3) from *in situ* canine testicles subjected to warm ischemia reveal a loss of ATP (as early as 7 minutes) with a slight increase in PME and a large, progressive increase in Pi. In testicles subjected to reperfusion after 3 hours of warm ischemia, ATP was successfully regenerated within 2.5 hours (Figure 4); similar findings were noted in testicles subjected to 6 hours of warm ischemia. Cumulative data (Figure 5) from 11 canine testicles revealed a time-dependant decrease in the PME/Pi ratio from 2.1 to 0.7 during 9.5 hours of warm ischemia. No significant histologic differences were

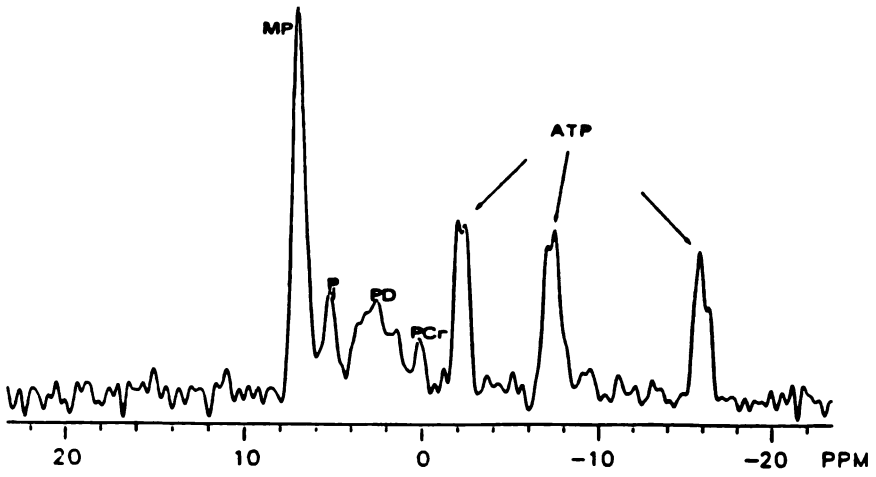

Figure 1. ^{31}P NMR spectrum of the normal canine testicle. Peak assignments are as follows: MP = phosphomonoesters (designated PME in text), Pi = inorganic phosphate, PD = phosphodiesters, PCr = phosphocreatine, ATP = adenosine triphosphate (with possible contributions from other nucleoside triphosphates). Chemical shifts are expressed as parts per million (ppm) relative to PCr.

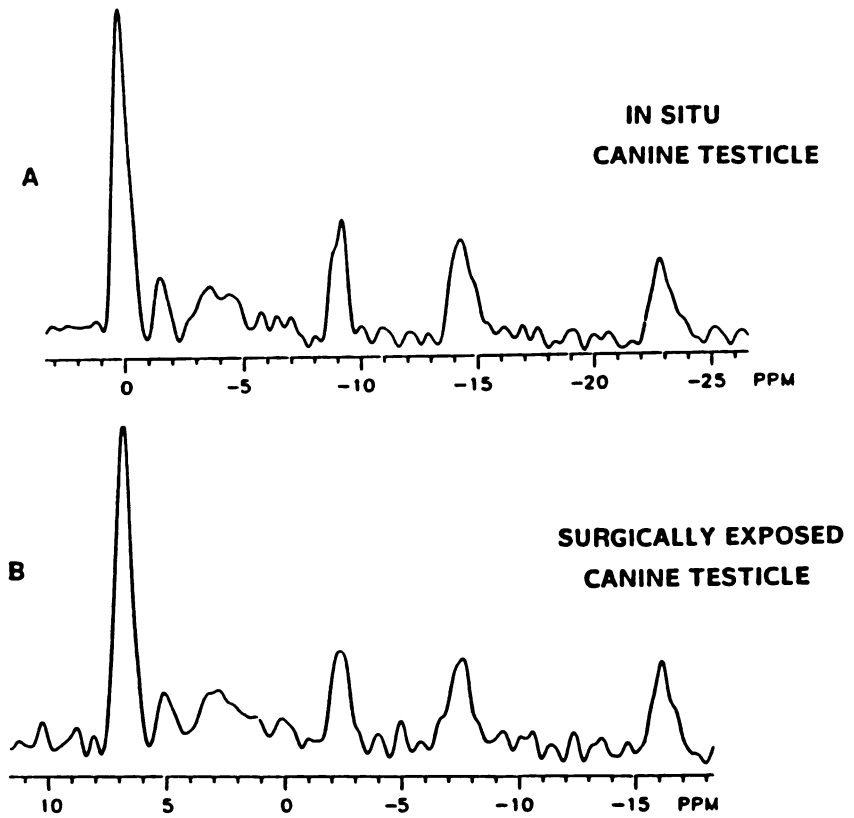

Figure 2. Fully relaxed ^{31}P NMR spectra of a normal *in situ* canine testicle (top) and a surgically exposed normal testicle (bottom).

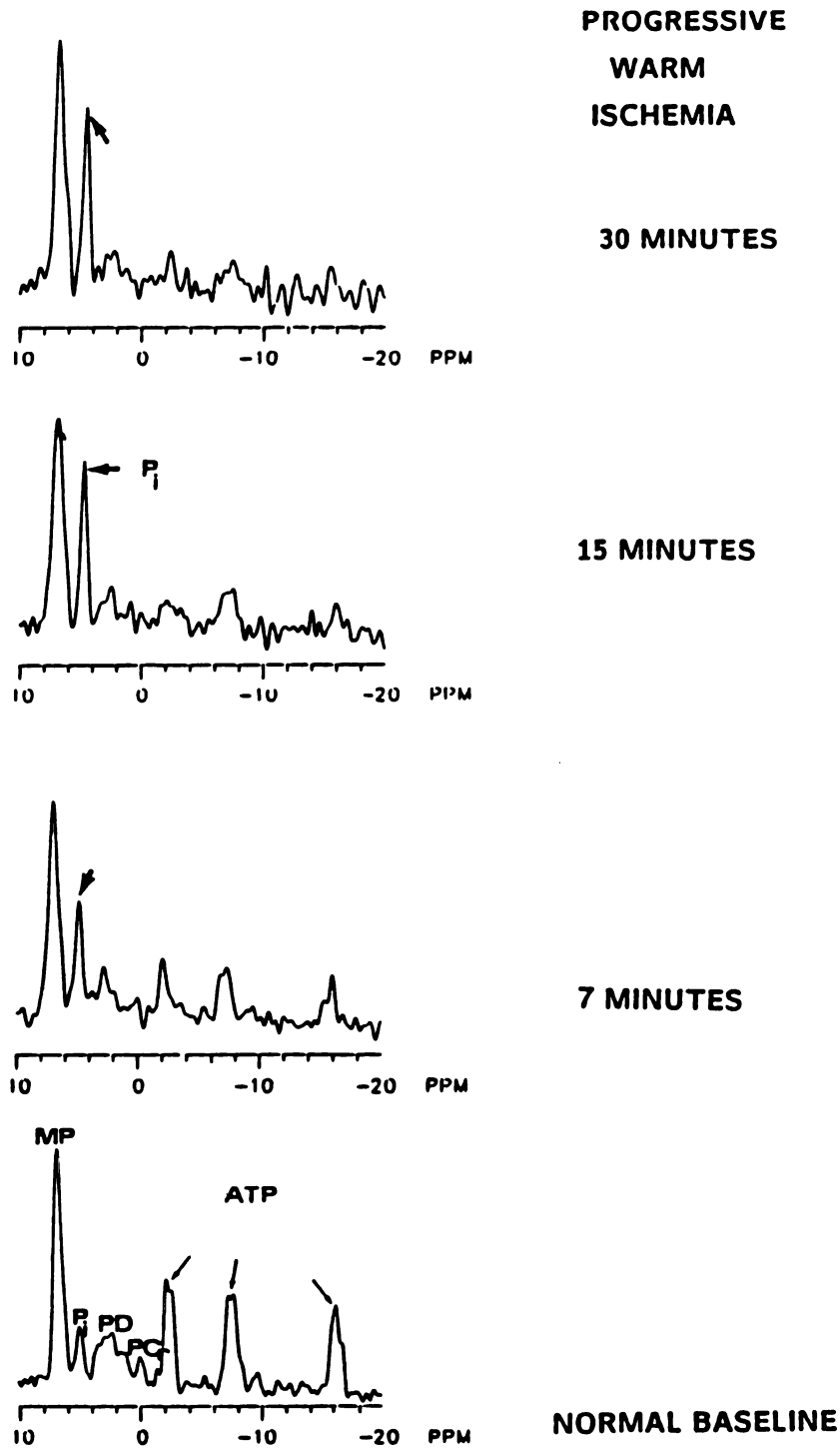

Figure 3. Serial ^{31}P NMR spectra of the effects of progressive warm ischemia on the canine testicle. The same peak assignments as in Figure 1 were used. Note the decrease in ATP resonances and the concomitant increase in Pi.

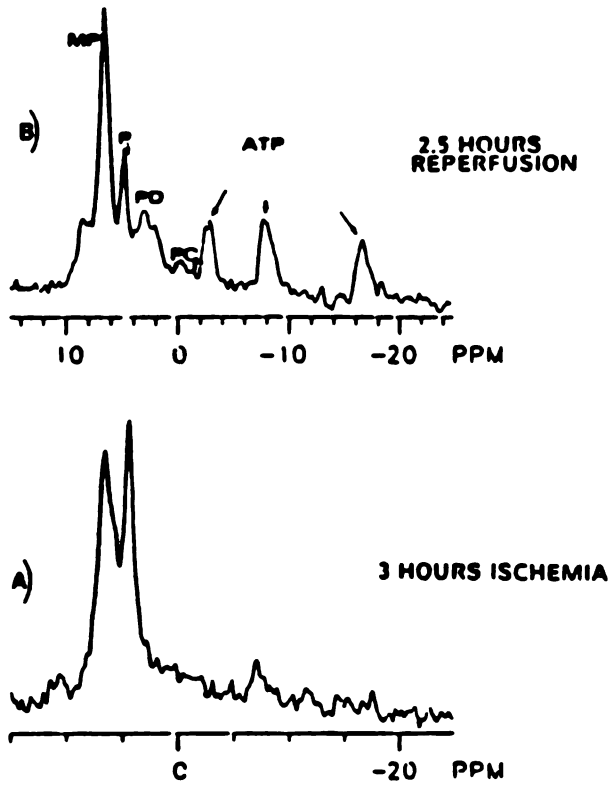

Figure 4. ^{31}P NMR spectra of the canine testicle after 3 hours of warm ischemia (bottom) and after subsequent reperfusion for 2.5 hours (top).

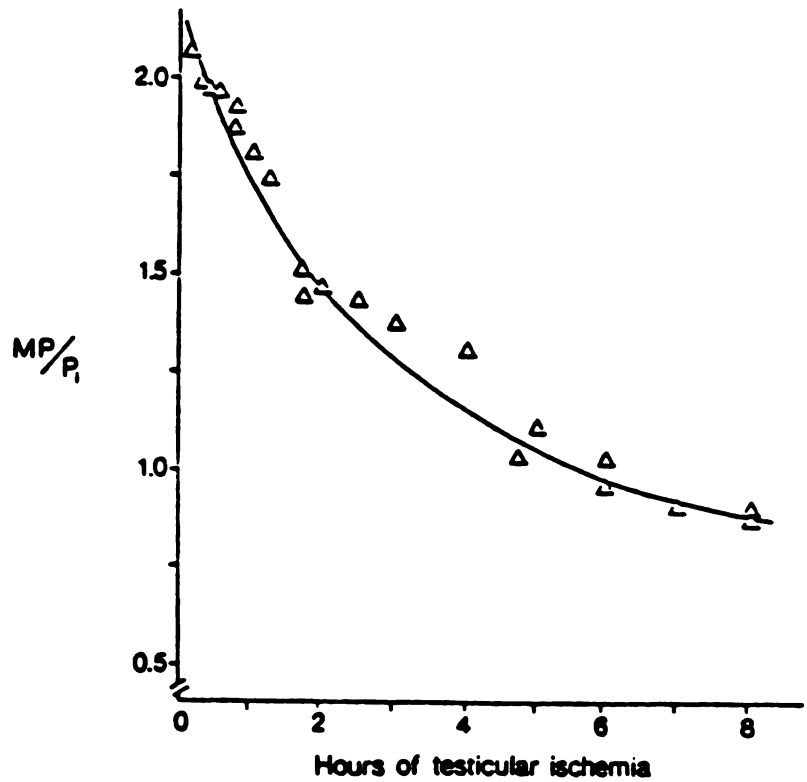

Figure 5. Cumulative data from 11 separate canine testicles monitored with ^{31}P NMR spectroscopy during warm ischemia show a time dependent decay of the phosphomonoester/inorganic phosphate ratio.

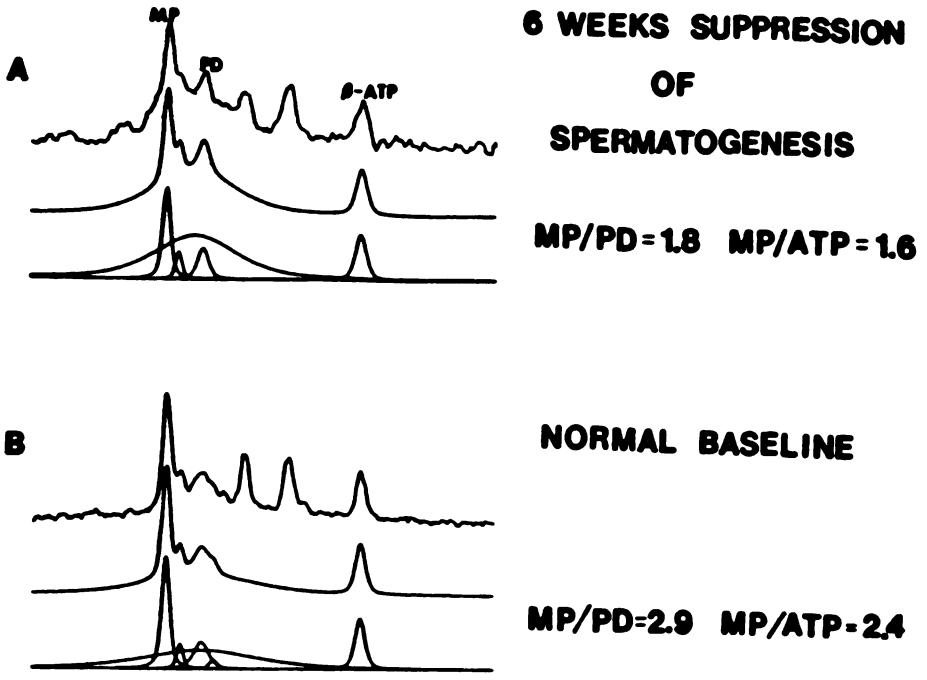

Figure 6. ^{31}P NMR spectra of the canine testicle after 6 weeks of pituitary gonadotropin suppression (top) and the of the normal canine testicle (bottom).

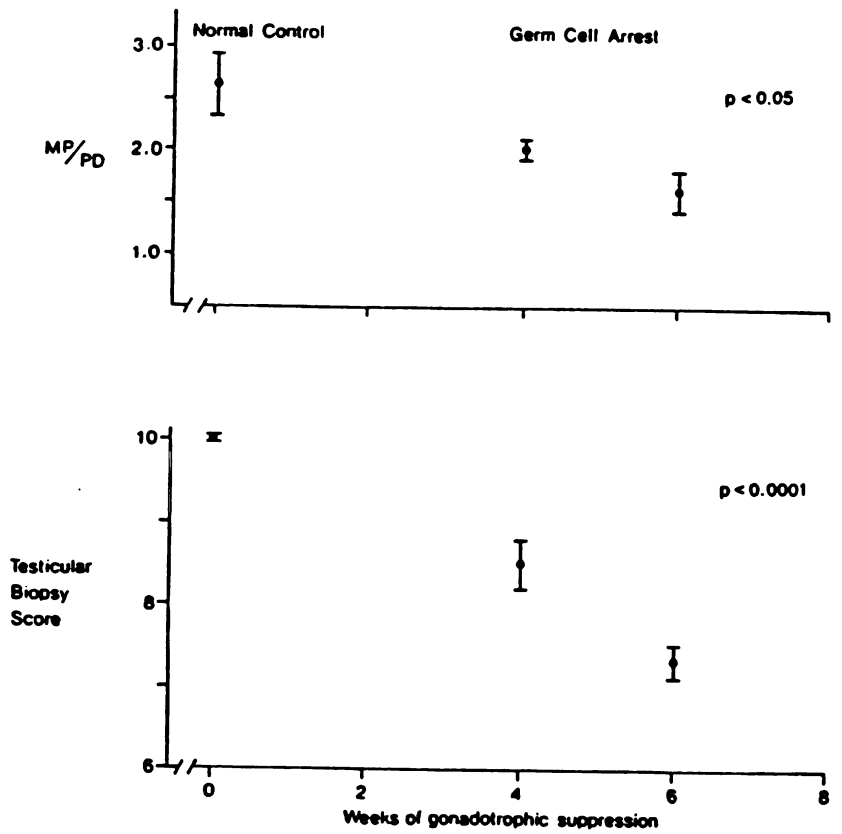

Figure 7. Cumulative data obtained from eight separate testicles during 6 weeks of pituitary gonadotropin suppression monitored with ^{31}P NMR spectroscopy (top) and testicular biopsy (bottom). A significant graded response is noted with both methods.

Table 1. ^{31}P NMR Derived Testicular Metabolite Ratios and Histologic Biopsy Scores - Changes with Suppression of Spermatogenesis

TIME	PME/ATP	PME/PD	BIOPSY SCORE
Initial	2.4 ± 0.2	2.6 ± 0.3	10.0
4 Weeks	1.9 ± 0.4	2.0 ± 0.2	8.5 ± 0.3
6 Weeks	1.8 ± 0.3*	1.6 ± 0.2*	7.3 ± 0.2*

* statistically significant from initial values ($p<0.01$)

noted with spermatogenesis throughout the period of ischemia, nor was there evidence of necrosis.

Serial NMR spectra of canine and primate testicles in which spermatogenesis was hormonally suppressed, reveal an appreciable decrease of PME concentrations and an increase in PD intensities (Figure 6). After six weeks of pituitary gonadotropin suppression, both PME/ATP and PME/PD ratios decreased significantly ($p < 0.01$) as did the testicular biopsy score (See Table 1). There were no significant differences between canine and primate testicles with respect to histology or ^{31}P spectra. No ischemic changes were detected by histology, spectroscopy or by autopsy.

Discussion

A noninvasive method for monitoring testicular metabolism has many potential clinical applications including the assessment of the degree of ischemic insult and of the status of spermatogenesis. This study demonstrates the feasibility of noninvasive transscrotal testicular ^{31}P NMR spectroscopy using a specifically designed surface coil. The signal contributions from overlying muscle and from the epididymis can easily be recognized and eliminated by proper coil placement. In this study, precise localization of the NMR signals to the testis was found to be relatively trivial.

The spermatic cord clamping experiments revealed that ischemia produced a rapid decrease in ATP peak intensities but that ATP remained visible for more than 7 minutes after occlusion of the arterial supply. In most organs, absence of ATP peaks is observed in

^{31}P NMR spectra within 2 minutes (5, 6). This suggests a lower metabolic oxygen demand in the testis. Although ratios involving ATP peak intensities are of very limited use in monitoring the duration and degree of ischemia, the PME/Pi ratio appeared to be quite adequate for quantitating the increase in low energy phosphates; i.e. the decrease in the bioenergetic status of the cells being observed. Both PME and Pi resonances are readily observed, and the PME/Pi ratio decreases in a time-dependant manner that presumably reflects ischemic intracellular damage. Progressive changes in this ratio were measurable during the 9.5 hour period, supporting its value as a clinical tool in assessing ischemic injury in the testicle.

The ability of tissues to regenerate ATP is one of the most consistent indications of acute viability known; shown both from freeze-clamping and *in vivo* NMR studies (7-9). The ATP regeneration, seen after 2.5 hours of reperfusion in testicles subjected to 3 and 6 hours of warm ischemia, is evidence of acute tissue viability and vascular integrity. This may not, however, be predictive of subsequent spermatogenesis and fertility. The testis contains several cell types with possibly different tolerances to hypoxia. The death of only a small number cells could result in impairment of spermatogenesis without substantially decreasing the ATP intensities in the ^{31}P NMR spectra. Nevertheless, the time-dependent decrease of the PME/Pi ratio during 9.5 hours of complete ischemia allows a practical assessment of testicular injury over the range in which the organ is still considered to be salvageable. After 8 hours of complete testicular ischemia caused by torsion, a complete lack of spermatogenesis is expected as well as immunologically mediated

alterations in the non-ischemic testicle (leading to functional infertility) (10, 11). Thus, testicular ischemic injuries equivalent to more than 8 hours of complete ischemia will result in dysfunction. In clinical cases of intermittent or partial testicular torsion, ^{31}P NMR spectroscopy may possibly be used to distinguish between viable and nonviable tissues using PME/Pi ratios. This technique could also be employed to determine whether testicular pain and swelling are caused by torsion or by infection (acute epididymoorchitis; which should not result in diminished intracellular ATP levels).

No species differences were found in the testicular ^{31}P NMR spectra between canines and primates. These spectra differed from those obtained from other organs in mature animals in that the PME peak is by far the most prominent peak in the spectrum. Navon et al. studied murine male reproductive organs via ^{31}P and proton NMR spectroscopy of perchloric acid freeze extracts (12). In our laboratory, freeze extracts from canine testicles have also been studied by NMR (13). In both of these studies, the PME peaks were identified as arising predominantly from phosphocholine, phosphoethanolamine and possibly phosphoserine by chemical shift and pH titration behavior. These compounds are involved in membrane phospholipid synthesis, which is particularly rapid during cell division and growth. High levels of these compounds have also been reported to occur in neonatal brain, neonatal liver, and neonatal kidney but not in fully developed organs (14).

After hormonal suppression of spermatogenesis, no significant change in ATP/Pi ratios was noted. This indicates that, although organ atrophy was occurring, no wide-spread ischemic effects resulted. At

any one time, the percentage of dying cells must have remained small. This suggests that the organ atrophy may have been a result of no new cell synthesis, rather than greatly increased rates of cellular necrosis. These experiments, however, indicate that ^{31}P NMR may be useful to assess the integrity of hormonally controlled spermatogenesis by measuring the PME/ATP and PME/PD ratios. In this study the relative PME peak intensities decreased after hormonal suppression of spermatogenesis. After 6 weeks of suppression, the mean PME/ATP ratio decreased 25%, while the PME/PD ratio decreased 38%. Both of these decreases were statistically significant ($p<0.01$) and were associated with a concurrent significant decay in spermatogenesis as quantified by the decrease in the mean testicular biopsy score from $10.0 \pm$ to 7.3 ± 0.2 ($p< 0.01$).

From these results it appears that the relative concentrations of these phosphorus metabolites is under hormonal control. In the absence of normal hormonal stimulation, the synthesis of the phospholipid precursors which comprise the PME peaks appears to decrease, presumably via control by the Sertoli cell, which serves as a "nurse" cell for the developing germ cells. The observed increase in PD concentration is most likely due to one of two factors. First, and hopefully more probable, is that the observed organ shrinkage caused by cell atrophy and death resulted in an increase in phospholipid degradation products which include the phosphodiesters. Secondly, some of this increase may be due to increased spectral contamination from the epididymis (which contains high concentrations of glycerophosphocholine, a PD) as the testicle atrophied. I took great care, however, in determining the correct size and placement of the

NMR coils and feel that spectral contamination from the epididymis was unlikely in these experiments. This contention is supported by the fact that there was not a great distribution in values for the PME/PD after hormonal suppression of spermatogenesis. One would expect that the contamination would differ greatly from testicle to testicle and from one coil placement to another, but this was not observed in these experiments. Therefore, I feel reasonably confident in proposing that the increase in the PD resonance was due predominantly due to the first explanation. In the phospholipid breakdown process, phosphodiesters are further degraded to yield phosphomonoesters. This may explain why the decrease in the PME peak is not larger than was observed after suppression of spermatogenesis. Although little PME is being synthesized for membrane synthesis, a substantial concentration arises from the phospholipid degradation associated with cellular atrophy. This unfortunately limits the sensitivity and usefulness of this technique since the cessation of hormonally controlled phospholipid synthesis affects two metabolic pathways; one resulting in decreased PME concentration and the other increased PME concentration. Although the increase of PD was associated with decreased spermatogenesis in this study, it would be difficult in a clinical situation to rule out the possibility of the PD peak arising from epididymal spectral contributions, resulting in a false diagnosis. Nevertheless a significant decrease in PME/ATP ratios appears to be a good indicator of hormonally-mediated suppression of spermatogenesis.

In summary, ^{31}P NMR spectral changes were observed after both testicular ischemia and hormonal suppression of

spermatogenesis. The changes associated with decreased spermatogenesis were easily distinguishable from ischemic damage; thus, vascular integrity can be assessed separately from spermatogenesis with the appropriate choice of phosphorus metabolite ratios. Although further investigations are certainly required, the present data suggest that testicular NMR spectroscopy may be useful for evaluating patients in the following clinical situations: (a) In cases where the severity of testicular ischemic damage after torsion is in doubt. (b) When the differentiating testicular torsion from inflammation due to infection is difficult and important. (c) When evaluation of spermatogenesis is required after treatment for torsion. (d) In patients with a varicocele or hormonal abnormalities, ^{31}P NMR may be useful in monitoring post-therapy improvement in spermatogenesis, since semen analysis often reveals minimal and inconclusive changes (3, 15).

References

1. Swerdloff RS, Palcios A, McClure RD, Campfield LA, Brosman SA: Male contraception: Clinical assessment of chronic administration of testosterone enanthate. In: Hansson V, Ritzen M, Purvis K, French FS, eds. Endocrine Approach to Male Contraception. Scriptor, Copenhagen, 1978.
2. Matsumoto AM, Bremmer WJ. Stimulation of sperm production by human chorionic gonadotropin after

prolonged gonadotropin suppression in normal men. J Androl 1985; 6:137-143.

3. Johnsen SG: Testicular biopsy score count: A method for registration of spermatogenesis in human testes-normal values and results in 335 hypogonadal males. Hormones 1970; 1:2-25.
4. Johnsen SG, Agger P: Quantitative evaluation of testicular biopsies before and after operations for varicocele. Fertil Steril 1978; 29:58-63.
5. Koretsky AP, Wang S, Murphy-Boesch J, Klein MP, James TL, Weiner MW: ^{31}P NMR spectroscopy of rat organs , in situ, using chronically implanted radiofrequency coils. Proc. Natl. Acad. Sci. 1983; 80: 7491.
6. Prichard JW, Schulman RG: NMR spectroscopy of brain metabolism in vivo. Annu Rev Neurosci 1986; 9: 61-89.
7. Southard JH, Senzig KA, Hoffman RM, Belzer FO: Energy metabolism in kidneys stored by simple hypothermia. Transplant Proc 1977; 9:1535-1539.
8. Calman KC, Quin RO, Bell PRF: Metabolic aspects of organ storage and prediction of organ viability. In: Pegg DE, ed. Organ Preservation. Churchill-Livingstone, Edinburgh, 1973; 225.
9. Bretan PN Jr., Vigneron DB, James TL, et al. : Assessment of renal viability by phosphorus-31 magnetic resonance spectroscopy. J Urol 1986; 135:866-871.

10. Nagler HM, Deitch AD, de Vere White RW: Testicular torsion: Temporal considerations. Fertil Steril 1984; 42:257-262.

11. Turner TT: Acute experimental testicular torsion: Effect on the contralateral testis. J Androl 1985; 6:65-72.

12. Navon G, Gogol E, Weissenbert R: Phosphorus-31 and proton NMR analysis of reproductive organs of male rats. Arch Androl 1985; 15:153-158.

13. Wendland MF: Personal communication, May 1986.

14. Schmidt HC, Gooding CA, James JL, Gonzalez-Mendez R, James TL: Comparison of *in vivo* ^{31}P-MR spectra of the brain, liver, and kidney of adult and infant animals. Pediatr Radiol 1986; 16:144-149.

15. Al-Juburi A, Pranikoff K, Dougherty KA, Urry RL, Cockett ATK: Alteration of semen quality in dogs after creation of varicoceles. Urology 1979; 13:535-539.

Chapter 10: Assessment of Male Infertility: Correlation Between Results of Semen Analysis and ^{31}P NMR Spectroscopy

Purpose

Previous studies have indicated that the concentration of glycerophosphocholine (GPC) in semen is contributed primarily by the epididymis, the structure in which sperm gain motility, and that the seminal levels of this compound may be a useful indicator of epididymal function and sperm motility (1, 2). The purpose of this study was to investigate the value of ^{31}P NMR-measured seminal GPC levels in assessing male infertility. To do so ^{31}P NMR spectra were obtained from thirty volunteers and patients, and the GPC to total phosphate ratio (GPC/TP) was compared with established semen analysis parameters.

Materials and Methods

Semen Analysis

Ejaculates were obtained from human volunteers after 2 to 3 days of abstinence. Semen analysis parameters established by the World Health Organization (3) were recorded within 1 hour of ejaculation. These were: volume, sperm concentration, total sperm count, percent motile sperm, percent normal morphology, mean progressive motility (0=none, 1=mild, 2=moderate, 3=severe). A

major portion of each specimen was refrigerated (-10°C) for subsequent NMR analysis.

Seven semen samples were obtained from healthy volunteer controls. They all had normal results on semen analysis, had fathered children within the previous 4 years, and were in excellent health.

Twelve semen samples were obtained from patients who had undergone vasectomy. Sperm was not present in any of these samples, consistent with complete surgical occlusion of both vasa deferentia.

Eleven semen samples were obtained from patients presenting to our infertility clinic for evaluation, but who were in otherwise good health. Many of these men were undergoing routine fertility assessment because their wives were infertile, while others had had poor motility scores on prior semen analysis.

Absolute concentrations of GPC were not measured because of the technical advantage of obtaining the concentration relative to total phosphate (TP). The ^{31}P-NMR-derived GPC/TP ratios were correlated with semen analysis parameters.

^{31}P-NMR Spectroscopy

Spectra were obtained at 35 MHz on a General Electric (CSI-II) spectrometer/imager with a 2-Tesla, 30-cm (horizontal bore) super-conducting magnet. ^{31}P NMR was performed on human semen samples using a home-built 1-cm-diameter solenoid coil. The spectra were obtained from the Fourier transforms of 400 acquisitions with parameters chosen to prevent saturation. Chemical shifts were references (in parts per million, ppm) relative to methylene

diphosphonate and the peak assignments described by Koretsky et al. (4) were used. Statistical analysis was performed with the unpaired Student t test.

Results

Characteristic ^{31}P-NMR of semen (Figure 1A) revealed high inorganic phosphorus (Pi) levels relative to GPC and phosphocholine (PC) in a specimen from a fertile control 15 minutes after ejaculation. In the same specimen after 3 hours of ambient storage (25° C), all measurable PC had hydrolysed to Pi and choline (Figure 1B), while GPC levels remained relatively stable. Since the total phosphate (TP) concentration (TP = GPC ± PC ± Pi) is constant (assuming no change in NMR visible phosphate concentration), we standardized all specimens for comparison by using the GPC/TP ratio. Repeat ^{31}P-NMR of selected semen specimens (n=5) after one week of -10°C storage revealed a mean decrease in GPC/TP ratios of 0.01 ± .005, reflecting stability in cold storage.

Semen from the normal volunteers (N=7) showed characteristic GPC/TP ratios of 0.10 ± 0.05, as did semen specimens (n=11) from the infertility clinic patients (Table 1). However, significantly fewer motile sperm ($p<0.001$) and a significantly lower number with normal morphology ($p<0.05$) were noted in the later group. When vasectomy patients' GPC/TP levels (0.05 ± 0.04) were compared with control values, the difference was significant ($p<0.05$) (Table 1 and Figure 2); however, 2 post vasectomy samples did demonstrate GPC/TP ratios in the normal range. An significant difference ($p<0.001$) was also found

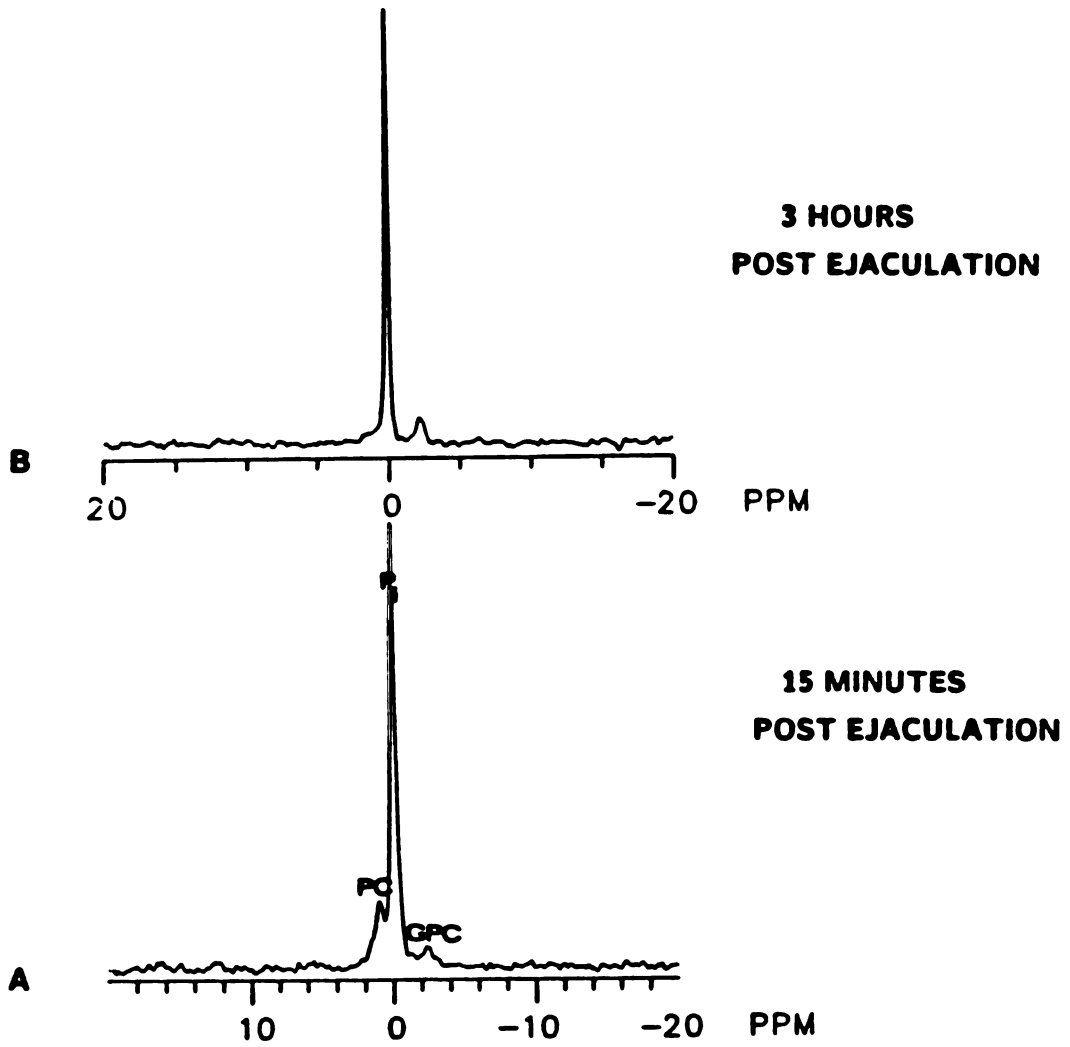

Figure 1. Sequential ^{31}P NMR spectra of a single semen sample from fertile control. (GPC = glycerylphosphorylcholine; PC = phosphorylcholine; Pi = inorganic phosphate.)

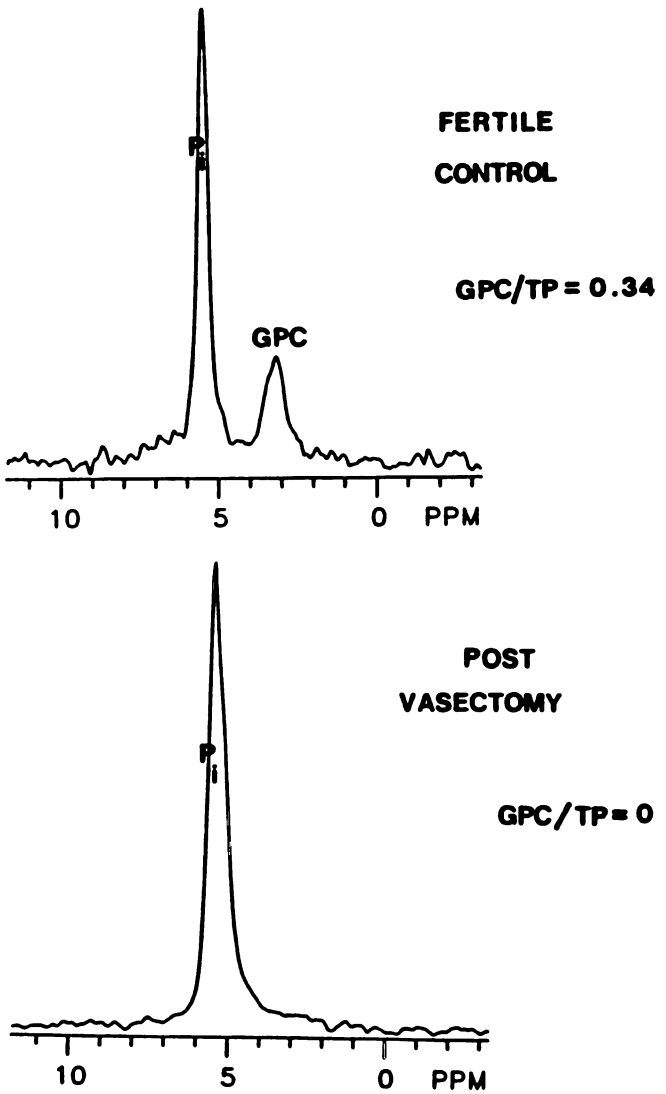

Figure 2. Representative ^{31}P NMR spectra of semen from a normal fertile control (Top) and an azoospermic postvasectomy patient (Bottom).

TABLE 1: COMPARISON OF GPC/TOTAL PHOSPHATE RATIOS AND SEMEN ANALYSIS PARAMETERS

GROUP	GPC/TP	SPERM CONCENTRATION (10^6/ml)	MOTILITY (%)	NORMAL MORPHOLOGY (%)
Normals	0.10 ± 0.05	85 ± 62	69 ± 8	75 ± 11
Vasectomies	0.05 ± 0.04*	0+	0+	0+
Infertility Patients	0.10 ± 0.05	51 ± 38	41 ± 21+	57 ± 17*

*p < 0.05 vs. control

+p < 0.001 vs. control

in sperm concentration, which reflected the complete lack of sperm in vasectomy patient samples, consistent with complete occlusion of the vasa deferentia in these patients. These findings are consistent with those of previous studies (12). The diminished GPC in semen specimens after vasectomy supports the contention that it is largely secreted from the epididymis. Other semen analysis parameters in the infertility patient group (volume, total sperm count, mean progressive motility and agglutination) and the vasectomy group (volume and agglutination) did not differ significantly from those of normal controls.

Discussion

GPC is synthesized by the epididymis and is bound closely to sperm; it has been postulated to be a protective coat associated with sperm motility (1, 5, 6). Although complete absence of epididymal secretions in semen is found after vasectomy, some of these patients still have levels of GPC that are not significantly different from those of fertile controls. Thus, GPC must be produced from tissues other than the epididymis (i.e., prostate and seminal vesicles). As a rule, however, normal patients will have levels greater than 0.07, and low levels (less than 0.03) are characteristic of vasal occlusion (Table 1). Although sperm motility is acquired in the epididymis, many factors should contribute to diminished sperm motility, such as the presence of a varicocele, sperm antibodies, or structural abnormalities (as suggested by the significant decrease in the percentage of sperm with normal morphology in the infertility clinic patients.

The infertility clinic patients were a heterogeneous group. Among this group were men who had presented to our infertility clinic to help establish the presence of infertility in their wives, and these men had normal GPC levels and normal results on semen analysis. This may explain this group's discrepant findings of a significantly lower mean motility rate without a concomitant reduction in GPC levels. To help link abnormally low GPC levels with diminished motility, a more appropriate sample of patients to study by GPC monitoring would be those with specific motility defects known to reflect epididymal dysfunction (such as patients with a good sperm count, poor motility and low antibody titers). Further clinical trials may support these contentions and help define precise indications for the clinical use of ^{31}P-NMR-measured GPC levels in assessing epididymal function and male infertility.

References

1. Arrata WSM, Tyler B, and Corder S. The role of phosphate esters in male fertility. Fertil and Steril 30:329 (1978).
2. Simmons FA. Medical progress. Human infertility. NEJM 255:1140-1146, 1186-1192 (1956).
3. World Health Organization (WHO). Laboratory Manual for the Examination of Human Serum and Semen - Cervical Mucus Interaction. Edited by M.A. Belsey, R. Eliasson, A.J. Galleges, K.S. Maghissi, C.A. Paulsen, MRN Prasad. Press Concern, Singapore, 1980.
4. Koretsky AP, Wang S, Murphy-Boesch J, Klein MP, James TL, and Weiner MW. ^{31}P NMR spectroscopy of rat organs, *in situ*, using chronically implanted radiofrequency coils. Proc. Natl. Acad. Sci. 80:749 (1983).
5. Mann T, and Mann CL. Male reproductive function and semen. New York, Springer-Verlag, 1981.
6. Turner TT. On the epididymis and its function. Invest. Urol. 16:311 (1979).

SECTION III: *IN VIVO* NMR STUDIES OF THE PROSTATE

Chapter 11: Introduction to Prostate Studies

This section presents studies assessing the utility of ^{31}P NMR spectroscopy and high signal-to-noise ^{1}H NMR imaging for studies of prostate pathophysiology, especially cancer. Prostatic carcinoma is the most common of all human cancers, being found in 50% or more of elderly men examined by autopsy (1,2). Prostate cancer is presently the second leading cause of cancer death in American men (3). Several variables in the occurrence and natural history of prostate cancer make it especially difficult to treat. Statistics indicate that less than 1% of prostate cancers cause clinical disease (4). Yet when they do, 50% of the patients present with metastases, and their average survival time is less than two years (5). Clinical management of this disease is further complicated by the fact that localized prostatic cancers of the same histologic grade do not behave uniformly (6,7). An understanding of the cellular bioenergetics of this cancer may help in understanding and perhaps predicting its biologic behavior. In the following two chapters, the ability of in vivo NMR techniques (primarily ^{31}P spectroscopy) to provide this kind of information was evaluated.

Studies of this type are especially significant, since present radiologic methods are often inadequate for clinical assessment of this pathology. Prostatic cancer is slowly progressive and is potentially curable if detected early (1,4). Unfortunately, there is currently no accurate screening test available for early detection of prostate cancer.

Conventional digital examination followed by core needle biopsy detects cancer in only 30-50% of suspicious prostates and is a primary diagnostic modality in only 13% of all prostate cancer (5). Serum assays of acid phosphatase is elevated usually only in metastatic disease and even then only in 60-80% of patients (8). Prostate specific antigen is elevated in 20-50% of patients with benign prostatic hyperplasia; so it is not useful as a screening modality (except for screening for metastases after radical prostatectomy) (9,10). Skeletal scintigraphy is useful only to screen for metastases, and this technique suffers from nonspecificity (11). Excretory urography in early prostatic carcinoma can detect only prostatic enlargement and nonspecific signs of lower urinary obstruction (11). Transrectal ultrasound has recently received attention as a technically simple and inexpensive screening and staging modality (12, 13). However, several recent studies have concluded that while its sensitivity is high, its specificity is too low for this technique to be considered as an accurate screening modality for prostatic cancer (14-16). CT is useful for detection of prostatic disease confined to the prostate gland (stage A and B) by the nonspecific findings of prostatic enlargement or asymmetry. In advanced prostate cancer, the sensitivity of CT for direct detection of stage C cancer (local extra-prostatic spread) has been determined to be 59% (17). Although MRI can provide quality images of the prostate, the lack of consistent distinguishing intensity characteristics between carcinoma and hyperplastic nodules also makes this technique presently inaccurate for cancer detection (18,19). In some cases, however, high quality T2-weighted MR images can differentiate the peripheral from the central and

transitional zones. The peripheral zone is where 70% of prostate cancers originate (1, 20). One study, on a limited number of patients, indicated that abnormal image intensities in the peripheral zone correlated well with the occurrence of cancer (21). Therefore, if high resolution MR images can be routinely obtained in which the prostatic zones are clearly demarcated, it may be possible to determine if a suspect nodule originates from the peripheral zone, thus making this technique more useful for cancer detection.

Once the prostate cancer diagnosis has been made, it is important to stage the disease accurately. Digital examination is very imprecise for determining tumor volume and local extent of the cancer. It is estimated that improper staging occurs in up to 42% of patients with local (clinical B_2) disease (22). Current radiologic imaging modalities also have have significant limitations in staging prostate cancer. Local staging using TRUS in the evaluation of capsular involvement has a reported accuracy of only 63% (23). The accuracy of CT for cancer staging has been the subject of several studies and has been determined to be from 61-67% (24-27). MRI has been shown to have the highest accuracy of any imaging modality. When T1- and T2-weighted images in multiple planes are obtained, accuracies of 83-89% have been reported (28-29). Improvements in MR image resolution and enhanced relaxation time weighting may improve this accuracy even further.

In addition to the lack of a good radiologic modality for prostate cancer detection and staging, there is also no accurate technique to monitor the efficacy of therapy. Evaluation of the effectiveness of therapy for prolonging the survival of prostate cancer patients has

remained difficult due to a number of factors. Chief among these is that this pathology occurs most commonly in elderly patients for whom mortality from other causes is especially high. Also, the autopsy incidence of prostate cancer is many times higher than the clinical incidence (30,31). This indicates that many patients with cancerous prostatic nodules do not require therapy. To date, no reliable tests have been developed to predict the biologic behavior of prostate cancer in an individual patient.

This uncertainty, coupled with the drawbacks and lack of clear effectiveness of each therapy, makes the clinician's decision as to proper therapy particularly difficult. The two most common therapies are: surgery and radiation therapy. Radical prostatectomy is a major operation with the associated operative mortality and surgical complications. Also erectile impotence and incontinence can occur in some cases. The success of this operation is dependent upon removal of all cancerous cells which is difficult (and often impossible) in cases of advanced prostate cancer. Radiation therapy also has several serious side effects including possibilities of radiation cystitis, impotence and rectal fibrosis requiring colostomy. Also, it is unclear whether this therapy is efficacious for larger cancerous prostates. There is also considerable variation in the reported efficacy of this therapy. Whereas some studies have shown radiation therapeutic results to be similar to those for surgery (32-34), other studies have found more recurrences and earlier progression following radiation therapy as compared with prostatectomy (35, 36). The efficacy and role of hormonal therapy in the management of prostate cancer is usually reserved for patients with metastatic disease. Its primary role is not

to effect a cure, but rather, to prolong patient survival by slowing tumor progression.

Although hormonal sensitivity of prostate tumors was first demonstrated over 40 years ago (37), there are currently no accurate methods to predict or assess response to endocrine therapy. Biochemical assays of androgen and estrogen receptor levels have demonstrated too low a correlation with hormonal sensitivity to be useful clinically (38, 39). There remains a clear need for a method which would provide early detection of hormone sensitivity and response to therapy and would then enable direction of nonresponsive patients to alternative therapies at an early stage of disease progression.

Chapter 12 presents studies assessing the ability of in vivo NMR to fulfill this need. In this chapter ^{31}P NMR spectra, ^{1}H MR images and ^{23}Na MR images were obtained from flank implanted tumors from two sublines (one hormone-sensitive and the other hormone-resistant) of the Dunning rat prostate cancer model. The Dunning rat prostate cancer is an established animal model for the study of human prostate cancer (40, 41). These rat cancers arise spontaneously, can metastasize to lymph nodes, and are hormonally responsive (40, 42). As in human prostate cancer, the effects of androgen manipulation on the cellular physiology in these tumors and the mechanisms involved are poorly understood, yet they are considered to be mediated by the same processes in both rat and human prostate cancer. In this study, ^{31}P spectra of each tumor line were compared, and the effect of androgen deprivation on the spectra obtained from hormone-sensitive tumors was followed over a 3 week period.

After the encouraging results described in chapter 12, a logical extension of this work is to initiate human prostate cancer studies to determine if this modality can provide useful medical insights as to tumor type and its biologic behavior. A major problem involved in doing this, as in most *in vivo* MR spectroscopy studies, is the difficulty of localizing spectra to a deep organ such as the prostate without contamination by surrounding skeletal muscle. To overcome this problem, a transrectal coil mounted on a plastic probe was constructed which could be inserted into the rectum and positioned close to the prostate. Using this probe, ^{31}P NMR spectra of the in situ prostate can now be obtained. In addition, the probe was designed to include either a double-tuned coil or a concentric two coil system so that ^{1}H MR images could be obtained along with the ^{31}P spectra. This is an important addition for two reasons. First, these transrectal images allow visualization of the area from which the ^{31}P spectra are obtained; thereby assisting in accurate coil placement. Secondly, the transrectal probe allows close proximity of the receiving coil to the prostate which results in much higher signal reception than can be obtained using external coils. This gain in signal-to-noise ratio can be exploited to provide images with a much finer pixel resolution than can be obtained using conventional body coil imaging techniques. Chapter 13 describes the construction of this probe and the images and spectra obtained by its use in canine prostates, similar in size to the human, before and after orchiectomy.

References

1. McNeal JE: The prostate gland: Morphology and pathobiology. Monographs in Urology 1983;4(1):3-33.
2. Franks LM: Latent carcinoma of the prostate. J Pathol Bacteriol 1954; 68:603.
3. Silverberg E: Cancer statistics 1985; 35:19.
4. Stamey TA: Cancer of the prostate. in Stamey TA (ed): Monographs in Urology 1982; 3:65.
5. Murphy GP, Natarajan N, Pontes JE, et al.: The national survey of prostate cancer in the United States by the American College of Surgeons. J of Urol 1985;129:928.
6. Heaney JA, Chang HC, Daly JJ, Prout G: Prognosis of clinically undiagnosed prostate carcinoma and the influence of endocrine therapy. J Urol 1977;118:283.
7. Rosenberg SM, Whitmore WF, Chopp RT: Delayed treatment of adenocarcinoma of the prostate. J Urol 1985;133:203A.
8. Heller JE: Prostatic acid phosphatase: Current clinical status. J Urol 1987;137: 1091-1096.
9. Seamonds B, Yang N, Anderson K, etal: Evaluation of prostate-specific antigen and prostatic acid phosphatatse as prostate cancer markers. Urology 1986; 28:472.
10. Myrtle JF, Klimly PG, Ivor LP, Bryni JF: Clinical utility of prostate specific antigen (PSA) in the management of prostate cancer. Hybritech Inc., San Diego, California.

11. Catalona WJ, Scott WW: Carcinoma of the prostate. In: Campbell MF. Campbell's Urology. WB Saunders, New York, Fifth Edition 1986; 1463-1534.

12. Fleischer AC: Prostatic endoscopy - a potential screening test. Diagnostic Imaging, April1987; 78-82.

13. Burks DD, Drolshagen LF, Fleischer AC, Liddell HT, McKougal WS, Karl EM, James AE: Transrectal sonography of benign and malignant prostatic lesions. AJR 1986; 1187-1191.

14. Chancellor MB, McHugh TA, Dorr RP, VanAppledorn CA: Transrectal prostate ultrsonography before transurethral prostatectomy, its value in screening for Stage A cancer. J Urol 1987; 137:241A.

15. Rosenberg S, Sogani PC, Palmer EA, Miller DG: Screening of ambulatory patients for prostate cancer by transrectal ultrasonography. J Urol 1987; 137:241A.

16. Babaian RJ, Evans R: In vitro prostate ultrasonography. J Urol 1988; 138: 178A.

17. Emory TH, Donovan BY, Hill AL, Lange PH: Use of CT to reduce understaging in prostatic cancer: Comparison with conventional staging techniques. AJR 1983; 141:315-318.

18. Ling D, Lee JK, Meiken JP, Balte DM et al.: Prostatic carcinoma and benign prostatic hyperplasia: The ability of MR imaging to distinguish between the two diseases. Radiology 1986; 155:103.

19. Byron PJ, Butler HE, Nelson AD, Lipuma JP, et al.: Magnetic resonance imaging of the prostate. AJR 1986; 146:543-548.

20. Sommer FG, McNeal JE, Carrol CL: MR depiction of zonal anatomy of the prostate at 1.5 T. J Comput Assist Tomogr 1986; 10:983-989.

21. Phillips ME, Kneget HY, Sprectar LE, Arger PH et al: Prostate disorders: MR imaging at 1.5 T. Radiology 1986; 386-392.

22. Fair WR, Kadmon D: Carcinoma of the prostate: Diagnosis and staging. Current status and future prospects. World J Urol 1983; 1:29-35.

23. Pontes E, Eisenkraft S, Watanabe H, Obe H, Saitoh M, Murphy GP: Preoperative evaluation of localized prostatic carcinoma by transrectal ultrasonography. J Urol 1985; 134:289-291.

24. Golimbu M, Morales P, Al-Askari S, Shulman Y: CAT scanning in staging of prostatic cancer. Urology 1981; 18:305-308.

25. Shankar Giri PG, Walsh JW, Hazra TA, Texter JH, Koontz WW: Role of computed tomography in the evaluation and management of carcinoma of the prostate. In J Radiation Oncol Biol Phys 1982; 8:283-287.

26. Morgan CL, Phil M, Calkins RF, Cavalcanti EJ: Computed tomography in the evaluation, staging and therapy of carcinoma of the bladder and prostate. Radiology 1981; 140:751-761.

27. Platt JF, Bree RL, Schwab RE: The accuracy of CT in the staging of carcinoma of the prostate. AJR 1987; 149:315-318.

28. Hricak H, Dooms GC, Jeffrey RG, Avallone A, Jacobs D, Benton WK, Narayan P, Tanagho EA: Prostatic carcinoma: Staging by clinical assessment, CT and MR imaging. Radiology 1987; 162:331-336.

29. Bionetti PR, Lee JK, Ling D, Catalona CSJ: Clinical Stage B prostate carcinoma: Staging with MR imaging. Radiology 1987; 162:325-329.

30. Franks LM: Latant carcinoma of the prostate. J Pathol Bacteriol 1954; 68:603.

31. Sheldon CA: Incidental carcinoma of the prostate: A review of the literature and critical reappraisal of classification. J Urol 1980; 124:626-632.

32. Leibel SA, Pino Y, Torres JL, Order SE: Improved quality of life following radical radiation therapy for early stage carcinoma of the prostate. Urol Clin N Am 1980; 7:593-604.

33. Neglia WJ, Hussey DM, Johnson DE: Megavoltage radiation therapy for carcinoma of the prostate. Int J Rad Oncol Biol Phys 1977; 2:873-882.

34. Bagshaw MA: Radiation therapy of prostatic carcinoma. In: Craford ED, Borden TA eds. Genitourinary Cancer Surgery, Lea & Febiger, Philadelphia, 1982; 405-411.

35. Scardino PT, Guerriero WG, Carlton CE Jr.: Surgical staging and combined therapy with radioactive gold grain

implantation and external irradiation. In: Johnson DE, Bolieau MA eds. Genitourinary Tumors. Fundamental Principles and Surgical Techniques. Grune & Stratton, NewYork, 1982; 75-90.

36. Paulson DF, Lin GM, Hinshaw W, Stephani S: The uro-oncology research group. Radical surgery versus radiotherapy for adenocarcinoma of the prostate. J Urol 1982; 128:502-504.

37. Huggins C, Hodges CV: Studies on prostatic cancer. The effect of castration, of estrogen and of androgen injection on serum phosphatases in metastatic carcinoma of the prostate. Cancer Res 1941; 1:293.

38. Ekman P, Barrack ER, Greeene GL, Jensen EV, Walsh PC: Estrogen receptors in human prostate: Evidence for multiple binding sites. J Clin Endocr & Metab 1983; 57:166-176.

39. Trachtenberg J, Walsh PC: Correlation of prostatic nuclear androgen receptor content with duration of response and survival following hormonal therapy in advanced prostatic cancer. J Urol 1982; 127:466.

40. Smolev JK, Meston WDW, Scott WW, Coffey DS: Charactization of the Dunning R3327H prostatic adenocarcinoma as an appropriate animal model for prostate cancer. Cancer Treat Rep 1977;61:273.

41. Thorndyke C, Meeker BE, Thomas G, Lakey WH, McPhee MS, Chapman JD: The radiation sensitivities of R3327H

and R3327AT rat prostate adenocarcinomas. J Urol 1985;134:191-198.

42. Pollack A, Block NL, Stover BJ, Irvin GL: Tumor Progression in serial passages of the Dunning R3327γ rat prostatic adenocarcinoma: Growth rate response to endocrine manipulation. Cancer Res 1985;45:1053-1059.

Chapter 12: Androgen Sensitivity of Rat Prostate Cancer Studied by ^{31}P NMR Spectroscopy, ^{1}H MRI, and ^{23}Na MRI

Purpose

^{31}P NMR spectroscopy, ^{1}H magnetic resonance (MR) imaging, and ^{23} Na MR imaging were used to study the biochemical difference between nine hormone-sensitive and six hormone-resistant rat prostate cancers and to follow bioenergetic and morphologic changes subsequent to androgen deprivation in the hormone-sensitive model.

The purpose of this study was to determine if use of magnetic resonance (MR) techniques could provide insights into the cellular metabolism of prostatic cancer. Specifically, ^{31}P NMR spectroscopy was used to compare the bioenergetics of hormone-sensitive with that of hormone-resistant rat prostate cancer. ^{1}H and ^{23}Na MR imaging was used to demonstrate any morphological differences between these tumor models. These *in vivo* NMR techniques were also evaluated for their sensitivity in following the effects of androgen deprivation on hormone-sensitive prostate cancer.

Materials and Methods

Tumor Lines

Hormone-sensitive and hormone-resistant sublines of the Dunning rat prostate cell line R3327H were obtained from Dr. David Lubaroff at the University of Iowa and from Papanicolau Laboratories in

Miami, Florida. Nine hormone-sensitive and six hormone-resistant cancers were implanted subcutaneously in the flanks of 15 male, 300-gram Copenhagen or Fisher rats. These cancers were in the form of 0.2-ml RPMI suspensions containing 1 x 10^5 cells or as 1-2 mm slices of tumor removed from tumor-bearing rats.

Procedure

After implantation, tumors were allowed to grow to a minimum diameter of approximately 1.5 cm (two months), then baseline MR images and NMR spectra were obtained. The rats with hormone-resistant tumors were then sacrificed. Orchiectomy (androgen deprivation) was then performed through a lower abdominal incision on four of the nine rats bearing hormone-sensitive tumors. After the testes were removed, the cords and vascular structures were ligated with 3-0 Dexon sutures; the wound was closed in two layers with 3-0 and 4-0 Dexon sutures. Three days after orchiectomy and weekly thereafter for three weeks, ^{31}P NMR spectra and ^{1}H MR images were obtained in these four rats and in the five untreated rats with hormone-sensitive tumors. The rats were then sacrificed.

All images and spectra were obtained with the rats anesthetized (50 mg/kg sodium pentobarbital administered intraperitoneally). For orchiectomy, an additional anesthesia of 1-2 ml of 1% lidocaine anesthesia was used locally. Tumor diameters were measured with calipers weekly throughout the study and when the rats were sacrificed.

MR Studies

A GE CSI-II spectrometer/imager with a 30 cm bore 2-Tesla magnet was used to obtain all the spectra and images for the study. The baseline ^{1}H MR images were obtained of all tumors to determine tumor shape, size and intensity characteristics and to direct placement of the ^{31}P NMR surface coil. For ^{1}H MR images, a 2.5" (diameter), low-pass "bird-cage" coil (1) constructed in our MR laboratory was used for radiofrequency excitation and reception at 85.6 MHz. Both T1- (TR of 500 msec/TE of 14 msec) and T2- (2500/80) weighted spin-echo (SE) 1H MR images were acquired using a slice thickness of 3 mm, 2 or 4 acquisitions at each of 128 phase encode steps, and a field of view (FOV) of 8 cm x 8 cm.

Baseline ^{23}Na MR images of 3 tumors (hormone-sensitive) were obtained and compared to the corresponding T2-weighted ^{1}H MR images. Another 2.5", low-pass, bird-cage coil, tuned to 22.6 MHz, was constructed and used to acquire the images (TR = 40 msec, TE = 9 msec, slice thickness of 5 mm, 200 acquisitions for each of 64 phase encoding steps, and FOV of 12 cm x 12 cm).

^{31}P NMR spectra were obtained for all tumors initially (baseline), three days post-orchiectomy (if done), and then weekly for a total of three weeks. A 1.4 cm (diameter) surface coil tuned to 34.6 MHz was used to acquire all spectra. Tape and plastic-cable ties were used to distance the tumor from the flank muscle; the surface coil was then secured directly above the tumor. For additional spatial localization, a "prepulse" pulse sequence (2) was used. This sequence employs a read pulse preceded by a pulse of one-third the read-pulse

duration; the prepulse is phase-cycled every other scan to attenuate the third harmonic of the read pulse. Imaging the response of this pulse sequence to a phantom showed that spectral contributions from high-flux regions just below the surface coil are substantially reduced and that the maximum depth of excitation is approximately 7 mm for the coil and pulse length we used. This technique, therefore, minimized spectral contributions from skin and subcutaneous tissues that lay between the coil and the tumor. Flank muscle, being at least 15 mm below the plane of the coil, was well beyond the sensitive volume of the experiment. A typical spectroscopic experiment utilized an interpulse delay of 3 sec, a 15-usec pulse length (180^0 tip angle at the surface), a sweepwidth of $\pm$ 2000 Hz, 4 K data points, and 256 to 400 acquisitions (depending on tumor size). Five fully-relaxed spectra with 20 sec between pulses were obtained in order to calculate T1-saturation factors; these factors were later used to correct all metabolite ratios. The Student's t-test for unpaired data was used for statistical analysis and ratios were expressed as mean $\pm$ S.E.M. (standard error of the mean).

Results

Representative T1- and T2-weighted ^{1}H MR images of a hormone-sensitive and a hormone-resistant tumor are shown in Figure 1. Baseline T1-weighted ^{1}H MR images of all fifteen tumors demonstrated an intermediate signal intensity for the cancers, higher than that of striated muscle but less than that of adipose tissue. The tumors demonstrated greater signal intensity on T2-weighted images

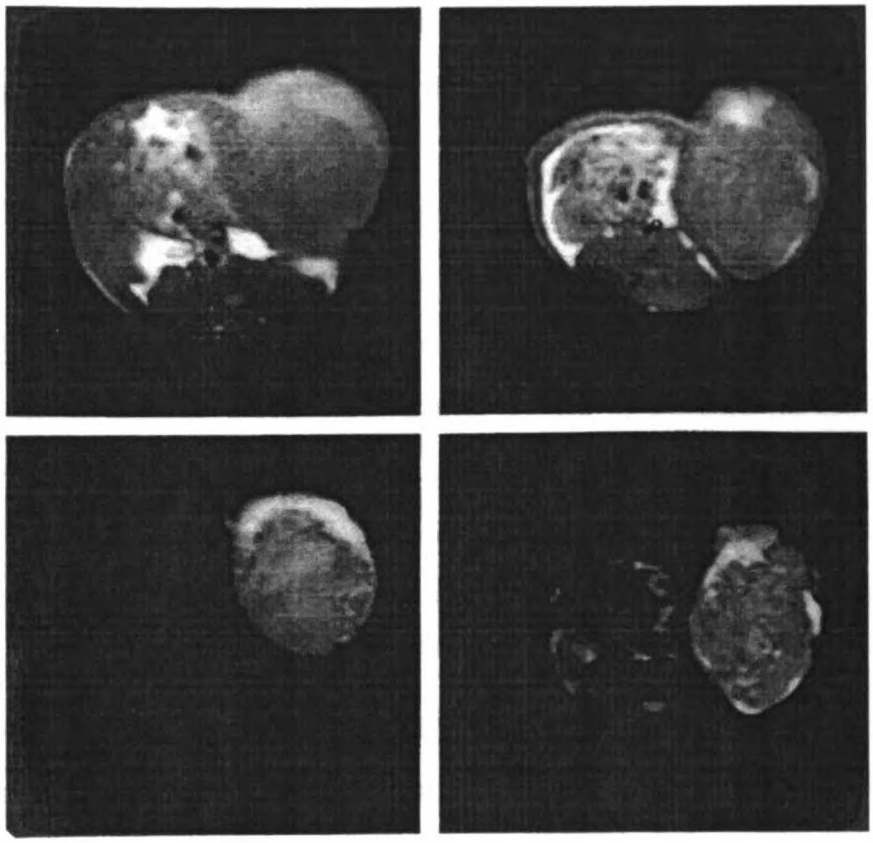

Figure 1. Comparison of T1-weighted (top) and T2-weighted (bottom) ^{1}H MR images of hormone-sensitive (left) and hormone-resistant (right) tumors. T1-weighted images were obtained with 4 acquisitions, a TR of 500 msec, a TE of 14 msec, an FOV of 8 cm x 8 cm, a slice thickness of 3 mm, and a 128 x 256 pixel matrix. T2-weighted images were obtained the same way except that 2 acquisitions were used with a TR of 2500 msec and a TE of 80 msec.

and only urine, CNS fluid, and subcutaneous edema showed higher intensity. No difference in signal intensity between hormone-sensitive and hormone-resistant tumors was observed. Orchiectomy produced no change in signal intensity on ^{1}H MR images, yet the effect of therapy was demonstrated by a much slower growth rate for the treated tumors (Figure 2).

^{23}Na MR images demonstrated a low-signal-intensity tumor surrounded by high-signal-intensity edema (Figure 3).

Baseline spectra disclosed a lower ATP/Pi ratio and a significantly higher PCr/ATP ratio for the hormone-sensitive tumors than for the hormone-resistant tumors of approximately the same size (Figure 4). The mean baseline PCr/ATP ratio for the hormone-sensitive tumors was 0.86 ± 0.9 S.E.M., whereas that for the hormone-resistant cancers was 0.26 ± 0.07 S.E.M. ($p<0.01$).

ATP/Pi ratios decreased significantly ($p<0.01$, at three weeks) with time for the hormone-sensitive tumors in both the control and orchiectomized rats, presumably due to an increase in Pi from edema, or necrosis, or both. No significant difference in ATP/Pi ratios was found between the control and orchiectomized rats.

PCr/ATP ratios decreased significantly over time in the hormone-sensitive tumors of orchiectomized rats; but in the control rats, only a small, non-significant decrease in this ratio was observed. The tumors of the orchiectomized rats showed a PCr/ATP decrease of one-third within three days after surgery; this decrease was statistically significant ($p<0.01$) one week later and remained so for the succeeding two weeks of the study (Figs. 5 and 6). Also, a significant difference ($p<0.01$) was found in the PCr/ATP ratios

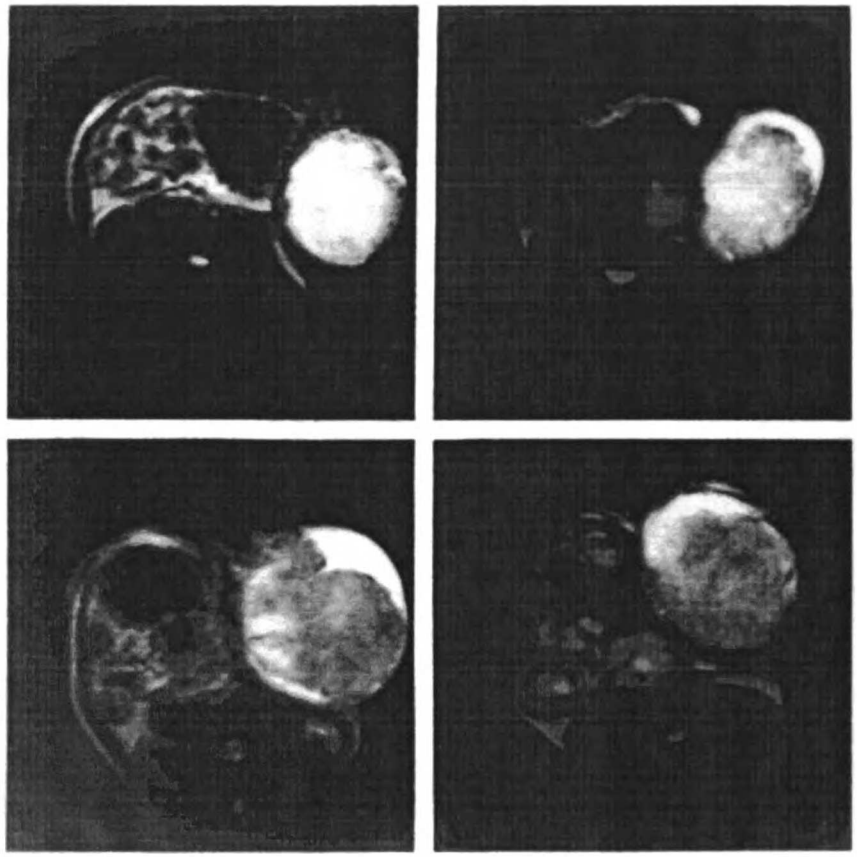

Figure 2. T2-weighted ^{1}H MR images of control (left) and androgen-deprived (right) tumors initially (top) and three weeks after orchiectomy (bottom). Imaging parameters were the same as for T2-weighted images in Fig. 1. Note the difference in tumor growth rate between the treated and untreated tumors, with no significant changes in tumor signal intensities.

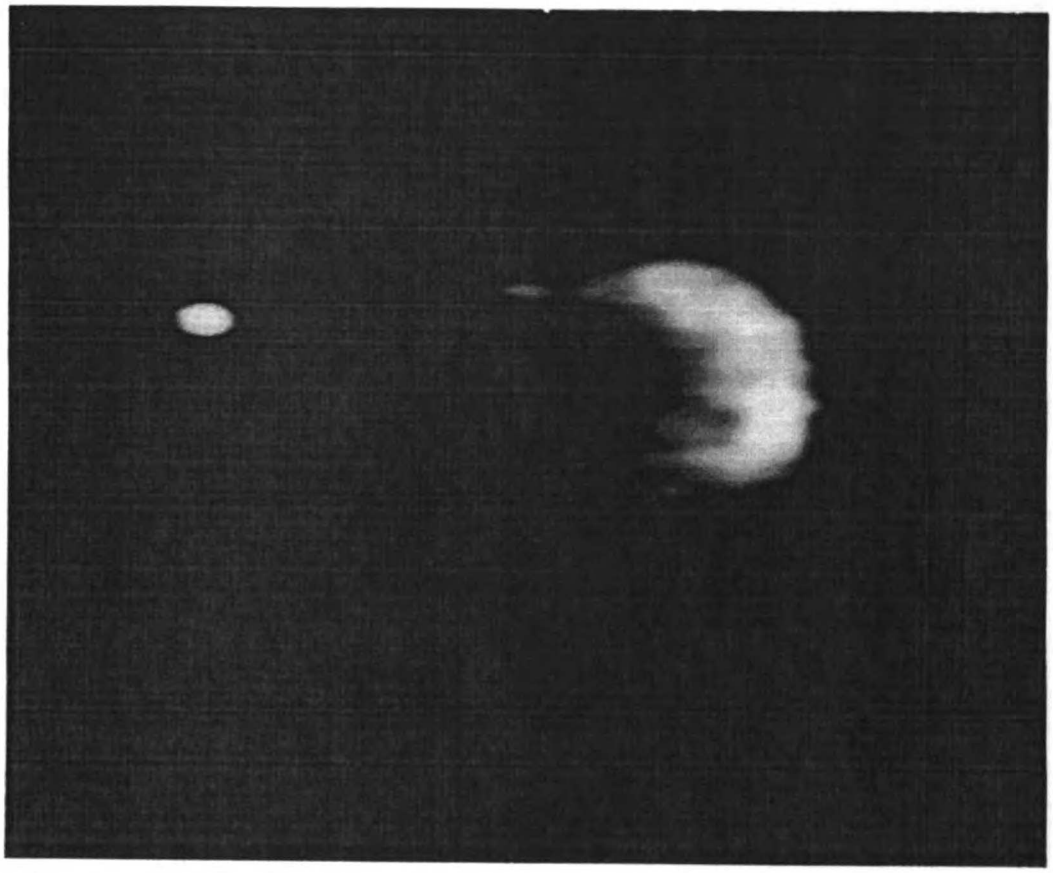

Figure 3. ^{23}Na MR image of an untreated androgen-sensitive tumor obtained with 200 acquisitions, a TR of 40 msec, a TE of 9 msec, an FOV of 12 cm x 12 cm, a slice thickness of 5 mm, and a 64 x 256 pixel matrix.

between the control and treated tumors from one week on (Figs. 5 and 6).

The chemical shift of the Pi resonance relative to that of PCr indicated pH values ranging from 6.9 to 7.2 with no correlation to hormone sensitivity nor to the time after orchiectomy.

HORMONE-SENSITIVE PROSTATE CANCER

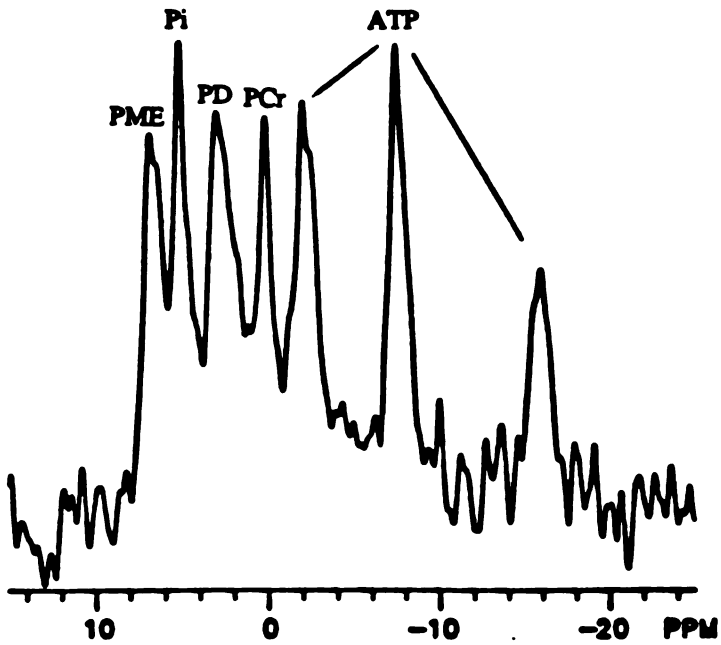

HORMONE-RESISTANT PROSTATE CANCER

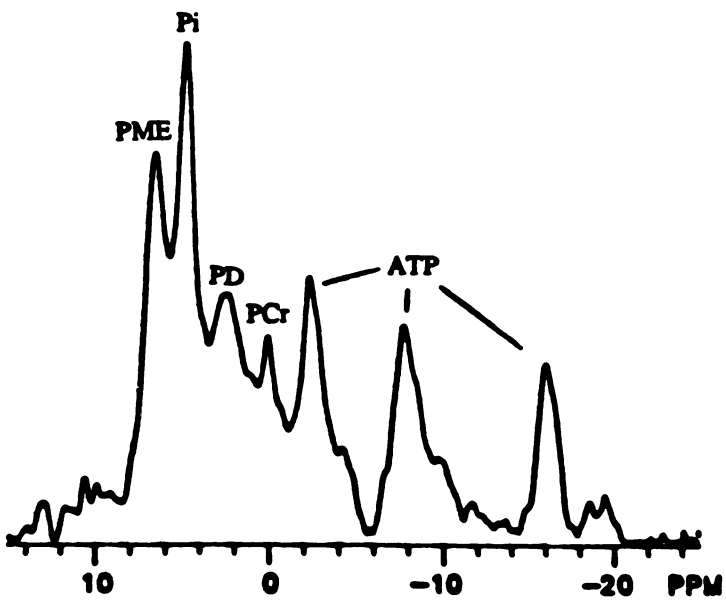

Figure 4. ^{31}P NMR spectrum from a flank-implanted prostate tumor that is androgen-sensitive (top) compared to that from one which is androgen-resistant (bottom). PME = phosphomonoesters, Pi = inorganic phosphate, PD = phosphodiesters, PCr = phosphocreatine, ATP = adenosine triphosphate with some possible contribution from other nucleoside triphosphates. Note the higher PCr/ATP ratio in the hormone-sensitive tumor.

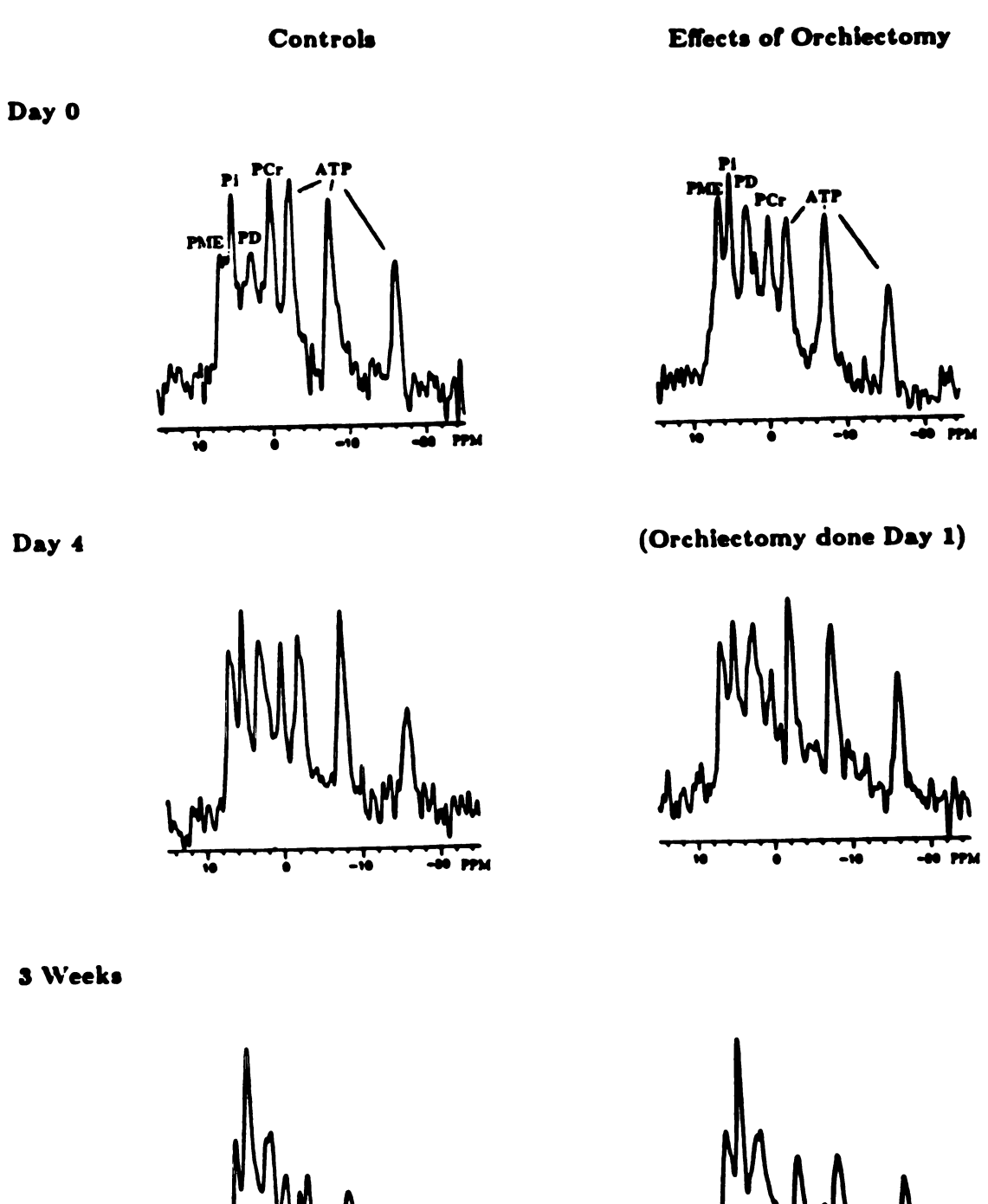

Figure 5. Serial ^{31}P NMR spectra of androgen-sensitive tumors implanted in control and orchiectomized rats. Spectra were obtained using the same parameters as were used for Fig. 2. The decrease in PCr/ATP ratio for the treated tumors was much larger than for the control.

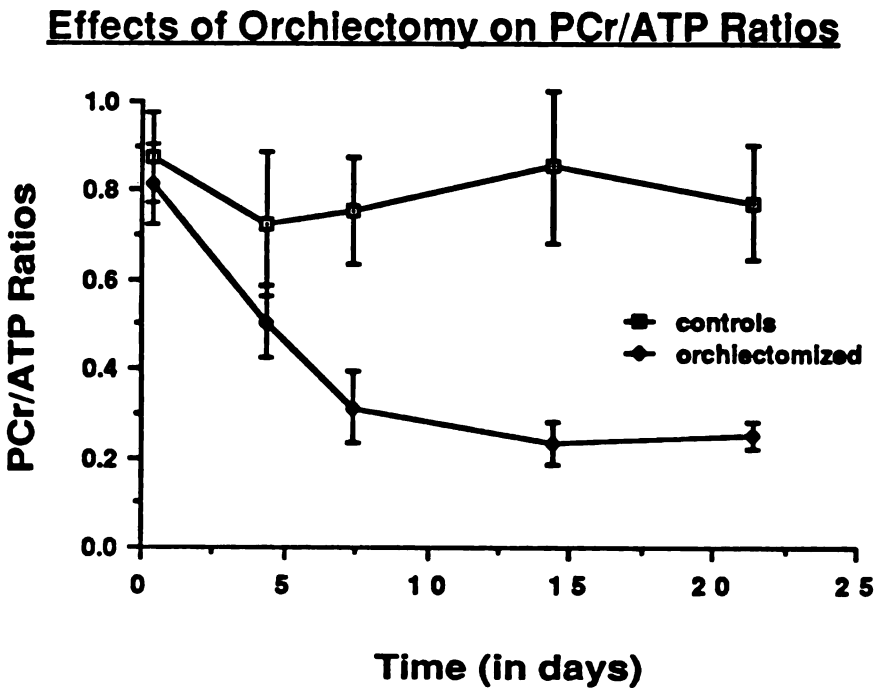

Figure 6. Graphic representation of the effects of orchiectomy on mean PCr/ATP ratios including S.E.M. After one week, orchiectomized tumors showed a statistically significant decrease in PCr/ATP ratios compared with those of the control tumors.

Discussion

The Dunning rat prostate cancer is an established animal model for the study of human prostate cancer (3, 4). These rat cancers arise spontaneously, can metastasize to lymph nodes, and are hormonally responsive (3, 5). As in human prostate cancer, in these tumors the effects of androgen manipulation on the cellular physiology and the mechanisms involved are poorly understood.

Unlike many tumor cells, prostate cancer cells have a substantial concentration of phosphocreatine. An enzyme assay study showed the concentration and isoenzyme pattern of creatine kinase (CPK) in prostatic cells to be under hormonal control (6). Changes in CPK concentration and isoenzyme pattern were also seen with neoplastic transformation of prostatic tissue. Another study, however, showed no significant correlation between CPK concentration (and isoenzyme pattern) and neoplastic transformation (7). In both these studies, enzyme patterns were not correlated with hormone sensitivity. Therefore, although CPK differences cannot be exploited to differentiate cancerous from noncancerous prostatic tissue, CPK concentration and isoenzyme pattern and, conceivably, PCr concentration may be useful in determining hormone sensitivity and in monitoring hormonal therapy.

Although studies of androgen stimulation of prostatic tissue are rare, the mechanism of hormonal stimulation may be similar to that of the better-studied steroid sex hormone, estrogen. Changes in CPK reaction rates have been observed with use of ^{31}P NMR spectroscopy

in uterine and ovarian cells after estrogen stimulation (8, 9). Also ^{31}P NMR spectroscopy of breast cancer has shown a correlation between PCr concentration and the presence of intracellular estrogen receptors (indicative of hormone sensitivity) (10, 11).

In our study, ATP/Pi and PCr/ATP ratios were elevated in the hormone-sensitive cancers as compared to the hormone-resistant ones of similar size. The observed Pi contains an undeterminable contribution from extracellular fluids and therefore is considered not to be a good indicator of cellular bioenergetics and the accuracy of pH measurements is compromised in these tumors. Qualitatively, however, the elevated concentration of Pi in the hormone-resistant tumors may indicate a larger proportion of necrotic cells. The difference in PCr/ATP ratios between these two cancer types does indicate a variation in cellular bioenergetics which may reflect the different CPK concentration and isoenzyme pattern.

The results of our study indicate that PCr/ATP ratios may be useful in monitoring androgen deprivation therapy. Although a sizeable range in PCr/ATP ratios was observed (probably due to individual differences in vascularization), the change in the mean value of this ratio was so large as to be statistically significant after one week. The spectral differences in the treated cancers preceded the change in growth rate by at least two weeks.

The usefulness of MR imaging for staging prostatic cancer is established, with an observed accuracy of 83% when T1- and T2-weighted images are obtained in multiple planes (12). However, MR imaging has not proved useful in detecting this cancer and, in our study, this technique was also not useful for determining hormonal

sensitivity or in rapidly monitoring the response to androgen deprivation.

The findings of our study, however, have several clinical implications. Prostate cancer is the second leading cause of cancer death in American men (13). It is highly metastatic, and therapy is often ineffective. Although the most effective and widely used therapy for metastatic prostate cancer is androgen deprivation, such therapy can only slow the progression of the disease. Resistance of the tumor to androgen deprivation eventually develops. The timing and mechanism of such resistance are presently unknown. Determinations of the hormone sensitivity of individual prostate tumors, even by invasive biopsy, are presently inaccurate and of little clinical use (14). Therefore, PCr/ATP ratios may aid both in detecting the hormone sensitivity of the tumor and monitoring tumor response to hormone deprivation. Although further studies are required to determine if the responses observed in this study hold for other prostate tumor lines (especially human prostate cancer) and for tumors of various sizes and degrees of vascularization, it appears that the unique chemical information provided by ^{31}P NMR spectroscopy can be used to predict the biologic behavior of prostate cancer to hormone therapy and to follow the course of this therapy.

References

1. Hayes CE, Edelstein WA, Schenck JF, Mueller OM, Eash M: A highly efficient, highly homogeneous radiofrequency coil for whole body NMR imaging at 1.5T. J Magn Reson 1985; 63: 622.
2. Shaka AJ, Freeman R: Spatially selective pulse sequences: Elimination of harmonic responses. J Magn Reson. 1985; 62:340-345.
3. Smolev JK, Heston WDW, Scott WW, Coffey DS: Characterization of the Dunning R3327H prostatic adenocarcinoma as an appropriate animal model for prostate cancer. Cancer Treat Rep. 1977; 61:273.
4. Thorndyke C, Meeker BE, Thomas G, Lakey WH, McPhee MS, Chapman JD: The radiation sensitivities of R3327H and R3327AT rat prostate adenocarcinomas. J Urol. 1985; 134:191-198.
5. Pollack A, Block NL, Stover BJ, Irvin GL: Tumor progression in serial passages of the Dunning R3327-γ rat prostatic adenocarcinoma: Growth rate response to endocrine manipulation. Cancer Res. 1985; 45:1052-1059.
6. Hall M, Silverman L, Wenger AS, Mickey DD: Oncodevelopmental enzymes of the Dunning rat prostate adenocarcinoma. Cancer Res. 1985; 45:4053-4059.
7. Truong T, Carmel M, Elhilali M, Cloutier D, Lehoux JG: Creatine phosphokinase isoenzymes in human prostatic

tissue. A comparison between benign hyperplasia and adenocarcinoma. Prostate. 1985; 7:143-149.

8. Degani H: MR studies of the reproductive organs and associated malignancies. In "Magnetic Resonance of the Reproductive System" S. McCarthy and F. Haseltine, Eds. SLACK Inc., Thorofare, New Jersey, 1987; 81.
9. Degani H, Neeman M, Rushkin E, et al: NMR studies of estrogen-induced metabolic activities in responsive organs and cells. "Workshop on Reproductive Biology and Magnetic Resonance Spectroscopy and Imaging" Center or Population Research, Bethesday, Maryland, 1986.
10. Degani H, Horowitz A, Itzchak Y: Breast tumor: Evaluation with P-31 MR spectroscopy. Radiology. 1986; 161:53-55.
11. Victor TA, Lawson CA, Wiebolt RC, Nussbaum S, Shattuck MC, Brodin AG, Degani H: Prediction of hormonal response of human breast carcinoma by ^{31}P MR spectroscopy. In Magnetic Resonance of the Reproductive System" S. McCarthy and F. Haseltine, Eds. SLACK Inc., Thorofare, New Jersey, 1987; 67-79.
12. Hricak H, Dooms GC, Jeffrey RB, Avallone A, Jacobs D, Benton WK, Narayan P, Tanagho EA: Prostatic carcinoma: Staging by clinical assessment, CT and MR imaging. Radiology. 1987; 62:331-336.
13. Silverberg E, Lubera J: Cancer statistics. CA 1987; 37:2.
14. Trachtenberg J, Walsh PC: J Urol. 1982; 127, 466.

Chapter 13: A Transrectal Probe for ^{1}H MRI and ^{31}P MR Spectroscopy of the Prostate Gland

Purpose

A major problem in obtaining spectra of the prostate is the difficulty of localizing spectra to such a small and deep organ without contamination by surrounding skeletal muscle. Even in the best case, localized prostate ^{31}P NMR spectra obtained using external coils (either body or surface coils) would suffer from far too low a signal strength to be at all useful. To obtain high-resolution images and well-localized spectra from the prostate, we devised a transrectal coil mounted on a plastic probe that can be inserted into the rectum and positioned close to the prostate. This chapter describes the construction of this probe and the images and spectra obtained by its use in canines before and after orchiectomy. The canine prostates of large dogs were chosen as experimental models since they are close to human size (approximately 3-4 cm in diameter whereas the human prostates range from 3.5-5 cm in diameter for adult males) and the response to hormone deprivation is similar.

Materials and Methods

Coil Design and Construction

Two types of transrectal NMR coils were used. Initially, a 2.7 cm-diameter coil double-tuned to obtain both ^{31}P spectra and ^{1}H images was employed. Later, a concentric coil design with a 3.0 cm-

diameter ^{1}H imaging coil surrounding a 2.0 cm-diameter ^{31}P spectroscopy coil was devised and constructed (Figure 1). For very small prostates (i.e. after months of androgen deprivation) a 1.5 cm ^{31}P MR coil was used. The coils were made of 3-mm copper wire with copper tape affixed to the probe just below and to the sides to effect rf shielding of all tissues except those directly in front of the coil. A ceramic chip capacitor was placed across the coil leads at the coil loop, and the leads were connected to either a double-tuned, balance-matched tuning and matching circuit (1) or to two single balance-matched circuits (2). The circuit board was covered with a plastic cover when the coil was being used, and tuning and matching was performed using plastic screws bored into the rear of the handle and connected to the variable capacitors. These long screws were adjustable from the outside, assuring minimal movement of the probe once positioned over the prostate.

Experimental Animals

Beagle dogs were obtained from Marshal Farms, New York, and were housed in the UCSF animal facility medical research building according to NIH guidelines. Two dogs were used for these experiments. One was 2 years old and the other was 8+ years old.

Anesthesia and Animal Preparation

Animals were fasted overnight. An enema was administered in the morning before the procedure to cleanse the rectum.

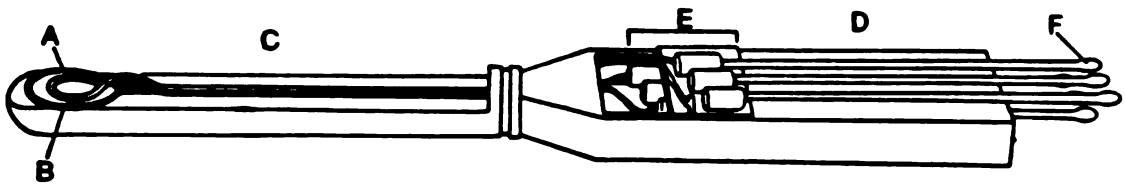

Figure 1. Transrectal MR probe with cut-away view of handle containing: (A) 2.0 cm-diameter ^{31}P spectroscopy coil. (B) 3.0 cm diameter ^{1}H MR coil. (C) Insertable portion. (E) Two sparate single-tuned tuning and matching circuits. (F) Tuning screws connected to the variable capacitors in E.

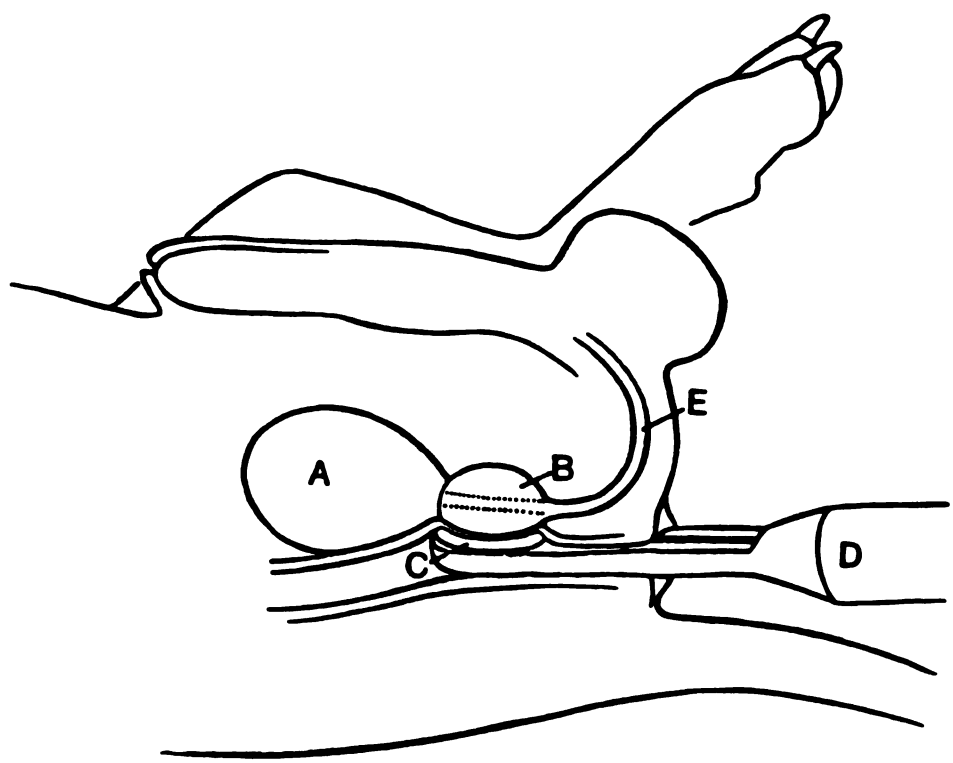

Figure 2. Schematic diagram showing placement of the probe in the canine rectum directly under the prostate gland: (A) Bladder; (B) Prostate; (C) MR coil; (D) Transrectal probe; (E) Urethra.

Preanesthetic medication consisted of 0.1 mg/kg of acepromazine given intramuscularly 1/2 hour before general anesthesia. General anesthesia consisted of sodium pentobarbitol 20-25 mg/kg given to effect intravenously and then as needed every half hour on the basis of vital signs and signs of animal awakening or movement.

Orchiectomy

Bilateral orchiectomy was performed under general anesthesia through a horizontal scrotal incision. Both testes were delivered out of the scrotal sac. Absorbable 2.0 Dexon suture ligatures were applied to the cord and vessels, and both testicles were removed. The scrotal skin was closed in two layers with interrupted 2-0 and 3-0 Dexon sutures.

Coil placement

Prior to each experiment, the coil and probe were washed with antiseptic solution (glutaraldehyde 2%; Cidex) or alcohol wipes, and two condoms, one over the other, were placed over the insertable portion. After the anesthetized dog was positioned in the magnetic resonance instrument, digital palpation was used to confirm the position of the prostate and to measure its location and its depth from the anal verge. The coil was then lubricated (K-Y jelly) and inserted into the rectum (Figure 2). Initially, the animal was placed face down with the prostate facing away from the coil. Subsequently, it was found that if the animal was placed face up in the magnet, the prostate (which in the dog is softer and more mobile anteroposteriorly than in the human) would rest directly above and closer to the insertable coil.

To prevent motion, the handle of the probe was then taped over soft foam supports to the acrylic half-tube upon which the dog lay. The optimum position was determined after prostate images were obtained. With experience it was possible to place the coil over the center of the prostate on the first attempt.

Imaging and Spectroscopy

Imaging and spectroscopy were performed on a GE CSI-II imager/spectrometer with a 30-cm-bore 2 Tesla magnet. Because of the small bore of the magnet, the dog could not be placed in a body coil, so the inserted coil was used both to transmit and to receive. To decrease B_1 inhomogeneity effects, a gradient-refocussing sequence and a short TR (100 msec) was used. Typically, a field of view (FOV) of 8.1 x 8.1 cm^2 was used so that the images acquired from a 256 x 256 pixel matrix yielded an in-plane pixel size of 0.3 x 0.3 mm^2 with a slice thickness of 3 mm (total voxel volume 0.27 mm^3). The older dog was used to look for evidence of benign prostatic hyperplasia (BPH). Following this, bilateral orchiectomy was performed to cause androgen deprivation and prostatic involution, and serial images and spectra were obtained 1 week, 2 weeks, 3 weeks and 3 months later.

^{31}P spectra were typically obtained from 200 acquisitions with a pulse width of 20 microseconds, an interpulse delay of 3 sec and a total time of 10 minutes using the 2.0 cm diameter coil. For the small prostate (3+ weeks after orchiectomy), a 1.5 cm coil and 800 acquisitions were required in order to obtain localized spectra with an adequate signal-to-noise ratio. To ascertain that the spectra obtained were solely from the prostate, additional spatial localization using both

B_1 (3) and B_0 gradient localization schemes (4) were employed to negate any spectral contributions from the rectal wall.

Results

Images obtained using the transrectal coil demonstrated much finer detail than those obtained by conventional clinical techniques on a 2T whole-body instrument (Figure 3 and 4). Specifically, better delineation of the peripheral zone of the prostate (where most cancers originate) was achieved and there was clearer delineation of the urethra and periurethral structures and finer resolution of the prostatic capsule, peristatic venous plexus, fat and levator muscles (Figure 3). After orchiectomy, serial images showed softening and change in rigidity of the prostate gland (Figure 3). A comparison image of the canine prostate obtained with a whole body coil at 2.0 Tesla is shown in Figure 4.

Using the transrectal coil, the first (to the authors' knowledge) *in situ* ^{31}P MR spectra of the canine prostate (or of any prostate, for that matter) were obtained (Figure 5). Relative to ATP, high levels of PME, Pi, PD and PCr were observed in canine prostatic tissue. The PME/ATP ratio was larger than that of most organs with the exception of the testicle and neonatal organs. Although smaller than for brain or muscle, the PCr/ATP ratio of 0.80 is higher than for most tissues. The Pi chemical shift relative to PCr indicated a pH of approximately 7.2 for prostatic tissue. Spectra obtained by both B_1 and B_0 gradient localization schemes were virtually identical, indicating minimal rectal

wall contributions. No differences between these spectra and those obtained without further localization were discernable.

After orchiectomy, the prostate shrank considerably: the width and height of transaxial slices at the prostate midline decreased from 3.8 cm x 2.9 cm to 3.2 cm x 1.5 cm at 1 week and to 1.9 cm x 1.3 cm at 3 weeks after orchiectomy. The ^{31}P spectra decreased in signal-to-noise because of the smaller organ size and the necessarily smaller coil (1.5 cm). Only minor spectral changes were observed. The PCr/ATP ratio remained at 0.80 throughout the study but the PME/ATP ratio decreased from 1.34 pre-orchiectomy to 0.89 by three weeks after orchiectomy. The PME/ATP ratio for the 8-year-old dog was 1.00; i.e. less than that for the 2-year-old dog prior to orchiectomy.

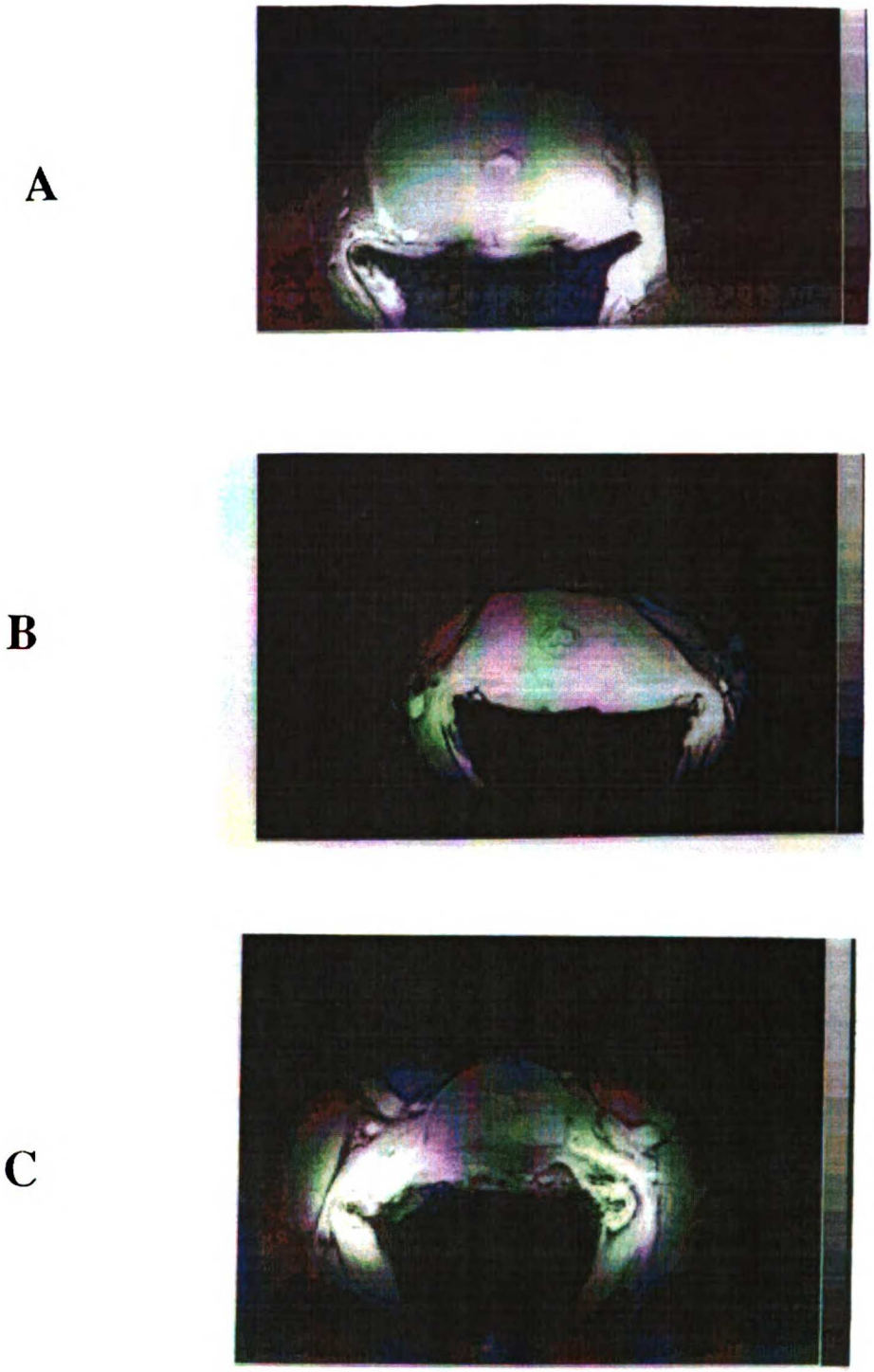

Figure 3. Serial transaxial gradient-refocussed MR images. (A) Prior to orchiectomy; (B) 1 week after orchiectomy; (C) 3 weeks after orchiectomy. Image parameters are: TR = 100 msec, TE= 9 msec, FOV = 8.0 x 8.0 cm^2, 256 x 256 pixel matrix, slice thickness = 3mm, and 2 acquisitions per phase-encoding step.

Figure 4. Whole-body coil T1-weighted MR image of the canine prostate obtained on a clinical imager/spectrometer operating at 2 Tesla. Spin-echo image parameters are: TR= 500, TE = 20, FOV = 40 x 40 cm^2, 256 x 256 pixel matrix, slice thickness = 1.0 cm, and 2 acquisitions per phase-encoding step.

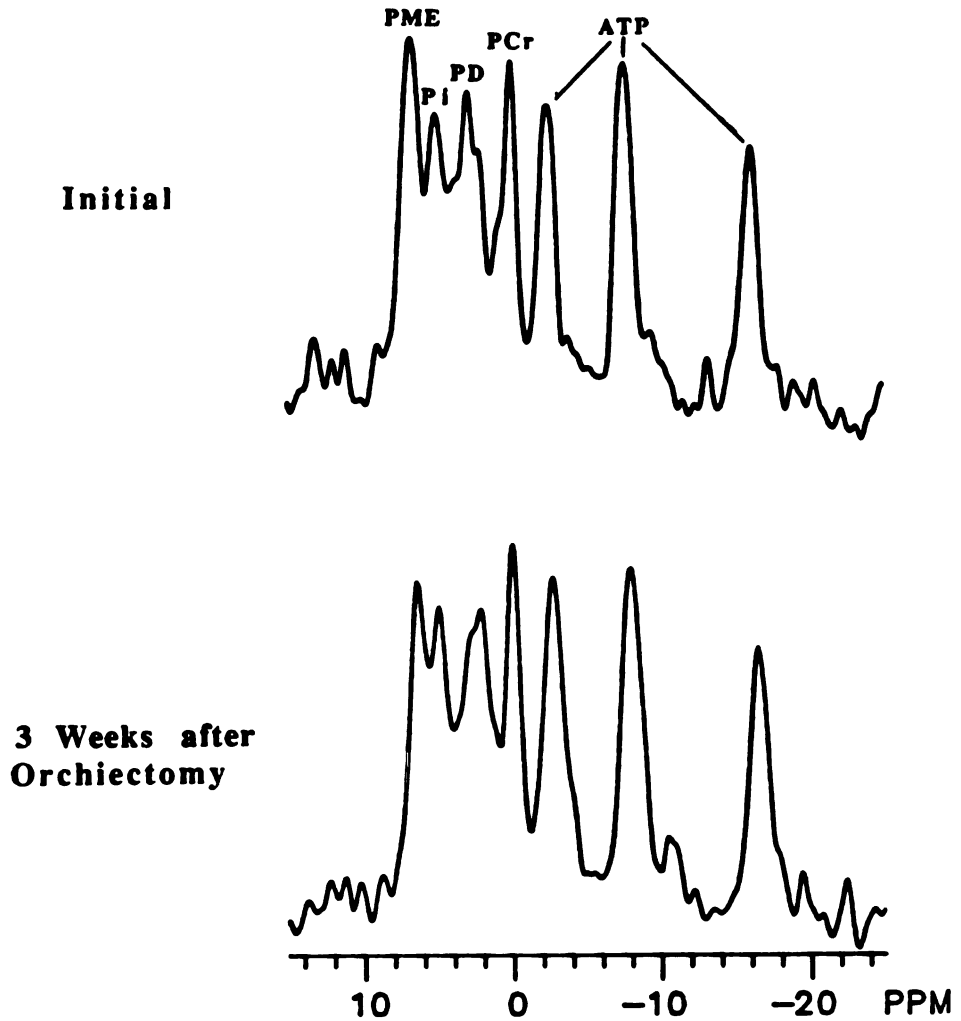

Figure 5. ^{31}P NMR spectra from the canine prostate initially (top) and 3 weeks after orchiectomy (bottom). Peak asignments are: PME = phosphomonoesters, Pi= inorganic phosphate, PD = phosphodiesters, PCr = phosphocreatine and ATP = adenosine triphosphate (with possible contributions from other nucleoside triphosphates).

Discussion

Prostate cancer is the second most common cancer in American men. In 1987, an estimated 97,000 new cases have been diagnosed (5). Unfortunately, accurate screening techniques to detect this cancer early and to stage it properly, once detected, are both lacking.

The transrectal MR probe may solve both these problems by producing high-resolution images of the prostate. The coil, being within a few millimeters of the prostatic surface, greatly enhances the signal-to-noise ratios of ^{1}H resonances from the prostate as compared with those obtained with body coils or conventional surface coils; this increases image clarity. Because the coil's sensitive volume is limited to the prostate and adjacent tissues tissues, a small FOV can easily be used without image distortion from signals outside the FOV. The images obtained had much finer detail than those obtained using a conventional clinical body coil with a typical slice thickness of 5 to 10 mm and a pixel size of 5 to 10 mm and a pixel size of 1.7 x 1.7 mm^2 to 2.2 x 2.2 mm^2 (or total voxel volume of 14.45 mm^2 to 48.40 mm^3 vs 0.27 mm^3 for the transrectal images). In this study, gradient-refocussed images were necessitated by instrument constraints, but in large clinical systems, conventional spin echo sequences will be possible using the body coil to excite and the transrectal coil to receive. Image quality is likely to improve even more. T2-weighted images, which differentiate well between the peripheral and central prostatic zones, can also be obtained easily, which is not the case for gradient-refocussing sequences.

The advantages of high-resolution images are several. First, better differentiation of zonal anatomy may improve the detection rates of cancerous nodules. Most cancers originate in the peripheral zone of the prostate, whereas benign adenomas are more common in the central zone (6). Conventional MRI currently is unable to differentiate this zonal anatomy consistently, a problem that may be overcome by high-resolution imaging. Also, the close proximity of the MR coil to the prostate effects a great increase in signal-to-noise ratio which could be exploited to provide images with greater T2-weighting than is obtainable using conventional imaging techniques (within an acceptable time period) This enhanced T2-weighting may allow better differentiation between neoplastic and normal tissue. Second, improved delineation of zonal anatomy will also allow precise biopsies of small nodules that otherwise are missed. Third, high-resolution imaging should increase the accuracy of staging and estimation of the volume of cancerous tissue within the gland by providing better delineation of the prostatic capsule, periprostatic fat and seminal vesicle anatomy. Cancer extension to periprostatic fat and, especially, to the seminal vesicles indicates a poor patient prognosis (7, 8) but is inadequately assessed by current imaging modalities (9-13). Pathologic step-sectioning studies have indicated that the extent of prostate cancer is incorrectly estimated clinically (10, 14, 15). Serial high-resolution images obtained transrectally may improve the volume estimation of cancer within the prostate, providing important accurate prognostic information.

High-resolution imaging will also be useful in the therapy of prostate cancer. For localized disease, accurate depictions of prostatic

and periprostatic anatomic details may help in planning surgical approach. Two major problems confronting surgeons during prostatectomy are bleeding from the venous plexus surrounding the prostate dorsally and laterally, and inadvertent injury to the nerves controlling erectile potency and continence, which travel close to the prostate laterally. Transrectal imaging, by depicting anatomic structures in detail, may help the surgeon avoid these problems. High-resolution imaging may also aid in assessing the impact of nonoperative therapy such as external or brachytherapy radiation, first by providing accurate staging and second by clearly delineating the changes in volume and perhaps image contrast differentiations in response to therapy. In more advanced disease, changes secondary to hormonal manipulation may be visible in the form of rapid shrinkage in volume as well as change in consistency and shape, as seen from the canine prostate studies.

Transrectal spectroscopy, although at present less applicable clinically than imaging, may also become valuable to study the bioenergetic differences between normal and neoplastic tissues, hormone-sensitive and hormone-resistant cancers, and treated and untreated tumors. A technique to monitor prostatic cellular metabolism and bioenergetics would be beneficial in several ways. First, the altered biochemistry of neoplastic cells could be studied. By comparing neoplasia with normal prostatic cellular metabolism, valuable insights may be gained into the fundamental biochemical alterations during human neoplastic transformations *in vivo* noninvasively. A great variety of prostate cancer behaviors (hormone sensitivity, growth rates, acid phosphatase, chromosomal content etc)

have been observed in different tumors and it will be interesting to correlate the incidences of the above to steady-state levels of high energy phosphates. Second, the metabolic "health" of both normal and cancerous cells could be monitored during therapy, yielding valuable information on the mechanism of action and the efficacy of specific treatments. Third, understanding prostatic physiology at a molecular level may provide new information on other prostatic diseases, especially benign hyperplasia, which is clinically ten-fold more prevalent than prostate cancer. Preliminary studies of rat prostate cancer (Chapter 12) suggest that ^{31}P NMR spectroscopy can detect differences between hormone-sensitive and hormone-resistant tumors and intracellular changes following androgen deprivation much earlier (3 days vs. 2 weeks) than can conventional changes in size and growth parameters (16, 17). The decrease in the PME/ATP ratio after orchiectomy and between the younger and older dogs may also have relevance. The PME peak has significant contributions from phosphocholine, phosphoethanolamine and phosphoserine, which are involved in membrane phospholipid synthesis (18-20). Hormonal suppression of spermatogenesis in canine and primate testicles has been shown to be accompanied by a decrease in PME/ATP ratios (20). It is possible that prostatic atrophy induced by androgen deprivation can be detected early by ^{31}P NMR monitoring of PME levels.

The transrectal coil described in this chapter has been used primarily to study prostate pathology. However, in concept and design, the device is meant for wider application. With experience from these studies, it is hoped that similar devices may be useful eventually in obtaining images and spectra from any cavity in the body.

References

1. Chang LH, Chew WM, Weinstein PR, James TL: A balanced-matched double-tuned probe for *in vivo* ^{1}H and ^{31}P NMR. J Magn Reson 1987; 72:168-172.
2. Murphy-Boesch J, Koretsky AP: An *in vivo* NMR probe for improved sensitivity. J Magn Reson 1983; 54:526-532.
3. Shaka AJ, Freeman R: Spatially selective pulse sequences: Elimination of harmonic responses. J Magn Reson. 1985; 62:340-345.
4. Ordidge RJ, Connelly A, Lohman JAB: Image selected *in vivo* spectroscopy (ISIS). A new technique for selective NMR spectroscopy. J Magn Reson 1986; 66:283.
5. Silverberg E: Cancer statistics. CA Cancer Journal 1985; 35:19-35.
6. McNeal JE: The prostate gland: Morphology and pathobiology. Monographs in Urology 1983; 4:3-33.
7. Gibbons RP, Correa RJ Jr., Brannen GE, Mason JT: Total prostatectomy for localized prostatic cancer. J Urol 1984; 131:73-76.
8. Lange PH, Narayan P: Understanding and undergrading prostate cancer. Urol 1983; 21:113.
9. Hricak H, Dooms GC, Jeffrey RB, Avallone A, Jacobs D, Benton WK, Narayan P, Tanagho EA: Prostatic carcinoma:

Staging by clinical assessment, CT and MR imaging. Radiology 1987: 161:331.

10. Emory TH, Donovan BY, Hill AL, Lange PH: Use of CT to reduce understaging in prostatic cancer: Comparison with conventional staging techniques. AJR 1983; 141:351-354.
11. Platt JF, Bree RL, Schwab RE: The accuracy of CT in the staging of carcinoma of the prostate. AJR 1987; 149:315-318.
12. Fleischer AC: Prostatic endoscopy - a potential screening test. Diagn Imaging, April 1987 : 78-82.
13. Burks DD, Drolshagen LF, Fleischer AC, Liddell HT, Mc Kougal WS, Karl EM, James AE: Transrectal sonography of benign and malignant prostatic lesions. AJR 1987; 146:1187-1191.
14. Lange PH, Moon TD, Narayan P, Mendini E: Radiation therapy as adjuvant treatment after radical prostatectomy: Patient tolerance and preliminary results. J Urol 1986; 136: 45.
15. Catalona WJ, Stein AJ: Staging errors in clinically localized prostatic cancers. J Urol 1982; 127:452.
16. Narayan P, Vigneron DB, Hricak H, Moseley ME, James TL: Biochemical response of prostate cancer cells to hormone deprivation detected by magnetic resonance spectroscopy. J Urol 1987; 137:113A.
17. Vigneron DB, Hricak H, Narayan P, Nunes L, Moseley ME, James TL: Detection of the biochemical response of prostate cancer to androgen deprivation by P-31 MRS.

Abstracts of VI Annual Meeting of the Society of Magnetic Resonance in Medicine. 1987; p.36.

18. Bretan PN, Vigneron DB, Hricak H et al.: Assessment of testicular metabolic integrity with P-31 MR spectroscopy. Radiology 1987; 162:867-871.

19. Navon G, Gogol E, Weissbart R: Phosphorus-31 and proton NMR analysis of reproductive organs of male rats. Arch Androl 1985; 15:153-158.

20. Schmidt HC, Gooding CA, James JL, Gonzalez-Mendez R, James TL: Comparison of *in vivo* ^{31}P MR spectra of the brain, liver and kidney of adult and infant animals. Pediatr Radiol 1986; 16: 144-149.

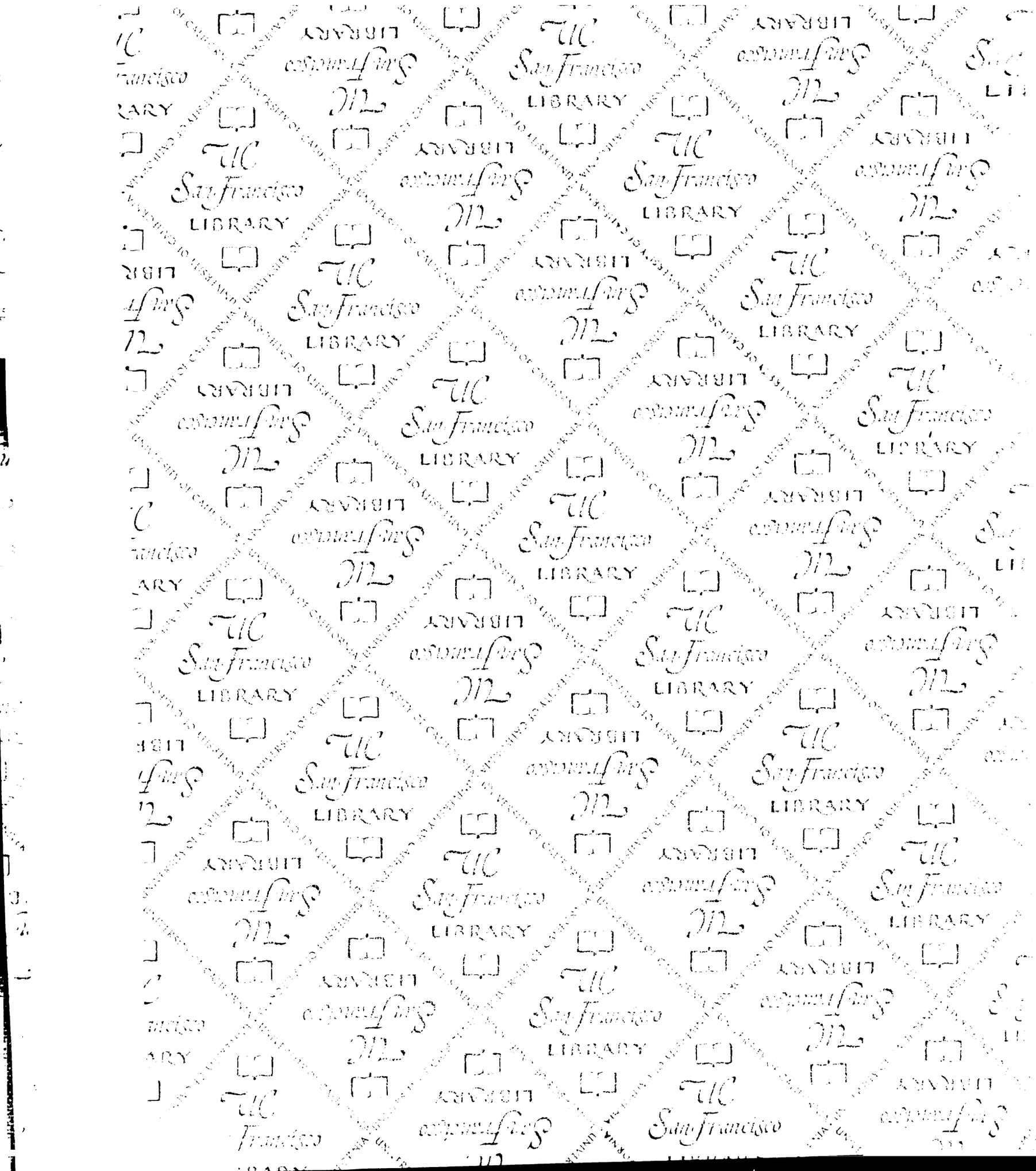
UC
San Francisco
LIBRARY